M.M. Nobel

The design of a manually operated compliant mechanism steerable needle for high doserate brachytherapy of the prostate





The design of a manually operated steerable compliant mechanism needle for high dose-rate brachytherapy of the prostate

M.M. Nobel

in partial fulfilment of the requirements for the degree of

Master of Science Biomedical Engineering

at the Delft University of Technology, to be defended publicly on April 9, 2020.

Supervisor: dr. J.J. van den Dobbelsteen Supervisor: M. de Vries

Thesis committee:

This thesis is confidential and cannot be made public until April 9, 2025.

An electronic version of this thesis is available at http://repository.tudelft.nl/.



Abstract

Prostate cancer is the most common cancer in men and third in terms of mortality. High dose rate brachytherapy is a common and effective treatment to treat this cancer. High dose rate brachytherapy requires the implantation of several needles into the prostate trough which a radiation source is introduced. This implantation can present a number of difficulties. Steerable needles have been proposed to address some of these difficulties. The literature review in Appendix A has identified a number of possible advantages using a steerable needle could have in high dose-rate brachytherapy of the prostate. This thesis aims to develop a steerable needle system enabling the surgeon to place a needle more accurately, combat pubic arch interference, and circumvent ureteral occlusion while not interfering in the general course of the procedure.

This steerable needle was developed according to several design guidelines and optimisation parameters. A mathematical model and simulation were used to predict the behaviour of the needle and identify which parameters influence its functioning. By developing a number of concepts and evaluating their performance according to the set design guidelines a final design was formulated. A phantom was developed to be able to evaluate the performance of the design. By comparing the performance of the developed steerable needle to commercially available non-steered needles we hope to show the possible performance benefit of the developed needle.

The steerable needle has shown to perform, at minimum, non-inferiorly to a commercially available non-steerable needle. A small cost-effectiveness analysis has shown the possibility of the developed system to be cost-effective. While the developed steerable needle allows a surgeon to steer a needle during needle implantation and possibly increase the needle endpoint accuracy, the question remains whether this will result in a more favourable outcome of the high dose-rate brachytherapy procedure.



Introduction

The literature review preceding this thesis describes the possible advantages steerable needles could have in the field of high dose-rate brachytherapy of the prostate. Steerable needles could provide a way to increase needle placement accuracy and reduce late toxicities.

This thesis will outline the design process used to design a manually operated, compliant mechanism steerable needle for high dose-rate brachytherapy of the prostate. The thesis will provide experimental data relating to the performance of this steerable needle and recommend a course of action for the further development of the steerable needle.

In the first chapter, design guidelines will be presented to ensure the product fulfils all requirements a physician might have. In chapter two the general design of the steerable needle will be presented, theory pertaining to the steering mechanism, materials choices and multiple concepts will be presented. Chapter three shows the methods used to evaluate the previously generated concepts and presents the method used to decide on the concept to develop further. The next chapter, chapter four, contains the optimisation of this chosen concept ad presents the final product. The fifth chapter present the final evaluation of the steerable needle in comparison to currently used instruments. The sixth and final chapter combines the previous chapters into a discussion about the performance of this steerable needle and the steps necessary to develop the instrument further.

Content

1 DESIGN GUIDELINES	
1.1 CONCLUSIONS FROM LITERATURE REVIEW	
1.2 SUPPLEMENTARY LITERATURE TO FORMULATE REQUIREMENTS	
1.3 DESIGN BRIEF	
1.4 REQUIREMENTS	
1.4.1 Functional requirements	
1.4.3 TECHNICAL REQUIREMENTS	
1.4.4 INTERACTION REQUIREMENTS.	
1.5 OPTIMISATION PARAMETERS.	
1.5.1 FUNCTIONAL OPTIMISATION PARAMETERS	
1.5.2 Usability optimisation parameters	8
1.5.3 TECHNICAL OPTIMISATION PARAMETERS	8
1.5.4 Technical optimisation parameters	8
2 DESIGN AND CONCEPT GENERATION	
2.1 Current prototype	10
2.1.1 THE COMPLIANT MECHANISM	
2.1,2 DEFLECTION OF EXISTING DESIGN	11
2.1.3 Steering in gelatine	
2.2 THEORY	
2.2.1 DEFLECTION	
2.2.2 YIELDING	
2.3 Material selection	
2.3.1 GENERAL MATERIALS	
2.3.2 Superelastic materials	
2.3.3 MATERIAL CHOICE	18
2.4 CONCEPTS	18
2.4.1 OPTIMISED CURRENT PROTOTYPE	
2.4.2 OPTIMISED CURRENT PROTOTYPE WITH STEERING MECHANISM	
2.4.3 WRE NEEDLE	
2.4.4 EXPANDED WIRE NEEDLE	
2.4.5 LINEAR ACTUATABLE EXPANDED WIRE NEEDLE	
3 CONCEPT EVALUATION	22
3.1 Phantom	23
3.1.1 Materials and methods	
3.1.2 RESULTS	
3.2 Prototypes	
3.3 EVALUATING PARAMETERS	
3.4 MATERIALS AND METHODS	
3.6 CHOICE OF FINAL CONCEPT	
4 OPTIMISATION AND FINAL DESIGN	



4.1 ADJUSTED DESIGN OBJECTIVES	32
4.2 MEDICAL DEVICE CLASSIFICATION	
4.3 MATERIAL SELECTION	
4.4 HANDLE	
4.4.1 STOP AND FLAT	
4.4.2 NJECTION MOULDED HANDLE	
4.4.4 ECCENTRIC LOCK	
4.5 Final design.	
5 PERFORMANCE EVALUATION	39
5.1 IMPROVED PHANTOM	40
5.1.1 MATERIALS AND METHODS.	
5.1.2 RESULTS	42
5.2 MATERIALS AND METHODS	
5.3 RESULTS	
5.4 COST-EFFECTIVENESS	
5.4.1 Cost of the steerable needle	
6 DISCUSSION	
6.1 THE BIG PICTURE.	
6.2 CHALLENGES.	
6.3 RECOMMENDATIONS	
CONCLUSION	
BIBLIOGRAPHY	54
ABBREVIATIONS	64
APPENDIX A - LITERATURE REVIEW	
APPENDIX B - STEERING EXAMPLE	
APPENDIX C - THEORY	
APPENDIX D - EXPERT CONSULTATIONS	107
D.1 ELEKTA	107
D.2 REN MOERLAND	
D.3 UMCU	
D.4 EMC	
APPENDIX E - IDEA GENERATION	
APPENDIX F -EXPERIMENT RUN TABLE AND RESULTS	
F.1 SMALL GELATINE EXPERIMENT.	
F.2 LARGE GELATINE EXPERIMENT	
F.3 PHANTOM VALIDATION.	
F.4 PERFORMANCE EVALUATION EXPERIMENT	



1 Design guidelines

Abstract

Based on the literature review (Appendix A) and consultations with experts (Appendix D), the following design brief was formulated; 'Developing a supplementary steerable needle system enabling the surgeon to place a needle more accurately, combat PAI, and combat ureteral occlusion while not interfering in the general course of the needle implantation.' Requirements formulated to evaluate future concepts include the ability to steer 15mm over an insertion distance of 50mm, compatibility with commercially available high dose-rate brachytherapy sleeves and enabling the surgeon to place a needle with the same accuracy as or higher accuracy then available instruments.



Every design process starts with formulating requirements to ensure the quality of the outcome, which also enable verification of the final product. This chapter will present the requirements of a manually operated steerable needle for high dose rate brachytherapy of the prostate theory. These requirements are derived from the preceding literature review and additional literature in this chapter. Optimisation parameters are presented in the second section. These will be used to evaluate generated concepts later in this paper.

1.1. Conclusions from literature review

The literature review revealed several possible advantages a steerable needle (SN) could have in high doserate brachytherapy (HDR BT). The first advantage being the increased manoeuvrability, allowing a surgeon to avoid anatomical obstructions and sensitive tissues. This increased manoeuvrability could increase the group of patients eligible for the procedure, decrease the difficulty of the procedure for the surgeon's and reduce the complication rate in HDR BT. The second advantage would be an increase in needle positioning accuracy, decreasing the number of required needle implants, possibly reducing the complication rate. Two possible drawbacks of a SN in HDR BT would be the additional complexity of the system, increasing the difficulty of the procedure for the surgeon, and a possible increase in intervention costs.

The literature review presented research into robotic steerable needle systems. When looking at instruments commercially available, we see only manually operated steerable needles. Our aim is to develop an easily adoptable steerable needle. We have therefore chosen to develop a manually steerable needle.

The literature review revealed a number of requirements a hand-operated steerable needle should fulfil. Some examples of these requirements are listed below. The requirements found in the literature review form the basis of the requirements found in the Section 1.4.

1.2. Supplementary literature to formulate requirements

Formulating a comprehensive list of requirements called for additional research. This section will give an overview of this literature.

One question that needed answering is what the required amount of steering for a SN for HDR BT is. The amount of steering required hinges on the three issues the steerable needle is looking to combat: unwanted needle deflection, avoidance of sensitive tissues and overcoming anatomical obstacles. The maximal reported unwanted needle deflection encountered in the literate review was highest for asymmetrical tipped needles, with values ranging from 4.9mm (Jamaluddin et al., 2017) to 8mm (Sadjadi, Hashtrudi-Zaad, & Fichtinger, 2014). For symmetrical tipped needles this deflection seems significantly lower, Blumenfeld et al. (2007) reported a needle deflection of 0.6-1.1mm (for symmetrical needles). These numbers however, do not consider the fact that it regularly takes multiple attempts to get the needles within the range reported possibly increasing patient trauma. The displacements above were measured at an insertion depth of between 60 and 80mm. In a porcine phantom, Strassmann et al. (2011) found an average positioning accuracy of 2.7 ± 0.7 mm with a HDR BT needle.

The required steering capability to avoid sensitive tissues is harder to quantify. Determining trauma to which tissues is responsible for needle implant related toxicities remains a challenge. An example of sensitive tissue avoidance is using the penile bulb as an indication of nervous and vascular structures (Lee, Spratt, Liss, & McLaughlin, 2016) and planning needle paths to avoid the penile bulb. However, evidence of the correlation between penile bulb trauma and erectile dysfunction is far from conclusive. Without definitive evidence of what structures are most vulnerable to needle implant related trauma, it is difficult to formulate an optimal trajectory. Of all structures implicated in needle implant related toxicity, the penile bulb and corpora cavernosa (the crura), which can be seen in Figure 1, are the largest. These structures would requiring the most steering to be able to circumvent. Being able to steer around the penile bulb and corpora cavernosa likely ensures the needles ability to steer around any sensitive tissues in surrounding the prostate.

There are several papers on trajectory planning for steerable needle while avoiding sensitive tissues. The paper by Xu et al. (2009) presents such an approach to plan needle trajectories in the prostate to avoid



sensitive tissues. In this paper a trajectory around the penile bulb is planned. Unfortunately, it is difficult to extract quantitative information from this paper. The paper by Wallner et al. (2002) on penile bulb imaging gives us Figure 1. From this MR-image we can estimate the size of the penile bulb to be about 75% of the width and 60% of the height of the prostate in the coronal plane and 55% of the width of the prostate in the sagittal plane.

There is no way to determine the actual size of the prostate or penile bulb depicted in Figure 1. Since the figure is depicting a diseased prostate, we will assume its width in the coronal plane to be 46mm (Lei et al., 2011). This would be an average dimension of a deceased prostate. This would make the width of the penile bulb in the coronal plane approximately 35mm. To be able to steer around this penile bulb would require 17mm of steering either over 31mm or 81mm to the caudal and coronal apexes of the prostate respectively. The needle path to the caudal and coronal apex of the prostate are indicated by the short and long dashed line in Figure 1 respectively. This approach is highly inaccurate, unfortunately we were unable to find higher quality data on the dimensions of the penile bulb.

MR coronal

prostate urogenital diaphragm

MR sagittal

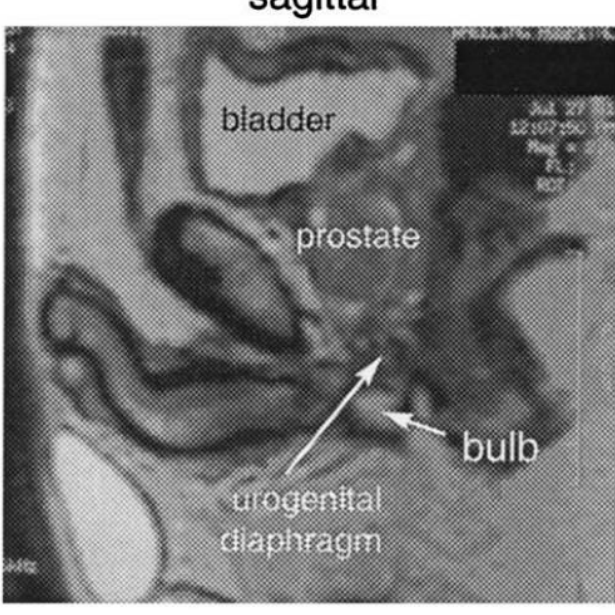


Figure 1 MR image of penile bulb in coronal (left) and sagittal (right) plane. Black dashed lines show the potential steerable needle path.

Pubic arch interference (PAI) is common in needle implantations in larger prostates. While the amount of PAI varies and can be up to 20mm (Bellon et al., 1999). PAI of more than 10mm is rare (Fukada et al., 2012). Using the prostate dimensions from the paper by Lei et al. (2011) this would mean a deflection of approximately 10mm over a distance of a little more than 47mm.



In HDR BT care is taken to avoid damage to the urethra. This means the deep section of the prostate, inferior to the prostatic urethra, is difficult to access. Figure 2 shows a schematic overview of the prostate. The black dotted line represents the path of a steerable needle to access the deep section of the prostate inferior to the urethra. The position, size, and orientation of the urethra with respect to the prostate varies between patients. To estimate the amount of steering required to access the deep section of the prostate, inferior to the urethra. We will assume a worst-case scenario. Namely, a urethra that runs from the superficial-inferior tip of the prostate to the deep-medial end of the prostate. This would mean the needle has to traverse approximately half the inferior-superior distance of the prostate over its insertion path.

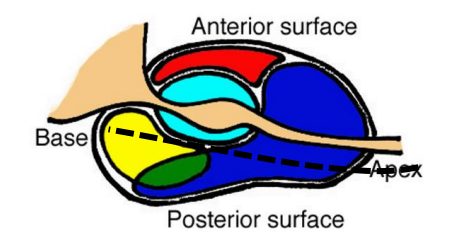


Figure 2 Prostate anatomy (Romero et al., 2012). Black dashed lines show the potential steerable needle path.

Using the prostate dimensions from the paper by Lei et al. (2011), this would mean a deflection of approximately 15mm over a distance of 47mm.

The maximum amount of steering required from the sources above comes to 15mm at a 47mm depth to avoid PAI and the urethra. To be able to steer around the penile bulb would require approximately 17mm at a 31mm depth. These values are rough approximations and will have to be revisited once more accurate dimensions become available.

Some requirements are derived from consultations with experts such as staff members of Elekta and medical staff from the UMCU and EMC. Information about these consultations and conclusions derived therefrom can be found in Appendix D – Expert consultations.

1.3. Design brief

Late toxicity from needle insertion in HDR BT is a highly controversial topic. Without definitive evidence of which tissues to avoided to reduce late toxicity, developing a steerable needle to avoid these tissues is futile. PAI and ureteral occlusion are well known difficulties in HDR needle implantation. We will therefore develop this needle to address these issues. This also means the minimum amount of steering we will require our SN to perform is 15mm over a 47mm insertion. This value is simply an approximation therefor going forward 15mm over a 50mm insertion will be used for ease of use. By using this 15mm over a 50mm insertion as an absolute minimum we ensure the needle is able to address PAI and urethral occlusion and possibly be valuable in possible future developments into sensitive tissue avoidance.

PAI, as well as ureteral occlusion is only relevant for a certain number of needles during the implantation. The majority of needles implanted are not affected by these issues. The needle developed in this paper should therefore be seen as an addition to the surgical toolkit, instead of a direct replacement of existing needles. This also means the developed system should be able to function harmoniously with existing templates and visualisation modalities.

The design brief of the steerable needle system will be: Developing a supplementary steerable needle system enabling the surgeon to place a needle more accurately, combat PAI, and combat ureteral occlusion while not interfering in the general course of the needle implantation.

1.4. Requirements

A useful steerable needle for HDR BT will have to fulfil several requirements. The next four sections sort these requirements into categories.

1.4.1. Functional requirements

- (R1) The system can steer a minimum of 15mm over 50mm of insertion: Among others this will mean the surgeon is able to circumvent most cases of PAI, and follow the curvature of the urethra. (Section 1.2)
- (R2) The system should allow the surgeon to implant a needle with at least as the same accuracy as systems currently in use: This should enable implantation with less tissue damage and possibly less required needles.



- (R3) The system can pierce tissue to reach a minimum depth of 90mm: From Podder et al. (2006) we know the insertion depth is generally around 80-90mm, this should be the minum depth the needle is able to penetrate.
- (R4) The system can steer in the sagittal and coronal plane: Steering in both the sagittal and coronal plane are required to be able to accurately place a needle in HDR BT.
- (R5) The system introduces a clean lumen trough which a radio source can be placed at a later stage in the procedure: A clean lumen is required for the afterloader to insert a radio source through (Appendix A, Section 3.1)
- (R6) The system enables the surgeon to steer in the sagittal and coronal plane simultaneously: steering in one plane at a time would likely mean needle retractions and increased tissue trauma.
- (R7) The system can be assembled and implanted without touching the tip-proximal half of the sleeve: The tip of the sleeve will come into contact with the patient, not handling this section of the sleeve should minimise the chance of contamination.

1.4.2. Usability requirements

- (R8) The system can be operable by a trained surgeon with little additional training: The more training required to operate the system the less likely adoption of the system is.
- (R9) To ease the adopting of the instrument the SN should be hand-operated. Either one or two handed: See Chapter 6 of the literate review (Appendix A).
- (R10) The system does not decrease the cost-effectiveness of HDR BT of the prostate: Decreasing the cost-effectiveness of the HDR BT procedure would make adoption of the steerable needle less likely.
- (R11) The system should not lengthen the procedure time of the HDR BT prostate needle implantation, approximately 30 to 45 minutes: Increasing procedure time in HDR BT will decrease cost-effectiveness and patient outcome. This would hinder adoption of the steerable needle.
- (R12) The system should not be less comfortable to use in a surgical setting then commercially available needle: If the system is uncomfortable to use it would put additional unwanted strain on the surgeon.
- (R13) The system can be retracted either both the stylet and sleeve, or only the stylet: During the procedure the surgeon should be able to retract either the stylet and sleeve to reposition the needle or only the stylet to attach the afterloader.

1.4.3. Technical requirements

- (R14) The system can be mass produced with existing manufacturing techniques: A steerable needle that requires exceedingly complicated manufacturing would increase the cost of the procedure.
- (R15) The system should not be thicker than the 15.5G systems currently in use: Larger diameters might result in increased tissue damage which we are trying to reduce. ("Prostate HDR Brachytherapy," 2019)
- (R16) A broken or damaged system should not injure the surgeon or patient: The system should be safe to use even when failing.
- (R17) The system should be able to withstand a minimum of 50 insertions if disposable and 500 if reusable: A implantation generally consists of approximately 15-20 insertions (Appendix A, Section 3.1), to allow for variation in procedures a minimum of 50 insertions when disposable is chosen. If reusable, to justify a cleaning and sterilisation procedure, the system should allow for a minimum of 500 insertions.
- (R18) The system should utilise an existing sleeve design: Developing a novel sleeve would result in additional cost and certification difficulties.

1.4.4. Interaction requirements

- (R19) The system is clearly visible on TRUS and CT imaging: Most used visualisation modalities should be compatible with the developed steerable needle to aid in adoption.
- (R20) The system is compatible with existing templates used in HDR BT needle implantation:

 Developing a novel sleeve would increase the cost and result in additional certification difficulties.
- (R21) The system should either be disposable or easily sterilisable: A difficult to sterilise system would result in increased operating cost and possible damage to the system during cleaning and sterilisation.



1.5. Optimisation parameters

Besides requirements, there are several parameters that should be optimised to develop a SN for HDR BT. The following sections will sort these parameters into categories.

1.5.1. Functional optimisation parameters

- (P1) The system should allow the surgeon to place the needle as accurately as possible: A more accurate needle placement should allow for less needle repositioning and possibly less required needles for an satisfactory implant (Appendix A Section 6.1.3).
- (P2) The system should allow the surgeon to avoid sensitive tissues as much as possible: Steering around sensitive tissue could allow the surgeon to improve procedure outcome (Appendix A Section 6.1.2).
- (P3) The system should be able to steer more than 15mm at a 50mm depth: The more steering the surgeon has at his disposal the more applications the needle would be suitable for.
- (P4) The system can be used for HDR BT procedures besides HDR BT of the prostate: Many high dose-rate procedures use the same template and sleeves. This would allow the developed system to be used for multiple procedures.
- (P5) The system should require as little additional equipment as possible: Additional equipment complicates the procedure and could reduce the cost-effectiveness of the procedure.

1.5.2. Usability optimisation parameters

- (P6) The system should increase the cost-effectiveness of HDR BT as much as possible: A more cost-effective procedure has a higher chance of being adopting assuming equal procedure outcome.
- (P7) The system should facilitate the surgeon to decrease the procedure time of the HDR BT needle implantation: Optimally using a steerable needle would reduce the time needed to position the needle satisfactory (Appendix A Section 6.1.4)
- (P8) The system should require as little training as possible to operate: Excessive required training to operate the system reduces cost-effectiveness and could decrease the adoption rate.
- (P9) The system should have as few parts as possible: Complexity could increase cost, increase user error, and decrease ease of certification.
- (P10) Assembly of the system in the OR should require as few steps as possible: Complicated assembly could result in assembly error and increased procedure time.
- (P11) The system should cost as little as possible per procedure: A high upfront cost regardless of costeffectiveness could present a hurdle to adoption of the system.
- (P12) The system should be more comfortable to use then current systems: A system that is uncomfortable to use might hinder adoption by surgeons.

1.5.3. Technical optimisation parameters

(P13) The diameter of the system should be as small as possible: A smaller needle diameter should reduce tissue trauma due to needle implantation. (Appendix A Section 4.5)

1.5.4. Interaction optimisation parameters

- (P14) The system should influence the general needle implantation procedure as little as possible: Requiring as little modification to the existing HDR BT procedure as possible should help in the adoption of the system.
- (P15) The system should be more visible on TRUS then current systems: Better visibility should allow the surgeon to perform more accurate manoeuvres.
- (P16) The system should be MRI compatible: Research is being done into using MRI to visualise HDR BT needle implantations. Optimally, the developed system should facilitate this development.



Design and concept generation

Abstract

In a compliant mechanism, forces are transmitted through the elastic properties of the material itself instead of through traditional joints. An existing prototype of the steerable needle is a nitinol rod with two slots machined through it, effectively splitting the rod in four while leaving both ends joined. By bending the end of the needle, the other end deflects in the opposite direction. While superelastic materials such as nitinol are suited to this application, a needle from a stiffer material would be desirable to ensure buckling does not occur during implantation. Theory shows the material choice only influences the maximum steering angle and not the relation between input and output angle. By designing five concepts for the steerable needle we increased the chance of finding a satisfactory design for this instrument.



This chapter will describe the process of designing a SN for HDR BT with the requirements and optimization parameters set in Chapter 1.

There are several HDR BT stylet and sleeve manufacturers. A popular design for an HDR BT needle can be seen in Figure 3. The stylet consist of a blunt stainless-steel stylet with a handle. The polymer sleeve is then slid over the stylet. The stylet and sleeve are inserted into the prostate after which the stylet is removed leaving behind the sleeve. This sleeve is later used to guide the radioisotope with an afterloader.

We will refer to the stainless-steel core as the 'stylet' and the polymer housing as the 'sleeve'. The sharp, conical side of the needle will be called



Figure 3 Mick FlexiGuide® needles 15.5G, 20cm and 25cm (retrieved from https://www.micknuclear.com)

the distal side and the side at which the surgeon manipulates the needle will be called the proximal side.

2.1. Current prototype

A prototype of a steerable stylet was presented to me at the beginning this thesis. This concept served as a starting point for the design process. The concept consists of a nitinol stylet with to slots machined through it, housed in a polymer sleeve. By manipulating the proximal end, an opposing deflection can be induced in the distal end. In a 10wt.% gelatine phantom, this needle was able to steer approximately 23mm over 85mm.

2.1.1. The compliant mechanism

Compliant mechanisms are a flexible, jointless mechanisms. Conventional mechanisms rely on pins and hinges to allow the transfer of forces, in a compliant mechanism these forces are transmitted through the elastic properties of the material itself. Figure 4 shows a pair of forceps based on a compliant mechanism. By using the elasticity of the material to replace hinges and more traditional connections, a reduction in part count, decrease in production cost or increase in performance can be achieved.

A compliant mechanism can also be used to create a steerable needle. Figure 5 shows the working Figure 4 Compliant forceps ("Compliant mechanisms principle behind a compliant steerable stylet. The explained," 2019)



ends of the thin midsection of the stylet act as hinges which allow the transfer of force. By manipulating the right side of the stylet in Figure 5, the midsections move relative to each other which in turn moves the left side of the stylet in the opposite direction.

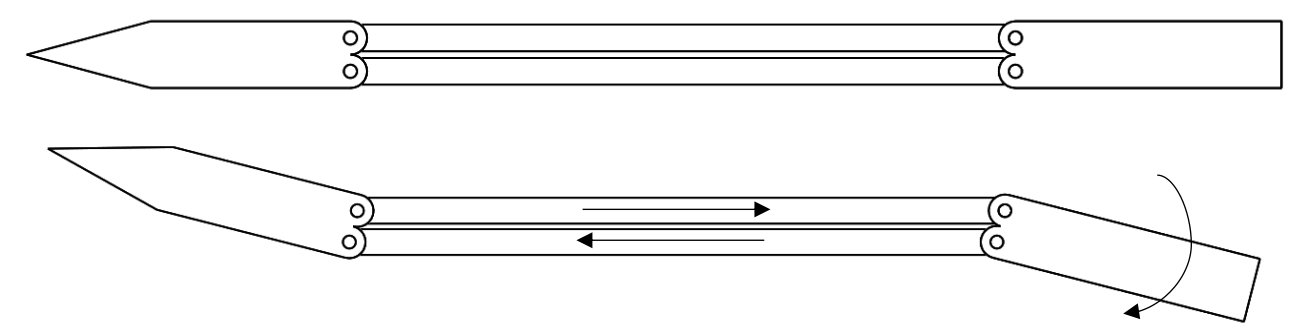


Figure 5 Compliant mechanism stylet concept. Top shows straight needle, bottom shows needle with moment applied to proximal end. Black arrows indicate relative motion of needle sections.



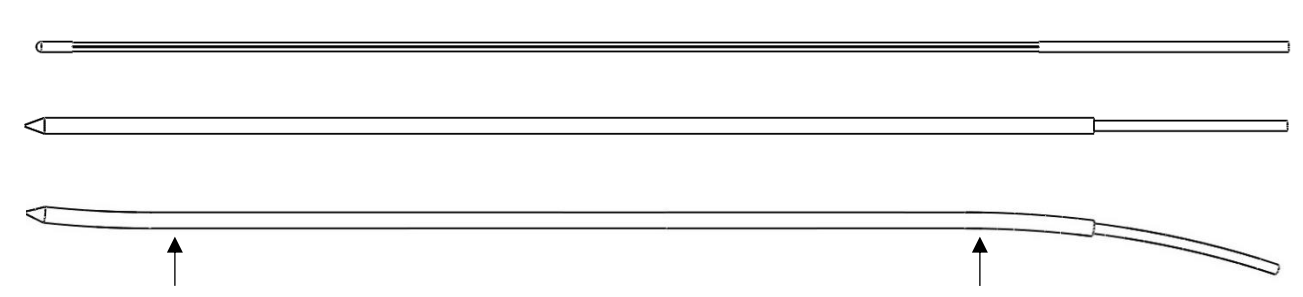


Figure 6 Steerable needle concept (Top: stylet, Middle: stylet with sleeve, Bottom: stylet and sleeve with small moment applied to proximal (right) section of the needle)

On this principle a solid nitinol stylet with electrical discharge machined (EDM) slots through its side and top was produced. In Figure 6 (Top) the slot through the side of the stylet is visible. The stylet is then placed in a sleeve (Figure 6 Middle), manipulating one end of the needle, the other end will deform in the opposite direction. (Figure 6 Bottom). When the proximal end of the needle is bent downward (right side in Figure 6) the top member moves to the right with respect to the bottom member. As this member is connected to the distal end (the tip of the needle), it forces the needle tip upward. The belief is that this simple compliant mechanism can be utilised to create an inexpensive and easy to operate steerable needle.

To be able to achieve this steering, a static equilibrium must be reached. This entails that a minimum of two points along the needle should be constrained. If no points along the needle length are constrained the needle would simply translate upon manipulation. If only one point is constrained, the needle would simply rotate. An example of these two points are the arrows in Figure 6.

To be able to operate this needle accurately and effortlessly, a manageable user interface is required. This mechanism should be attached to the needle and enable the surgeon to steer and control the needle precisely. The goal of this thesis will be to develop a cost-effective and hand-operated steerable needle implantation system for high-dose rate brachytherapy of the prostate based on the compliant steering concept presented above.



Figure 7 First steerable needle prototype (Top: stylet and sleeve separate, Bottom: stylet in sleeve)

This section presents the methods and results of the tests performed with the first prototype. The only purpose of these results is to determine an order of magnitude of possible steering and gain a better understanding of the behaviour of this needle. To establish a baseline for the performance of this concept, a first prototype was manufactured, which can be seen in Figure 7. To evoke the bending effect, a minimum of two points along the shaft of the sleeve need to be fixated. This behaviour could be enlisted by sliding a ridged tube over the sleeve providing multiple point of support along the shaft. However, when inserting this ridged tube through a template used in HDR BT, it will impede any steering of the needle. If the shaft is not flexible, the needle will not be able to follow the path the needle tip cuts. A more favourable alternative is to use a template with two support points to elicit the desired bending. Figure 8 shows the template used to estimate the deflection of the existing concept. To estimate the performance of this first concept it is important to determine the relation between the deflection of the distal and proximal end. Unfortunately, due to the slots in the design, the needle does not bend in a circular fashion. This makes it difficult to estimate the exact

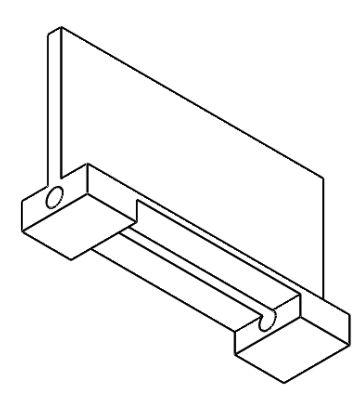


Figure 8 Needle fixation template, used to fixate section of the steerable needle to enable steering.

angle of deflection achieved. For this test the angle used is the angle between a line drawn through the tip of the needle and the base. These lines can be seen as dashed lines in Figure 9. The left image in Figure 9



shows the stylet and sleeve in the neutral position. The middle image in Figure 9 shows a deflection of 20° in the proximal end resulting in a deflection of approximately 6,5° in the distal end. The middle image in Figure 9, shows a deflection of 40° in the proximal end resulting in a deflection of approximately 11° in the distal end. At a deflection of 70° on the proximal end, the distal end deflects approximately 20°. Greater deflections might be possible, to aid the lifespan of this prototype we did not attempt larger deflections at that point in time.

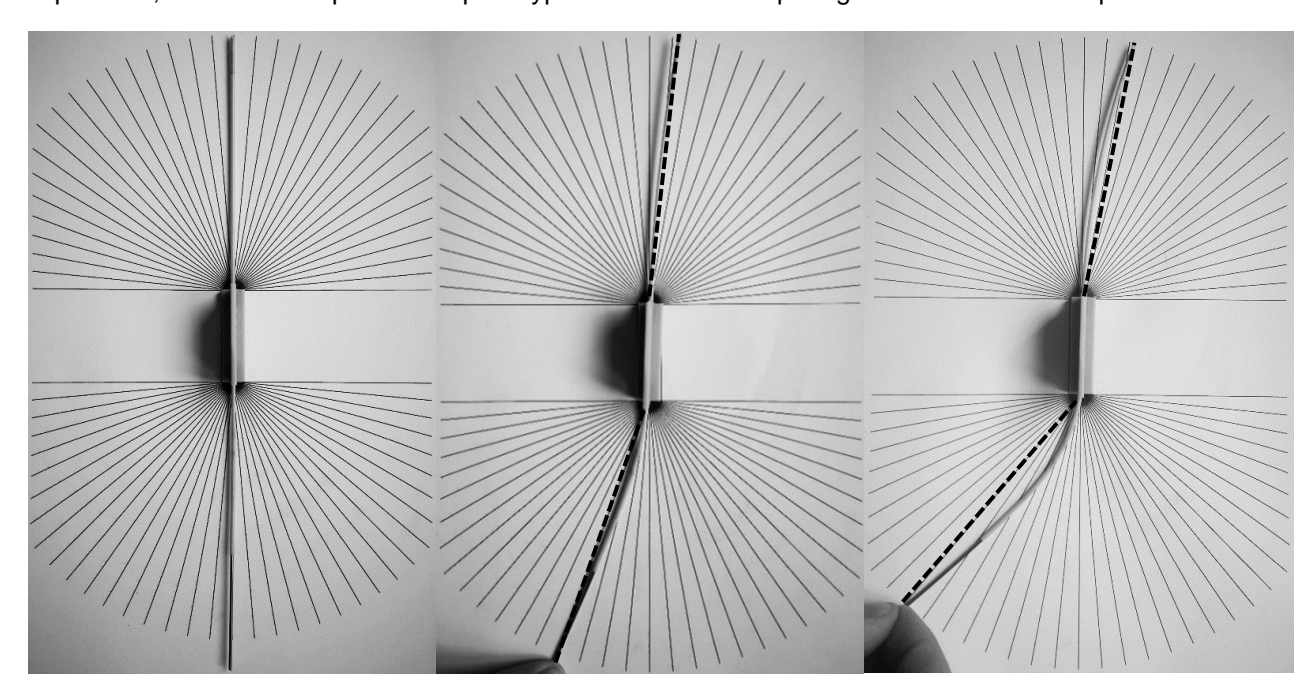


Figure 9 Deflection test first prototype (Left: no moment applied, Middle: 20° proximal angle, Right: 40° proximal angle.

2.1.3. Steering in gelatine

Swaney, Burgner, Gilbert, and Webster (2013) use a 10 wt.% gelatine and pork loin phantom for their needle steering experiments. By using a 10 wt.% gelatine phantom, we hope to be able to extrapolate some of the needle's behaviour observed in gelatine to pork loin. The insertion depth is generally between 70 and 80mm (Moreira et al., 2018; Sadjadi et al., 2014). 85mm was chosen to show the prototypes capabilities even in larger insertion depths. Steering in vivo will likely differ significantly to these experiments due to inhomogeneity and tissue movement. This experiment therefore only served to give an indication of steering capabilities and clarify the working of the steerable needle.

To give the needle a reproducible bend we used the template shown in Figure 10. This template can be set to 60°, -40°, -20°, 0°, 20°, 40° and 60° in the proximal part of the needle. For every configuration two needle insertions were performed. Giving four needle insertion per angle. An image was taken after each insertion. An example of such an image can be seen in Appendix B. The run table can be found in Appendix F1. The pattern on the bottom of the container and photoshop were used to determine the needle tip displacements. Displacement is defined as the horizontal distance between the tip of the sleeve and insertion point. The results of this experiment can be seen in Table 1.

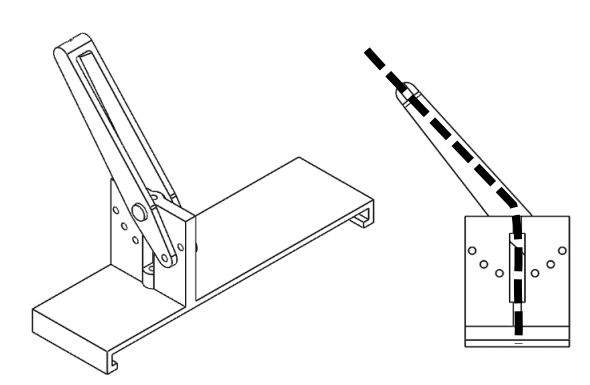


Figure 10 Gelatine needle template, needle path indicated with black dashed line.



Proximal angle (n = 4)	Range of displacement at 85mm (mm)	Mean displacement at 85mm (mm)	Mean angle at 85mm
0°	0.55 - 3.8	2.1	0.37°
20°	6.0 - 9.9	6.9	6.6°
40°	9.4 – 19.4	14	9.1°
60°	18.7 – 37.1	23	15°

Table 1 10% Gelatine steering test

Table 1 shows a reasonable amount of steering. More steering is achievable with larger proximal angles. It seems due to the flexibility of this needle that inserting the needle without actively steering, results in deflections larger than a solid needle. Controlling the steering is a concern in this prototype. The needle tends to buckle during insertion making insertion more difficult. A more robust control mechanism will be necessary to enable the surgeon to effectively steer a needle. Another concern is whether the steering capability enables more accurate needle placement in practice.

2.2. Theory

This section will introduce some theory about bending and buckling that should prove useful throughout the design process.

Inducing a curvature in the stylet, shortens one half of the stylet relatively to the other, according to Equation 1. With ΔS being the difference in length relative to one another, r being the radius of the curvature, R being the radius of the stylet (and the distance between the centres of both halves of the stylet) and θ being the angle of the arc. Equation 1 shows that for a given stylet radius (r), the relative difference in length of the stylet parts to each other is determined solely by the angle of the arc (θ).

(1)
$$\Delta S = \left(r + \frac{R}{2}\right) * \theta - \left(r - \frac{R}{2}\right) * \theta = R\theta$$

With R being constant along the length of the stylet this means, not considering strain in the material, the deflection of the stylet tip would adhere to Equation 2. With S1 and S2 being the relative change in length between the stylet parts in the bottom and top section respectively, and θ 1 and θ 2 being the arch angles of the proximal and distal section of the stylet respectively.

$$R = \frac{\Delta S1}{\theta 1} = \frac{\Delta S2}{\theta 2}$$

Without strain Δ S1 and Δ S2 would be equal, resulting in equation 3. Meaning a deflection of θ in the lower section of the stylet would result in a deflection of θ in the upper part of the stylet, regardless of the dimensions of the stylet.

$$\theta 1 = \theta 2$$

In practice $\theta 2$ is generally lower than $\theta 1$ due to the strain and other losses in the material. The strain is the result of the stress induced by the force applied at the lower section of the stylet. Adjusting equation 2 to account for strain results in equation 4.

(4)
$$R = \frac{\Delta S}{\theta 1} = \frac{\Delta S + \Delta S strain}{\theta 2}$$

Simplifying the stylet to a beam and assuming no friction, a negligible slot thickness and small deflections (below 5 degrees), we were able to establish a formula for the relation between the deflection of θ 2 and θ 1.



The entire derivation can be found in Appendix C. Equation 5 shows the formula describing the relation between θ 1 and θ 2. Notable is the fact that material characteristics, and stylet radius do not seem to play a factor in its bending behaviour. Figure 11 shows the stylet in a bent position with the relevant dimensions.

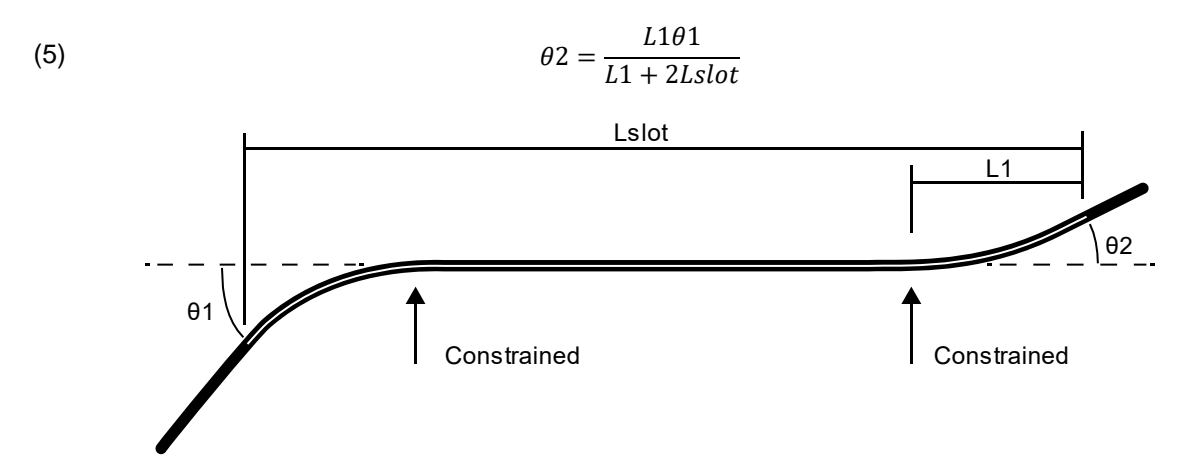


Figure 11 Bending stylet free body diagram with moment applied at proximal end (left)

From this equation we can deduce that, to maximise $\theta 2$ for any given $\theta 1$, L1 should be maximised and Lslot + L1 should be minimised. One thing this formula does not account for is yield strength. When moving L1 closed to Lslot, the deflection of the stylet might increase, but so will the resistance of the proximate part of the stylet to bending. This will result in higher localised stresses and eventually the breaking of the stylet.

Noticeable from equation 5 is the fact that neither material or stylet diameter seem to play a role in its bending behaviour. This lead us to conclude the only thing influencing the maximum deflection of the stylet is the amount of elastic deformation the material can undergo. Which would be indicated by its yield strength divided by its Young's modulus. Another conclusion we can draw from equation 5 is the fact that for a constant L1 and Lslot, the relation between $\theta 1$ and $\theta 2$ is linear. This could be beneficial to the surgeon as it makes the behaviour of the tip of the needle predictable. If the needles behaviour remains (pseudo) linear in vivo remains to be seen.

Simulation of the stylet and its sleeve in Ansys discovery AIM, corresponds with equation 5. The current prototype was modelled and its dimensions changed one by one from the baseline. A 20mm deflection of the proximal part of the needle resulted in tip deflection of 0.077 rad in the baseline model. Table 2 shows the Ansys simulation results.

Manipulation	Proximal deflection(mm)	Distal deflection (rad) in Ansys	Effect in formula	
Baseline	20mm	0.077	No effect	
Increased Young's modulus	20mm	0.077	No effect	
Decreased radius	20mm	0.072	No effect	
Decreased Lslot	20mm	0.11	Increased tip deflection	
Increased L1	20mm	0.11	Increased tip deflection	

Table 2 Ansys simulation results, comparing changes in distal deflections from Ansys with the predicted effect of the manipulation in the formula shows the formula to be an effective predictor of the deflection in the steerable needle.

The simulation shows similar behaviour to what the equation predicts in most cases. The equation predicts decreasing the radius to have no effect on the deflection slope, the simulation however shows a little decrease. Equation 5 gives us some insight into the behaviour of the needle. However, this equation represents a highly oversimplified situation. Friction, non-circular bending, and deflections larger than 5° do play a significant role in the needle's deflection. Therefore, this equation will serve as a tool to better understand the needles behaviour, but will not be used to determine any actual deflections.



2.2.2. Yielding

Equation 6 describes the axial stress as a result of force F. From Podder et al. (2006) we know the maximum axial force in a HDR BT implantation is approximately 15N in a 17G diamond shape tipped needle. With a typical 17G needle this results in a stress of approximately 3 MPa. With a minimum yield strength of 100 MPa, there is little to no chance the nitinol needle or any other metal needle would yield during insertion due to axial load.

$$\sigma = \frac{F}{A}$$

The stress induced by the bending is more likely to present a significant limitation. Equation 7 shows the formula for bending induced normal stress in a solid needle. The distance from the neutral line is indicated by y. When y equals the stylet radius, the stress will be largest. Because we are interested in the maximum stress, we can substitute y for r.

(7)
$$\sigma = \frac{My}{I}$$

Substituting the moment of inertia equation for a round cross section into equation 7 results in equation 8.

(8)
$$\sigma = \frac{4M}{\pi R^3}$$

A 1N load at the tip of the stylet perpendicular to the surface would result in a maximum stress of approximately 600MPa. Additionally, due to the slot in the stylet, stress concentrations are likely present at the start and the end of the slots. It is likely yielding will be the limiting factor in the maximal deflection the needle can achieve. The stylet radius and yield strength of the material will determine the maximal deflection achievable.

2.2.3. Buckling

In long slender tools such as needles, buckling is of considerable concern. Equation 8 describes the critical load for Euler bucking. With E being the Youngs modulus, I the moment of inertia, K the effective-length factor and L the unsupported length (Hibbeler & Fan, 2011). Brazier buckling will likely not be relevant to this design as the stylet is not hollow.

$$Pcr = \frac{\pi^2 EI}{(KL)^2}$$

With an axial load of 15N, a solid 17G nitinol needle has a maximum unsupported length of approximately 6 cm (K=1). This makes buckling a significant problem for this instrument. Substituting the moment of inertia equation for a round cross section into equation 8 results in equation 9.

(10)
$$Pcr = \frac{\pi^2 E R^4}{4(KL)^2}$$

From equation 8 we can see increasing the radius of the needle would dramatically decrease chances of buckling. However, increasing the size of the needle will likely increase implant related trauma. This leaves us with the K-factor, which could be increased by a stiffer connection between the needle and the hand of the surgeon (for example by introducing a handle) and the Young's modulus.

2.3. Material selection

The existing stylet prototype is fabricated from a 1.48mm superelastic nickel titanium wire (NiTi). This superelasticity is caused by the phase transformation between the austenitic and martensitic phases in the metal. This means strains of up to 8% can be fully recovered (Bhattacharya & Kohn, 1996).



2.3.1. General materials

From Section 2.1 we learned a number of things:

- The relation of deflection between the proximal and distal ends of the stylet is not influenced by the material;
- A material with a higher Young's modulus will require more force to achieve an equal bend compared to a material with a lower Young's modulus;
- The maximal achievable deflection is determined by the yield strength divided by the Young's modulus. Also known as the elastic strain;
- To combat buckling a high Young's modulus is favourable.

CES (Cambridge Eengineering Selector) was used to select a suitable material for the stylet. From the requirments above we can conclude we need a material with a high elastic strain and high Young's modulus. Composit materials were excluded as it is unlikely the stylet could be produced from composits. Materials with Young's moduli below 10GPa were also excluded as they would be exceedingly prone to buckling. This resulted in Figure 12. A material to the right of the graph indicates a material which allows high elastic strains, while a material towards the top of the graph represents a material with a high Young's modulus. Some materials with favorable characteristics are indicated with names. According to this graph, silicon carbide and carbon fiber allow most elastic strain. However these material cannot be made into the required geometry.

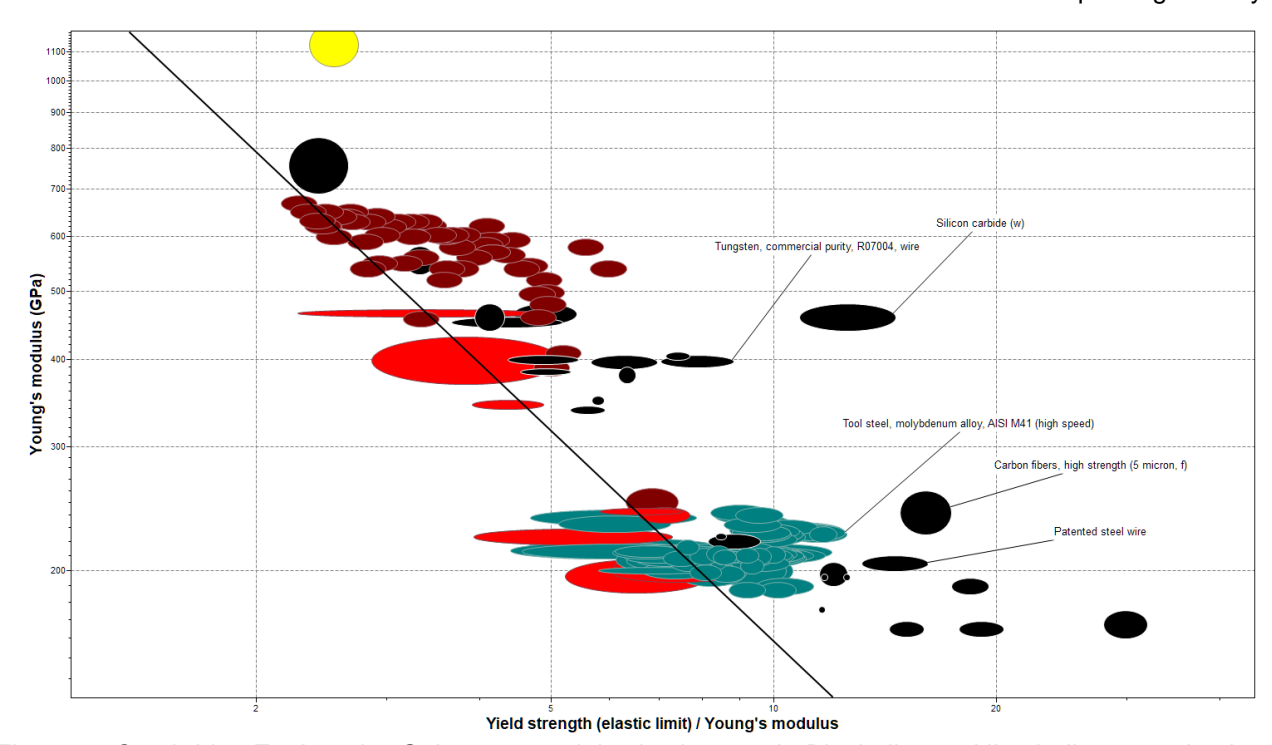


Figure 12 Cambridge Engineering Selector material selection graph. Black diagonal line indicates optimal material behaviour. Materials with a larger perpendicular distance to the right of the line present more favourable characteristics.

Materials that can be manufactured in the appropriate geometry are molybdenum alloy tool steel, tungsten and patented steel wire. These materials present reasonable elastic stain combined with a high Young's modulus. Unfortunately, CES does not take into account super-elastic behaviour. Even if it did, our approach of calculating the maximum elastic strain by dividing the yield strength by the Young's modulus would be innapropriate.

From Figure 12 we can conclude that, excluding super elastic materials, patented steel wire, molybdenum alloy tool steel (especially AISI M4x), and tungsten present favorable characteristics.



2.3.2. Superelastic materials

We have identified possible candidates for the stylet material from the non-superelastic material pool. Now we turn our attention to the super elastic materials.

A superelastic material has the unusual characteris that extremely large strains can be recovered. This is due to a reversable stress-induced phase transformation. This effect closely ties in with the shape memory effect. When a superelastic (or shape memory) material is stressed sufficiently, a phase transformation occurs

allowing the rearangement of the cristal lattice. Once the stress is removed, the deformation persists until the material is brought to an activation temperature, after which the cristal lattice transforms back to the original arrangement and the strain is fully or partially recovered. In the case of a superelastic material, the activation temperature is lower then the amient temperature and the transformation to the original lattice phase is near instantaneous giving the illusion of superelasticity.

Figure 13 show a stress-strain diagram for a superelastic NiTi alloy. When the sample is loaded, the forward transformation occurs, transforming the material from it austenitic to its martensitic phase. When unloaded, the reverse occurs.

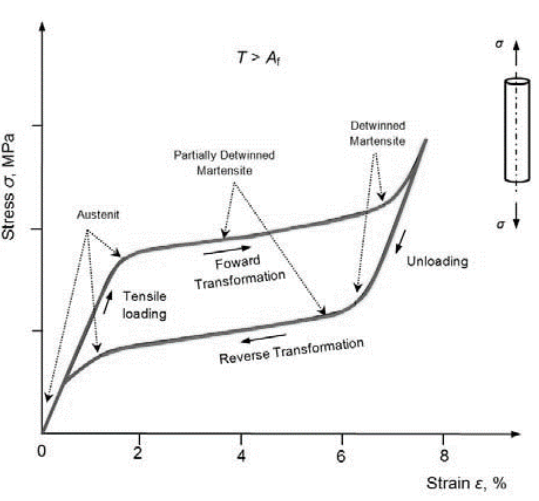


Figure 13 Superelasticity of NiTi alloy (Rebeka & Ferčec, 2013). Notable is the hysteresis and plateau.

Shape memory alloy	Maximum elastic strain (%)	Young's modulus (GPa)	Availability of wires and/or rods	Source
Ni-Nb-X	±4	20-30	Very Limited	Fukui, Inamura, Hosoda, Wakashima, and Miyazaki (2004)
Ni-Ti	8	28-83	Good	(Huang, 2002)
Ni-Ti-Cu	-	30-90	Good	(Huang, 2002; Jayachandran et al., 2019)
Ni-Mn-Ga	±5	±10-20	Very Limited	Hamilton, Dilibal, Sehitoglu, and Maier (2011)
Ti-Nb	±4	60	Limited	(Li et al., 2012)
Fe-Mn-Si	2.5-4.5	170	Very Limited	Yamauchi, Ohkata, Tsuchiya, and Miyazaki (2011)
Cu-Zn-Al	4-6	70-100	Fair	(Design of shape memory alloy (SMA) actuators, 2015)
Cu-Zn-Ni	2	80	Very Limited	Duerig, Melton, Stöckel, and Wayman (1990)
Cu-Al-Ta	2.5	±6	Very Limited	(Wang, Su, Yang, Shi, & Liu, 2014)
Cu-Al-Ni	5-6	80-100	Fair	(Design of shape memory alloy (SMA) actuators, 2015)
Co-Ni-Al	6	±60-100	Very Limited	(Dilibal, Sehitoglu, Hamilton, Maier, & Chumlyakov, 2011)

Table 3 Properties of shape memory alloys



The number of canditates here is significantly smaller, Table 3 gives an small overview of some materials that can have superelastic properties. Of the materials in Table 3, Ni-Ti and Ni-Ti-Cu are readily available. Cu-Zn-Al and Cu-Al-Ni are available on order.

The are to our knowledge no superelastic materials with Young's moduli as high as the varieties of steel found in the preceding section. Of the superelastic materials, Co-Ni-Al or Cu-Al-Ni would be the best choice for the stylet. They have excellent maximum elastic strain combined with a relatively high Young's modulus to combat buckling. While Fe-Mn-Si on paper also present a viable candidate, obtaining the actual material would prove exceedingly difficult.

2.3.3. Material choice

We have identified several materials suitable for this application. The amount of strain required to enable the steering determines the final material choice. AISI M42 tool steel or patented wire would be an excellent choice for the stylet if the amount of required deflection is limited. AISI M42 tool steel and patented steel wire are significantly cheaper and easier to obtain then any superelastic material will be. Secondly the high stiffness will reduce the deflection effect of tissue interactions as the needle itself will be stiffer. A possible downside of using a very hard steel could be its low toughness. Fabrication defects could result in brittle failure.

DELISSING

Figure 14 shows an Ansys Aim simulation of a M42 tool steel needle with a 0.3 N/m moment applied to the end. This resulted in a tip displacement of approximately 24mm.

Figure 14 Ansys simulation M42 tool steel steerable needle with moment applied to proximal end (right)

The maximum equivalent elastic strain this simulation produced was approximately 1%. AISI M4x tool steel and patented steel wire should be able to accommodate 1% elastic strain. Larger deflections require superelastic materials such as Co-Ni-Al or Cu-Al-Ni.

2.4. Concepts

After generating a large number of partial solutions, I generated a number of concepts for a compliant steerable needle. This section will present these concepts. The idea generation process can be found in Appendix E.

2.4.1. Optimised current prototype

The first concept is an optimised version of the current design. This SN is optimised according to the theory in Section 2.2. The length of the slot is minimised while the slot continues further down the tip of the stylet (increasing L1). Two prototypes will be manufactured, one from a high strength steel and the other from a superelastic material according to Section 2.3. The diameter of the stylet will be 17.5G to enable the use of standard sleeves. To enable the needle to be held, steered, and withdrawn easily, a small collet will be fitted. Figure 15 shows the concept consisting of a stylet, a sleeve, and a collet (top). Figure 15 (bottom) shows only

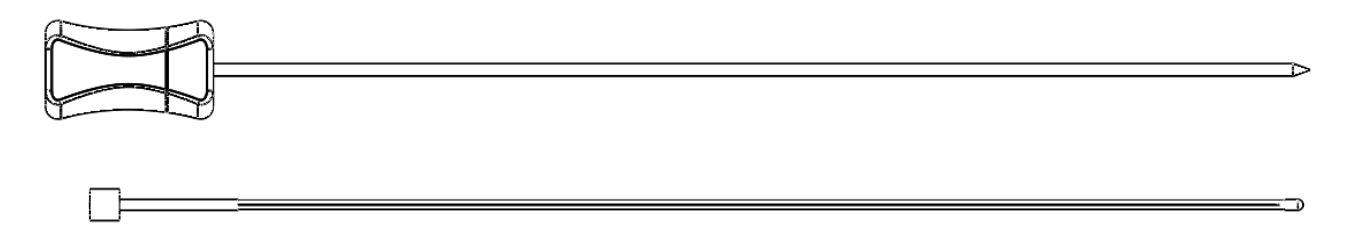


Figure 15 Optimised needle concept. Top shows assembled steerable needle, Bottom shows the stylet only



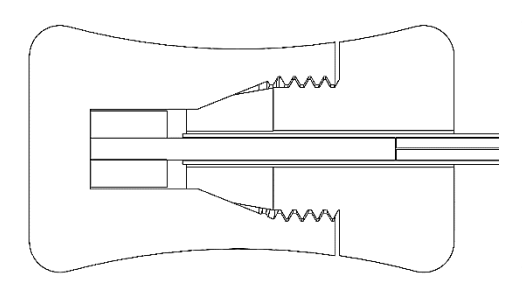


Figure 16 Collet of optimised current concept

the stylet. On the proximal side (left), the stylet has a crimped on collar that indexes in the collet to enable the stylet to be easily retracted from the sleeve.

Figure 16 shows the screw on collet. The collet consists of two parts, the right side is slid over the sleeve after which the left side is screwed onto it. When screwed tight, the collet grips the sleeve such that any force applied during the procedure is transferred to the sleeve. After insertion, the collet can be loosened slightly, releasing the sleeve. The collet and the stylet can then easily be retracted from the sleeve. The collet also acts as a handle which can be manipulated during the procedure making the manipulation more comfortable and controllable.

The stylet in this concept will likely be diffucult to sterilise between procedure and will therefore have to be diposable. The collet should be easier to sterilise. However, the collet can cheaply be mass produced by injection molding and could therefore also be disposable. The cost of sterilisation and related risk likely outweight the costs of the parts.

The simplicity of this concept and therefore it's presumable low cost, are very attractive qualities. There are however a few issues this concept could have. To elicit a sufficient curvature in the tip, the needle has to be bent a reasonable amount. This could interfere with allready placed needles. Secondly, even with the change in material, the needle could be insufficiently stiff, resulting in buckling.

2.4.2. Optimised current prototype with steering mechanism

This concept consists of the same stylet and sleeve as the previous prototype. Instead of the collet, a steering mechanism is attached to the end. The purpose of the steering mechanism is to decrease the interference with previously placed needles by decreasing the amount of required deflection.



Figure 17 Steering mechanism concept

According to Section 2.2 the amount of deflection the tip experiences is dependent on the angle $(\theta 1)$ and not the radius of curvature. This means bending a short section of the proximal part of needle should result in an equal deflection as bending a larger section. By minimising the size of the bent section, we can decrease the amount of interference with surrounding equipment. An added benefit of a dedicated steering mechanism is the ability to limit the maximum bending of the needle, ensuring the needle is not damaged.

Figure 17 shows the concept of the steering mechanism. By manipulating the joystick on the left, the rest of the needle deflects in the opposite direction. A collet similar to the first concept fixates the sleeve during insertion. After insertion, the collet can be loosened after which the whole system with the stylet can be withdrawn leaving the sleeve behind.



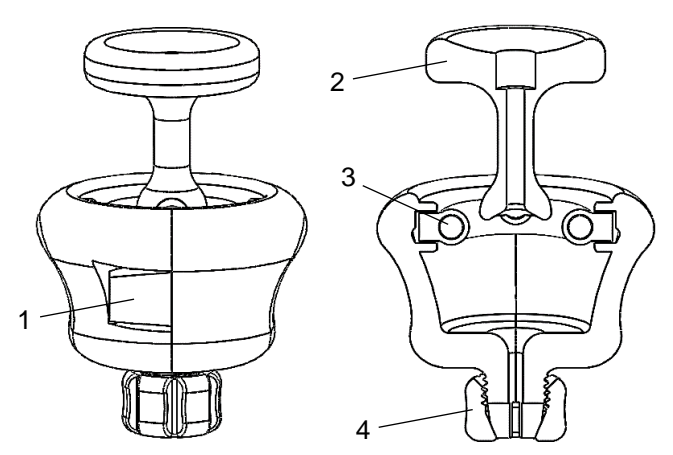


Figure 18 Steering mechanism in detail. Left shows an overview, right shows an section view. (1: snap finger, 2: thumb stick, 3: hinge, 4: collet)

Figure 18 Shows the mechanism in detail. The concept lacks fasteners and instead assembles with two snap fits (1). The joystick (2) is thumb actuated and transfers the input to the needle. Two hinges ensure the joystick can be moved in both planes, but is unable to rotate due to the orientation of the hinges (3). A collet (4) tightens around the sleeve during insertion and can be loosened to release the sleeve.

This concept should give the surgeon more control over the needle in addition to allowing him to operate in tighter spaces. The main drawback of this concept is the added complexity and additional components. Secondly, bending the needle over a shorter section increases stress in this section. This could decrease the maximum bending angle before damaging the stylet.

2.4.3. Wire needle

The current prototype is made by EDM two slots trough a solid wire. To simplify the production, four thin wires could be soldered together at each end instead (Figure 19). Regarding dimensions and material this stylet concept will be identical to the stylet in the first two concepts. The total length is dictated by the sleeve and the materials can be either AISI M42 tool steel/patented steel wire or Co-Ni-Al/Cu-Al-Ni. While there are many similarities between this and the first concept, there are two possible advantages this stylet could have. Firstly, the soldering for four sections of wire could be significantly easier and cheaper than the EDM process. Secondly, stress localisations in the EDM stylet and minute deviations in the production process could have significant influence on its durability and performance. The simplified production process and reduced chance of stress concentrations due to the production process could make for a SN that is more durable and easier to produce.



Figure 19 Soldered wire concept

2.4.4. Expanded wire needle

One of the main requirements of this SN it that is steers sufficiently. Unfortunately, according to the theory, there are not a lot of parameters that we can manipulate to increase the steering potential. With the current stylet much of the geometry is determined by the production process. However, the wire needle concept gives the ability to separate the sections of the stylet.

In equation 2 (Section 2.2.1) we assumed the stylet diameter (R) to be constant, but what if it was not? If the stylet diameter is larger in the controlled section then in stylet tip, ignoring strain, any deflection would be magnified according to equation 11. While strain will reduce the magnifying effect, a larger stylet radius in the controlled section will always result in increased tip deflection.

$$\theta 2 = \frac{R1}{R2}\theta 1$$

Figure 20 shows the concept. The stylet is largely the same as the previous concept. The stylet also consists of four wires that are partially soldered together. However instead of also soldering the proximal end (left side in Figure 20) together, the wires (4) are routed through a solid guide (3), then a flexible spacer (2) and are then fixated with set screws in a solid block (1). This means effectively that the radius of the stylet, in the section



that is bent by the controller, has a significantly larger radius then the rest of the stylet. This should increase the steering potential. To steer the needle, one holds the solid guide (3) with one hand and with the other hand bends the flexible section (2). To fixate the sleeve to the assembly, a collet is fitted (5) which can be loosened after needle placement and allows the assembly to be withdrawn leaving behind the sleeve.

This concept has the potential to steer more than the previous concepts, without interfering with surrounding equipment. However, the complexity of the necessary parts and their accompanying cost makes that at minimum the control mechanism should be reusable and therefore sterilisable.

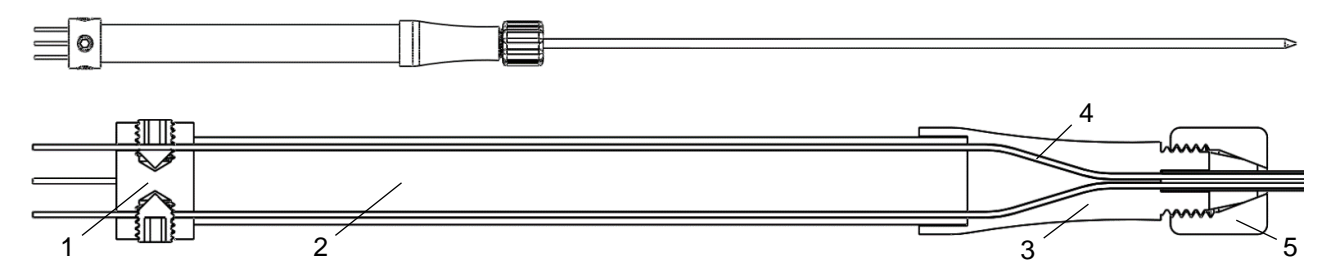


Figure 20 Expanded wire concept. Top shows an overview, bottom shows an section view.(1: block with set screws, 2: flexible spacer, 3: wire, 4: wire guide, 5: collet)

2.4.5. Linear actuated expanded wire needle

Figure 21 shows the fifth and final concept. It uses the wire stylet presented in Section 2.4.3. The wire stylet is placed through a guide (5) and fixated in a piston (3). The piston can move inside its cylinder (4). The

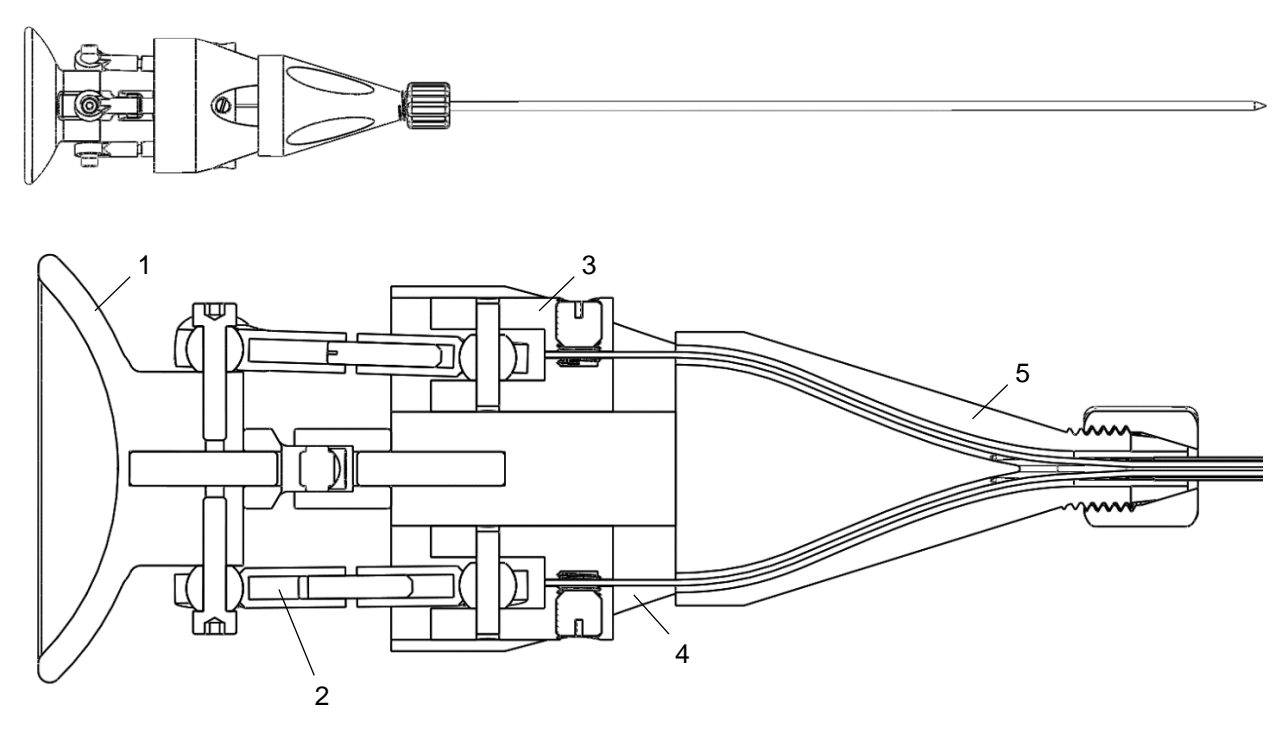


Figure 21 Linear actuatable wire needle. Top shows an overview, bottom shows a cross-section (1: thumb stick, 2: pushrod 3: piston, 4: cylinder, 5: wire guide)

cylinders are linked by pushrods (2) to the thumb stick (1). By manipulating the thumb stick, the pistons push and pull on the wire stylet resulting in the stylet bending. This approach could have several advantages. Firstly, eliminating the necessity to bend the proximal part of the stylet to enlist a bend in the distal part of the stylet should reduce the chance of interference with pre-existing equipment. Secondly, the thumb stick could prove to be a more comfortable way to elicit the required steering. However, this concept is significantly more complex than previous solutions.



3 Concept evaluation

Abstract

A 10 wt.% gelatine phantom, topped with a .15mm sheet of PVC closely mimics a human prostate and surrounding tissue regarding the required penetration force. In this phantom the steering capability and buckling tendency of the prototypes are evaluated. Several of the prototypes did not meet the requirements set previously and are therefore excluded from further evaluation. The patented steel stylet, with a polymer handle, was found to be most favourable according to the optimisation parameters set previously.



This chapter will describe the methods and outcomes of the experiment used to evaluate the performance of the concepts described in the previous chapter. The goal of this chapter is to select the most suitable concept for further development

3.1. Phantom

To evaluate the steering capabilities of the needles to one another, the phantom used for this experiment is of limited importance as the test will only serve to compare different designs. Another factor that will be assessed through this experiment is buckling. While with any phantom one could compare the buckling tendencies of different designs, to gain some insight into the magnitude of the problem, a more accurate phantom will yield more valuable results. To be able to evaluate buckling performance of the needles somewhat accurately, the phantom needs to elicit a similar insertion force to perineal and prostatic tissue.

In the initial steering evaluation described in 2.1.3, a 10 wt.% gelatine mixture was used. This phantom was similar to the one used by Swaney et al. (2013). The paper by Wilkin and Hamm (2010) on a cheap and simple prostate phantom uses a similar concentration gelatine mixture. Section 5.4 in the literature review describes several phantoms being used, from a 5 to 15 wt. % gelatine mixture, canine liver, canine kidney, plastisol, and PVC. To my knowledge none of these papers validate the accuracy of the used phantoms by measuring the elicited insertion force.

For this experiment the transparent nature of gelatine gives the benefit of measuring needle deflection without the use of complex imaging modalities. Ng, Goh, Foo, Ting, and Lee (2013) developed a gelatine phantom to mimic porcine tissue, as porcine tissue is a good phantom for human soft tissue. While this phantom likely mimics porcine tissue well, whether it is a suitable phantom for HDR BT needle insertions is unclear. Podder et al. (2006a) provide insertion force and motion trajectories for 17g and 18g needle insertion in brachytherapy (LDR). For a 18g needle, the paper gives an average peak insertion force in the perineum of 8.87N (±2.32) (while puncturing the skin) and an average peak insertion force in the prostate of 6.28N (±1.64). The authors note the high insertion speed of the needles in the perineum and subsequently note the high insertion speed does not affect the insertion force.

Podder et al. (2006a) provide highly relevant insertion force data to compare a prostate phantom to. Ng et al. (2013) used thin polymer sheets to replicate anatomical obstructions that increase required insertion force to simulate peak forces seen in practice. By using a single polymer sheet on top of a gelatine phantom we will attempt to reproduce insertion forces found by Podder et al. (2006a).

3.1.1. Materials and methods

A linear stage will drive a 18g stainless steel diamond tipped needle through a template +/- 90mm into a gelatine phantom topped with a polymer sheet. The gelatine will be chilled to around 10° and will not be allowed to come up to room temperature as the lower concentrations of gelatine might return to their liquid state. Five gelatine concentrations will be prepared, 2, 4, 6, 8 and 10wt.%. three polymer sheets with thicknesses 0.1, 0.15 and .2 will be used to replicate skin. First the five concentrations gelatine will be tested to find the approximate concentration to achieve the correct peak insertion force in the prostate (around 6N). Once several suitable concentrations of gelatine are found, these samples will be covered by the polymer sheets. This way we hope to find a sheet thickness to mimic the peak insertion force in the perineum. The aim is to find a combination of sheet thickness and gelatine concentration that gives a peak insertion force of between 7 and 9N and a peak insertion force in the rest of its trajectory of approximately 6N. While this approach will not yield a perfectly representative phantom, it should yield relatively realistic insertion forces and enable a comparison between prototypes. Five needles will be inserted in each gelatine concentration and gelatine sheet combination. A 10N force sensor (Futek) will be used to measure the insertion force generated by the phantom.



3.1.2. Results

The results were processed using MATLAB. The insertions were averaged and plotted against the insertion depth. These results can be found in Figure 22. Only 6, 8 and 10 wt.% gelatine concentrations were combined with polymer sheets as 2 and 4 wt.% provided insufficient resistance to the needle. The 0.2mm sheet was not tested as it overloaded the 10N force sensor and therefore provided to much resistance.

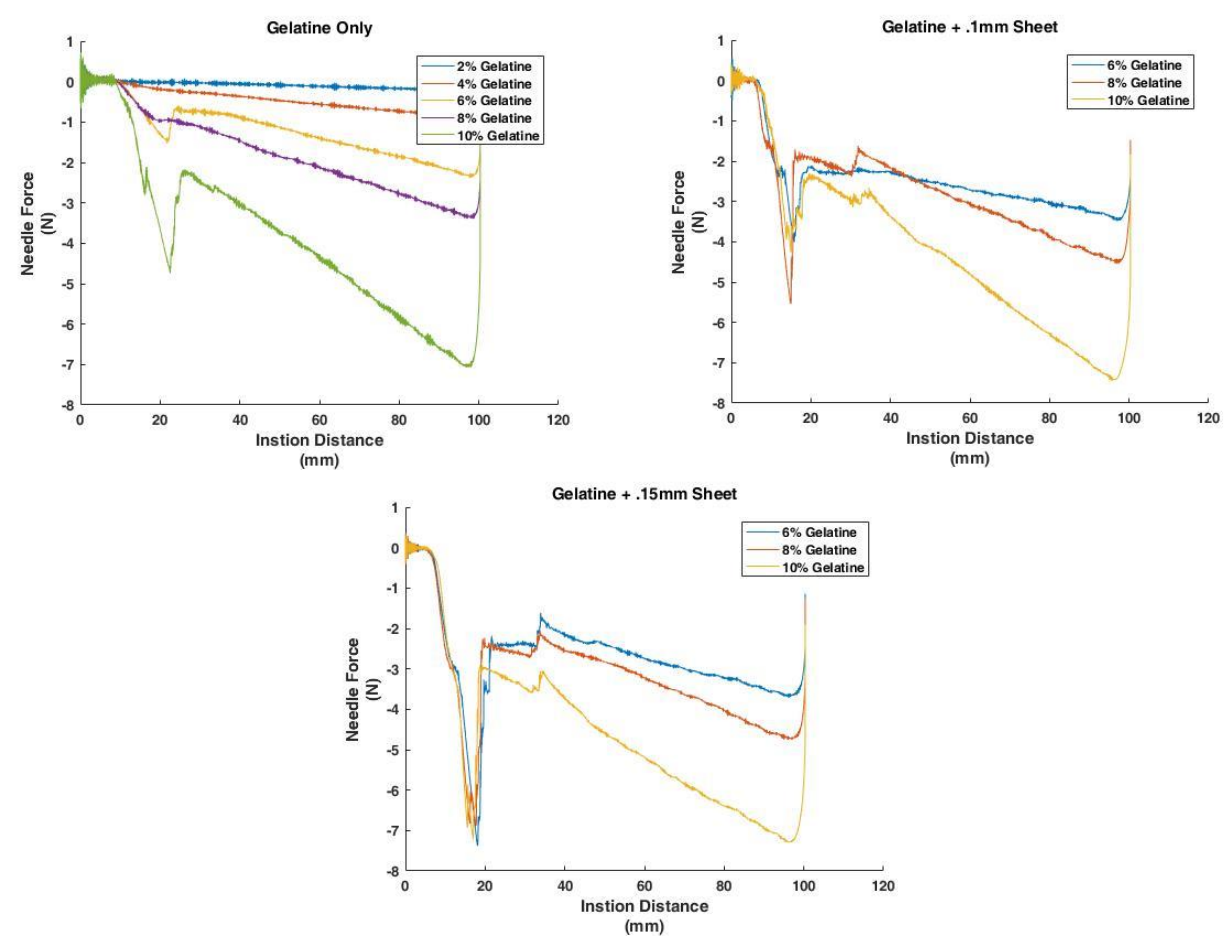


Figure 22 Gelatine concentration phantom experiment. Top left shows insertions into only gelatine, top right shows insertions into gelatine topped with a 0.1mm sheet of PVC, bottom shows insertions into gelatine topped with a 0.15mm sheet of PVC.

Podder et al. (2006a) found a peak insertion force in the perineum and prostate of 8.87N (\pm 2.32) and 6.28N (\pm 1.64) respectively. This is are the values our phantom should approach. The 10 wt.% gelatine phantoms topped with a .15mm PVC sheet yielded average peak insertion force in the perineum and prostate of 7.21N and 7.29N respectively. This is within the 95% confidence interval of the data provided by Podder et al. (2006a). To compare the different prototypes, a phantom consisting of a 10wt% gelatine mixture and a .15mm PVC top layer should be sufficiently representative.

3.2. Prototypes

Of the first two needles presented in Section 2.4 two prototypes are produced, one in a high carbon steel and one in a superelastic material. Piano wire (patented steel wire) is chosen for the manufacturing of the first half of these prototypes. Optimally a superelastic material with a higher Young's modulus then NiTi would be used to manufacture the other half of these prototypes. However, obtaining any superelastic material other than NiTi or NiTiCu in the dimensions and limited quantity we require is nearly impossible. Therefore, we will produce the second half of the prototypes from NiTi.



The last three concepts are only produced from piano wire as the deflection of these concepts is much less limited by the elastic limit of the material. Therefore, a more elastic material will not result in better steering performance.

Figure 23 Shows the five finished prototypes. The first two prototypes in Figure 23 are produced with both a patented steel wire and NiTi stylet. This brings the number of prototypes to be tested to seven.

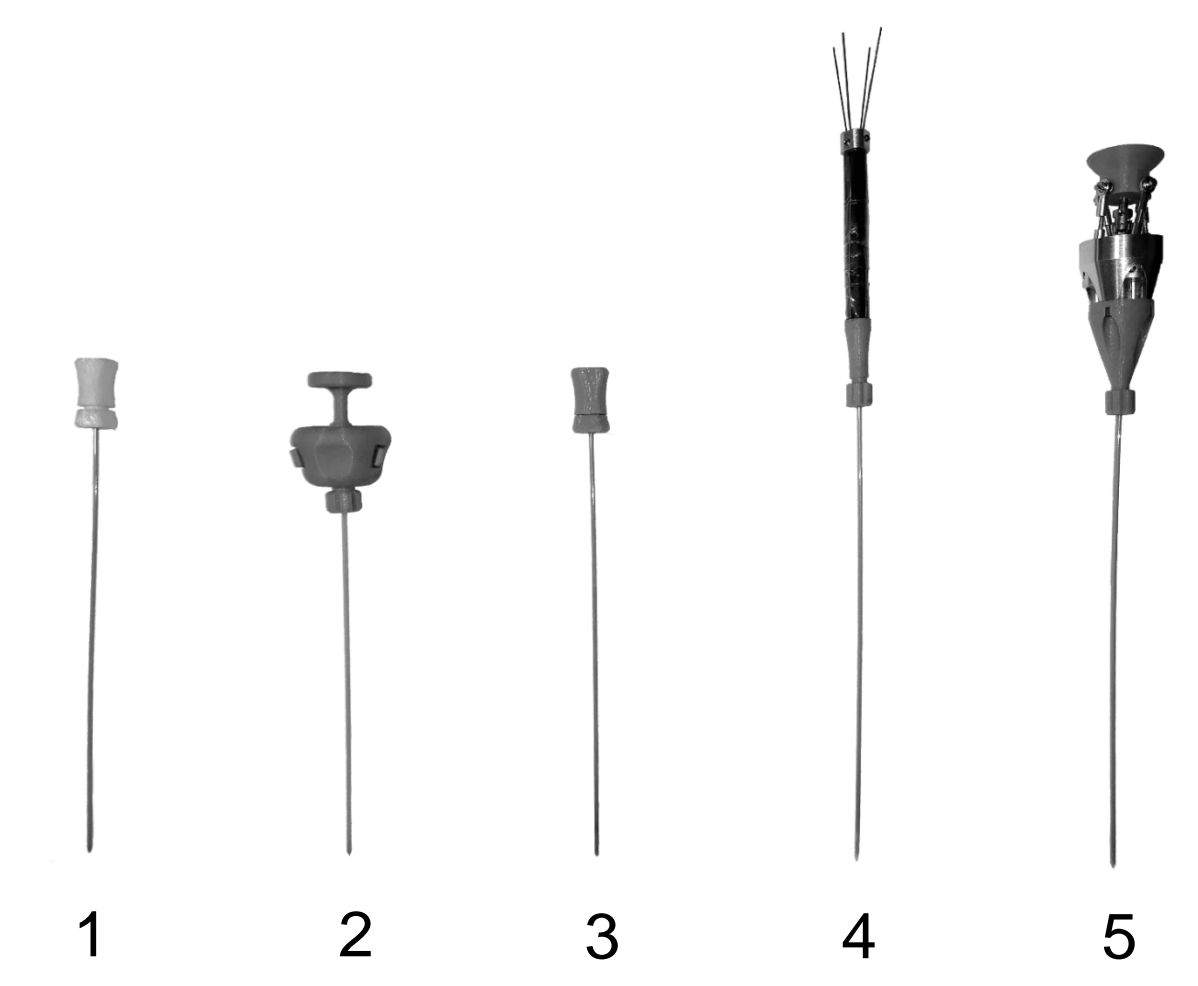


Figure 23 Finished and assembled prototypes (From left to right concept 1 to 5)

3.3. Evaluating parameters

The final concept must meet all the requirements presented in section 1.4. Multiple concepts could meet these requirements. All concepts meeting the requirements presented in section 1.4 will be ranked according to the optimisation parameters presented in section 1.5.

The ability to steer 15mm over a 50mm insertion depth is an important requirement and one that is verifiable with relative ease. Some of the other requirements however, are easier judged subjectively. We will evaluate the concepts by manually steering the needles into a phantom. After each insertion, the amount of steering will be recorded and a short questionnaire will be filled out to evaluate parameters such as ease of control and buckling issues. Table 4 shows the questionnaire that will be used to evaluate parameters that are not easily measured.



	Strongly disagree	Disagree	Neutral	Agree	Strongly Agree
This concept does not interfere with existing equipment.					
This concept requires practice to operate.					
This concept is prone to buckling.					
This concept increases implantation time.					
This concept requires a long assembly in the OR.					

Table 4 Questionnaire

3.4. Materials and methods

This experiment aims to provide the data needed to select the most suitable concept for further development. The tip geometry and sleeve design are identical in all prototypes, therefore it is likely the prototypes would perform similar in comparison to each other in any phantom. While using a more representative phantom (such as an animal or human cadaver) would yield a more valuable evaluation, using the phantom described in Section 3.1 should suffice to make a comparison.

As interference with other equipment is one of the parameters that should be evaluated, it is important to create a representative environment. This means, a template populated with several sleeves and a mock-up of a TRUS setup.

We have five concepts with the first two concepts having two material variations. This means there are seven distinct prototypes and seven experimental conditions. For each variation we will perform 20 insertions per concept at a maximal comfortable achievable deflection. In some of the prototypes the maximal comfortable achievable deflection will likely be limited by the surrounding equipment and in others by the needle itself. Of the twenty insertions per prototype, five will be steered 'up', five 'down', five 'left' and five 'right'. The template position will be randomly chosen from the middle seven holes on the horizontal middle line, as the number of runs and number of hole positions are not divisible. All seven of the prototypes will be tested in a random order, a random steering direction, and a random

n = 20	NiTi	Patented Steel Wire
Concept 1	EC ₁	EC ₂
Concept 2	EC ₃	EC ₄
Concept 3		EC ₅
Concept 4		EC ₆
Concept 5		EC ₇

Table 5 Experimental conditions

template position. Table 5 shows the experimental conditions. Appendix F.2 shows the entire run table.

To evaluate the complete use-cycle of the product, the stylet and its sleeve will be placed separately next to the test setup. Before each run the system must be assembled. The SN is then implanted. The stylet is withdrawn and placed aside. Finally, after measurements and filling out the survey the sleeve will be retracted.

We will use the phantom described in Section 3.1, a 10% wt. gelatine phantom topped with a .15mm PVC sheet. Each needle will be inserted approximately 40mm into the phantom through a template. After which, they will be steered in one of four directions at the maximal comfortable achievable deflection to an insertion depth of 90mm. The deflection of the needle tip from the neutral line will be measured with callipers and noted. The template, neutral line indicator and ultrasound mock-up will be stationary while the phantom is moved between them. In every run a random prototype will be placed in a random template position and steered in a random direction. After each seventh run an identical chilled phantom will replace the phantom to ensure a constant temperature of around 10 degrees Celsius. The next insertion location will be 50mm from the previous insertion location to ensure no crossing of needle paths. After each insertion the researcher will fill out the form



in Table 4. Because the EC's are ranked and the results, due to the small sample size, will likely not be normally distributed, a Kruskal-Wallis test is most appropriate. The null hypnosis is that there is no difference between the EC's. The alpha used is 0.05.

Figure 24 shows the setup used to evaluate the prototypes. The timber is a stand in for the ultrasound probe. In the template several sleeves can be seen that represent already implanted sleeves. Beneath the template and phantom, a ruled sheet of paper can be seen which indicates the neutral line from which the deflections are measured.



Figure 24 Gelatine concept experiment setup. Top left shows the gelatine phantom (1) and the TRUS stand in (2). Top right shows the template (3) thought which the needles are inserted. The bottom shows an overview of prototypes tested.

3.5. Results

A total of 140 implantations were performed with the seven prototypes. During these implantations several observations were made:



- The prototypes based on the nitinol stylet are not stiff enough to insert one handed.
- Loosening the mechanism that secured the stylet to the sleeve can be hard to loosen when it is close to the template;
- Previously implanted sleeves present little obstacle to the SN as they can easily be slightly moved out
 of the way due to their flexibility;
- The screw caps on the fastening mechanisms should not come off as easy as they could be lost during retraction:
- In prototype four, the steering mechanism tends to permanently deform the steel stylet;
- Prototype five, the wire stylet, depends heavily on the tightness of the template to combat the inner wires shifting in the stylet;
- Partly due to the lack of torsional rigidity, prototypes six and seven are difficult to accurately steer;
- The steel stylet tends to permanently deform after several insertions. This seems to have little influence on its performance. The stylet is also easily bent straight;
- The plastic 'stop' on EDM'ed stylet comes off too easy upon retraction.

Table 6 shows the results of the concept experiment. The light grey and dark grey squares show the most and least favourable results respectively.

N=20	EC ₁	EC ₂	EC ₃	EC ₄	EC ₅	EC ₆	EC ₇
Deflection (mm)	27.0	28.4	16.8	13.6	6.3	10.4	13.2
This concept does not interfere with existing equipment.	4.7	4.8	2.6	2.4	4.6	4.7	4.3
This concept requires practice to operate.	2.7	2.5	1.6	1.6	3.3	3.4	3.0
This concept is prone to buckling.	4.6	1.2	3.6	1.1	2.5	3.5	4.0
This concept increases implantation time.	2.1	2.1	2.0	2.1	2.0	2.1	2.2
This concept requires a long assembly in the OR.	3.3	3.0	2.8	2.8	3.3	1.6	1.4

Table 6 Gelatine concept experiment results. (Light grey: highest value, dark grey: lowest value) Implantation time results were ignored due to negligible effect.

Prototype one, two and three show average deflections above the 15mm threshold set in section 1.4. However, the confidence interval of other prototypes might include the 15mm threshold. The prototypes without a steering mechanism interfere less with existing equipment due to the lack of a bulky mechanism running into previously placed sleeves. However, when placing a needle in the lower holes of the template and subsequently steering upwards, the issue of interference with the ultrasound probe can be reduced by having a steering mechanism. Having a steering mechanism could also help to reduce the learning curve required to perform the steering implantation. Buckling was most prevalent in the nitinol stylets and the longer wire needle concepts. There is no clear difference between the implantation time of the different concepts as they are too alike to significantly differ in this regard. The assembly time needed in the OR was least for the sixth and seventh prototypes as they only require the sleeve to be placed and the cap to be tightened.



The 95% confidence intervals of EC_1 and EC_2 fall well above the 15mm threshold. As expected, the 95% confidence interval of multiple of the prototypes encompasses the 15mm threshold, namely prototypes three and four. With some optimisations, prototypes three and four could likely be improved to meet the 15mm threshold. Prototypes five, six and seven do not meet the threshold.

The data collected fails normality tests, likely due to the small sample size (n = 20). The non-normal ranked data makes a Kruskal-Wallis test the most appropriate statistical tool. Figure 25 shows a boxplot of the Kruskal-Wallis test performed on the deflection results of the concept experiment. This test shows statically significant differences between the measured deflections of the different EC's (χ^2 _(6, N = 20) = 84.14, p = <0.01). Comparison of mean ranks shows EC₁ and EC₂ to be significantly different from EC₄, EC₅, EC₆ and EC₇. EC₃ is significantly different from EC₂ but not EC₁. From this test can be concluded that EC₁ and EC₂ meet the 15mm threshold and perform significantly better than EC₅, EC₆ and EC₇. Appendix F.2 contains a table with mean rank comparison between every EC.

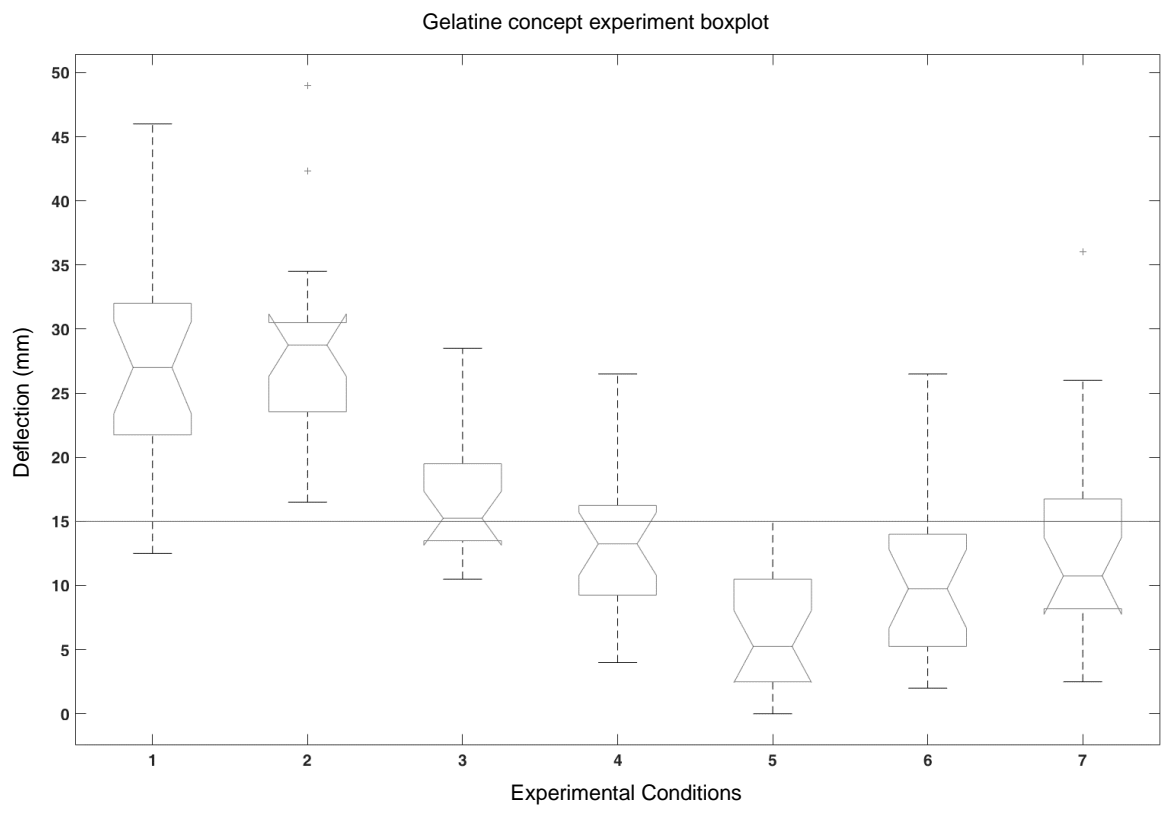


Figure 25 Boxplot with 95% confidence interval concepts experiment. The horizontal line represents the 15mm minimum steering requirement presented in section 1.5.

3.6. Choice of final concept

The requirements set in section 1.4 will eliminate some of the concepts, the remaining concepts will be chosen according to the optimisation parameters described in section 1.5.

Prototypes 4 to 7 do not fulfil R1, however because the 95% confidence interval of prototype 4 does envelop the 15mm threshold we will only exclude prototypes 5 to 7. Prototypes 1 to 4 fulfil most of the requirements, the following is a list of the requirements that have not been mentioned or investigated sufficiently:

- (R8) The system can be operated by a trained surgeon with little additional training;
- (R9) To ease the adopting of the instrument the SN should be hand-operated. Either one or two handed;
- (R10) The system does not decrease the cost-effectiveness of HDR BT of the prostate;



- (R11) The system should not lengthen the procedure time (Approximately 30 to 45 minutes) of the HDR BT prostate needle implantation;
- (R12) The system should not be less comfortable to use in a surgical setting then current needles;
- (R14) The system can be mass produced with existing manufacturing techniques.

The mechanism by which steering is achieved is quite easy to understand and intuitive to use. Therefore, we believe R8 should not pose an issue. However, in further development this issue should be considered. The four prototypes fulfil R9, however, the nitinol stylets (prototypes 1 and 3) can only be used two handed, as they buckle when used with one hand. To evaluate the cost-effectiveness of the prototypes (R10) we would need information about the value of improved needle position and possible reduced toxicities. Doing this for all the prototypes would, in this stage of the design process, be highly time consuming and yield inconclusive results as the prototypes are in an early stage of development. Nevertheless, we can safely assume the relatively inexpensive type of steerable needle being developed has the possibility to be cost-effective. The steel stylet will be easier and less expensive to manufacture then the nitinol version as the material is less expensive and easier to machine. Prototypes with more parts and more complex mechanism will probably be more expensive to manufacture. R11 refers to the time needed to implant the needles. The ability to steer a needle could result in slower implantations as the surgeon steers towards the target. The lost time however should be offset by the reduced number of insertions required to reach a satisfactory position. This is another point that will require further research. During the concept experiment we found the collets of some concepts to be hard to release comfortably. Otherwise the concepts fulfil requirement R12. Some of the parts of the prototypes are 3D printed, this could be an obstacle to mass production. However, these parts could, with only minor adjustments, be injection moulded.

A weighted objectives evaluation will be used to determine the final concept. The optimisation parameters will be used as criteria and will each be weighted. The optimisation parameter P1, will not be included in the weighted objectives matrix as this would require an addition experiment to determine the prototypes accuracy. The potential accuracy gain will have to be determined in a future experiment. Parameters that are very similar between concepts will be omitted as they would not influence the outcome. The four prototypes will then be scored from 0 to 10 on each of these criteria. The criteria weight and prototype scores are multiplied and added, the highest score indicates the preferable concept.

	Weight	Pro	totype 1	Prot	otype 2	Prot	totype 3	Pro	totype 4
P3 - The system should be able to steer more than 15mm at a 50mm depth.	25	8	200	9	225	6	150	5	125
P6 - The system should increase the cost- effectiveness of HDR BT as much as possible	20	8	160	9	180	5	100	6	120
P8 - The system should require as little training as possible to operate.	20	5	100	5	100	8	160	8	160
P9 - The system should have as few parts as possible.	15	7	105	7	105	4	60	4	60
P10 - Assembly of the system in the OR should require as few steps as possible.	10	5	50	5	50	7	70	7	70
P12 - The system should be more comfortable to use then current systems.	10	6	60	6	60	7	70	7	70
Total	100		675		720		610		605

Table 7 Weighted objectives

Table 7 shows the weighted objectives table. Prototype 2, the optimised stylet from patented steel wire scores highest with prototype 1 the nitinol optimised stylet as a close second. Difference between the two concepts results from the slight difference in amount of steering and the cost of a nitinol versus steel stylet. We will use the optimised stylet from patented steel wire as starting point for the rest of this design process.



4

Optimisation and final design

Abstract

The medical device being developed is classified as an IIa medical device. Due to the width of the slots in the stylet, sterilisation is not an option. The stylet and handle are not to be taken apart and should be disposed of after each procedure. Final material for the stylet should be available in medical grades. The most favourable material available in a medical grade is AISI M42 tool steel. An eccentric lock ensures the stylet is secured to the sleeve during implantation, but can comfortably be loosened to retract the stylet after implantation.



The previous chapter has provided an evaluation of the different prototypes and the selection of the most suitable prototype. While this prototype performed most favourable in comparison to the other prototypes, there is always room for improvement. This chapter iterates on the prototype selected in the previous chapter and presents the final design.

4.1. Adjusted design objectives

In the previous chapter the second prototype was chosen to base further development on. The evaluation of the prototypes revealed several limitations and characteristics of the prototypes. For the second prototype these were:

- Loosening the mechanism that secured the stylet to the sleeve can be difficult when close to the template;
- The screw caps on the fastening mechanisms should not come off as easily, as they could be lost during retraction;
- The steel stylet tends to permanently deform after a number of insertions. This seems to do little against its performance. The stylet is also easily bent straight
- The plastic 'stop' on EDM'ed stylet comes off too easyily upon retraction;
- The prototype scored relatively high 'This concept requires practice to operate.' in the gelatine experiment;
- The prototype scored relatively high 'This concept requires a long assembly in the OR.' in the gelatine experiment;
- In the weighted objectives evaluation, the prototype scored relatively low on the optimisation parameter 'Assembly of the system in the OR should require as few steps as possible.'.

The items in the list above should receive additional attention in the optimisation of the second prototype.

4.2. Medical device classification

The classification of medical device will influence the cost of developing said medical device and determine its cost and therefore cost-effectiveness. This section will describe how this medical device was classified and its implications.

To classify this device the European medical device regulation ("COUNCIL DIRECTIVE 93/42/EEC" 1993) was used. Firstly, the duration of use is important in determining the classification for CE marking. Because the stylet is used for a few minutes to place the sleeve and then retracted, the continued use is never more than 60 minutes. This makes its duration classification 'transient'. The sleeve however does stay in the body for more than 60 minutes continuously, and its duration is therefore classified 'short term'. Secondly the invasiveness of the device. Surgically invasive is defined as: 'An invasive device which penetrates inside the body through the surface of the body, with the aid or in the context of a surgical operation.' By this definition, our device is surgically invasive. Lastly, because the slots in the design would be exceedingly difficult to properly clean and the instrument should be discarded if excessively bent, the device should be disposable.

The sleeves used in HDR BT can remain in the patient for up to days a time. Their duration of use is therefore 'short term'. The stylet on the other hand will only be used during the implantation and has a duration of use that is 'transient. Point 5.2 of Annex VIII, Rule 6 ("COUNCIL DIRECTIVE 93/42/EEC," 1993) states; 'All surgically invasive devices intended for transient use are in Class Ila unless…'. The exceptions to this rule do not apply to this device, the steerable stylet is therefore classified as an Ila medical device. Using the previously certified commercially available sleeves lowers the medical device classification and potential reduces cost and time required to certify the developed system.

4.3. Material selection

Section 2.3 found patented steel wire to be the most suitable material to produce a non-superelastic stylet from. However, to comply with medical device directives, materials used in a medical device should be certified and documented conforming ISO-10993. It is therefore desirable that the material used in the stylet already has this certificate. According to the Cambridge Engineering Selector, there is no patented steel wire grade conforming with ISO-10993. Figure 26 shows the same graph as Figure 12, this time showing only materials



that have a medical grade conforming with ISO-10993. From this graph we can see AISI M42 tool steel has the closest yield strength over young's modules ratio to patented steel wire. AISI M42 tool steel does have a slightly higher Young's modulus. AISI M42 tool steel can be found in the ASM medical materials datasheet under 'Fe-9Mo-8Co-4Cr-2W (M42)' (ASM, 2020).

One of our optimisation parameters was to have a MRI compatible steerable needle. Unfortunately, none of the materials that score well in Figure 26 are MRI-compatible or pose a low-risk of MRI interference. When only including MRI compatible materials and materials that pose a low risk of MRI interference, tungsten wire becomes the most suitable material. Unfortunately, tungsten has a significantly less favourable yield strength over young's modules ratio to AISI M42 tool steel (note the scale is logarithmic). Using MRI in HDR BT is rare, we have therefor chosen not to ensure MRI compatibility with this system.

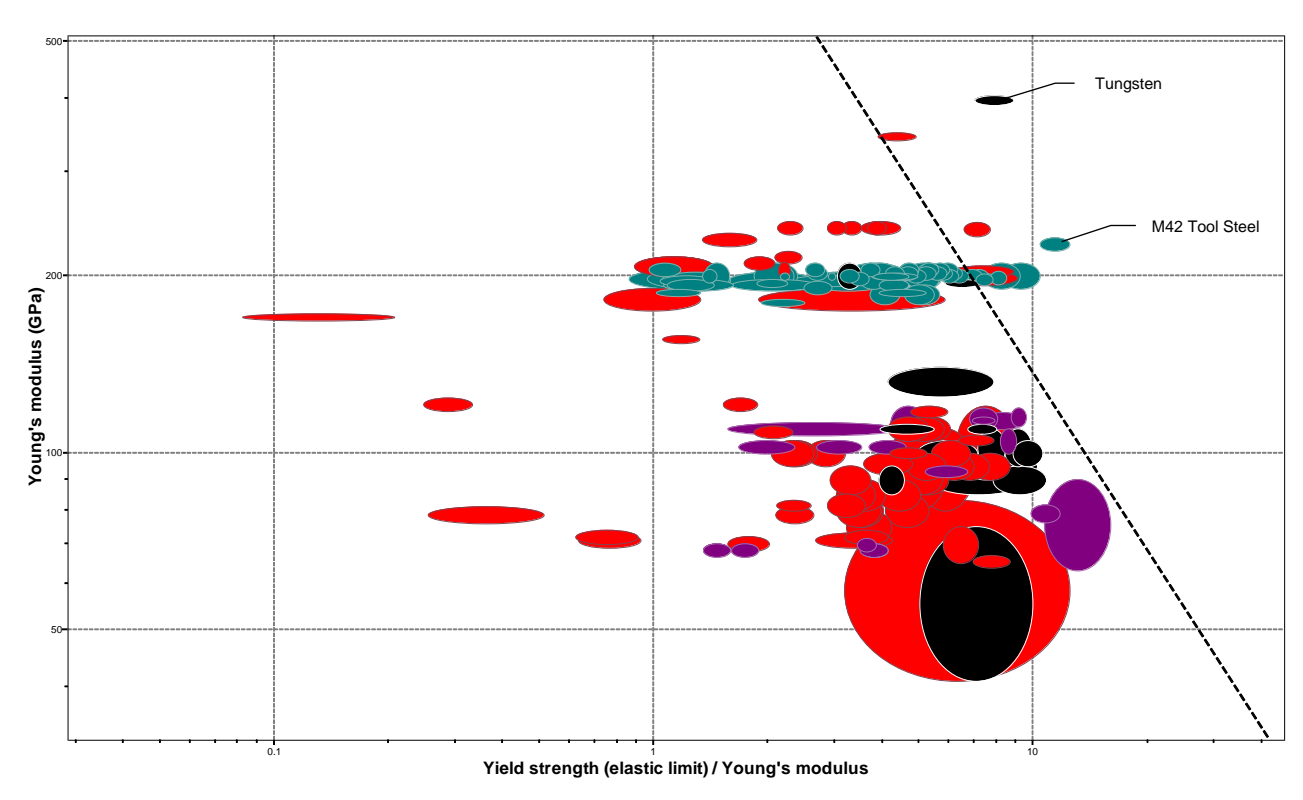


Figure 26 Material selection using Cambridge Engineering Selector. Only materials included with medical grades available. Black diagonal line indicates optimal material behaviour. Materials with a larger perpendicular distance to the right of the line present more favourable characteristics.

4.4. Handle

Having a handle on the SN could be beneficial for multiple reasons. Firstly, a handle gives the surgeon a better grip of the needle reducing the chance of buckling. Secondly, a handle could allow a surgeon to perform more controlled and precise movements without worrying the system might slip from his hand even if the system gets wet. Lastly, a well-placed handle can prevent the stylet from penetrating through the sleeve under excess force.

The stylet and sleeve are generally not fixated to one another during implantation. The ProGuide® obturators do have a kink in the end of the stylet to ensure the sleeve remains in its place during implantation. If the stylet is not fully inserted into the sleeve during implantation there is a chance the unsupported sleeve will kink and possibly break during implantation. This, at best, makes the implant unusable to an afterloader and at worst brings the radio source in contact with tissue or leaves fragments of the sleeve in the patient. The developed SN will likely encounter more extreme manipulation and larger insertion angles then currently used alternatives. This increases the importance of good fixation between the stylet and sleeve.



HDR BT needles typically have either a small plastic handle (Mick FlexiGuide Needles® - Eckert & Ziegler) or a small metal stop (ProGuide® Needles - Elekta) that allows the surgeon to withdraw the stylet from the sleeve after implantation. This metal stop also acts as the control surface of the system. When a needle is inserted straight with little manipulation, this surface provides the surgeon with enough control. In the developed SN, the surgeon needs to bend the needle during insertion. This insertion should be possible one-handed to enable the surgeon to, if necessary, operate other equipment (such as the TRUS probe). To give the surgeon accurate control even in wet condition, we believe a handle is required.

The Mick FlexiGuide® Needles handle placement ensures the tip of the stylet stays just shy of the tip of the sleeve. The handle transfers any force applied to the system, to the sleeve. This is done to ensure the stylet can never penetrate the tip of the sleeve. This again prevents the breaking of the sleeve and possibly bringing tissue into direct contact with the radiation source.

The stylet will have to be disposable as the slots would be difficult to clean. The handle could be detachable and reusable. Reusing the small polymer handle however would probably not be cost-effective as the sterilisation and assembly of the handle can be costly (Van Meter & Adam, 2016). A reusable handle would also have the drawback of consisting of small parts that could come apart during use. We have therefor chosen to use disposable handles. The next sections present concepts for the handle design.

4.4.1. Stop and flat

The first concept is the minimum viable product. Figure 27 shows the stylet and sleeve separately. The tool steel stop (1) is press fit to the stylet and a small flat (2) is pressed into to proximal end of the stylet. The stop gives the surgeon something to hold onto and transfers forces applied to the system, to the sleeve. This ensures the stylet can never penetrate through the end of the sleeve. The flat holds the sleeve on the stylet for the duration of the procedure. This concept closely resembles the approach taken in the ProGuide® system from Elekta.



Figure 27 Stop and flat (1: stop, 2: flat)

4.4.2. Injection moulded handle

Concept two replaces the stop for an injection moulded handle to allow for more comfortable manipulation of the needle. A flat is still pressed into the stylet to ensure the sleeve remains in place, but now a second flat at the proximal end of the stylet is simultaneously pressed. The stylet is then placed in an injection moulding machine and a polymer handle is moulded around the stylet. The handle again ensures any force applied to the system is applied to the sleeve and gives the surgeon better control. This concept resembles the approach taken in the Mick FlexiGuide® Needles.



Figure 28 Injection moulded handle cross section



4.4.3. Improved screw collet

A significant drawback of the previous two concepts is the fixation of the sleeve to the stylet. The sleeve is held in place by a flattened part in the stylet. This holding force cannot be very large as the stylet has to be easily removed from the sleeve after implantation. The screw collet presented in Section 2.4.1 prevents the stylet from sliding during manipulation and allows easy retraction after implantation. The adjusted objectives in Section 4.1 show some limitations of the prototypes. Loosening the collet presented an issue. This redesign addresses this issue. Figure 29 shows the redesign of the screw collet. The collet consists of two parts, the first part (1) is injection moulded over a flat on the stylet much like the previous concept. The second injection moulded part (2) can then be locked into place. The shallow angle of the collet generates a large amount of

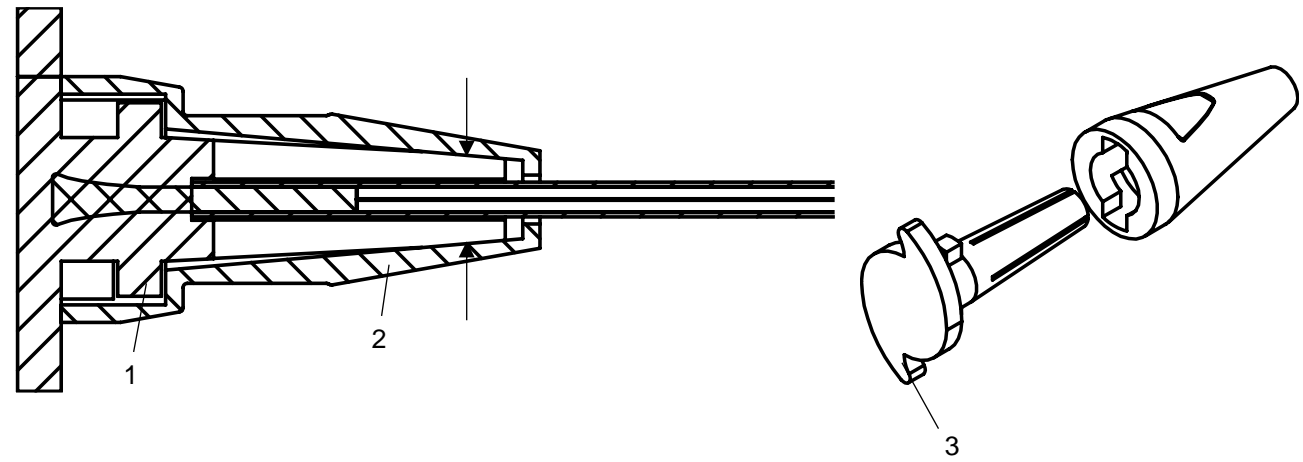


Figure 29 Improved screw collet. Left shows a section view, rightshows an isometric view. Black arrows show clamping force. (1: base part injection molded over stylet, 2: second clamping part, 3:directional fins)

holding force while still being easy to loosen. The first part has directional fins (3) to ensure the user does not accidentally loosen the mechanism. The depth the sleeve can be placed in the handle again ensures the stylet does not penetrate the sleeve.

4.4.4. Eccentric lock

A second issue that surfaced during the experiment in Chapter 3 was that the handle could be dropped and/or lost. Figure 30 shows an eccentric lock consisting of two parts. The first part (1) is injection moulded around a flat on the stylet. The second part (3) is then snapped into place and held in place by snap hooks (2) and a groove. This means the whole system cannot be disassembled after assembly. The holding force is generated by rotating the part 90 degrees in respect to each other. Because the axis of rotation is eccentric, the sleeve is compressed and held in place when the components are rotated in relation to each other. The depth the sleeve can be placed in the handle again ensures the stylet does not penetrate the sleeve. The flats on the

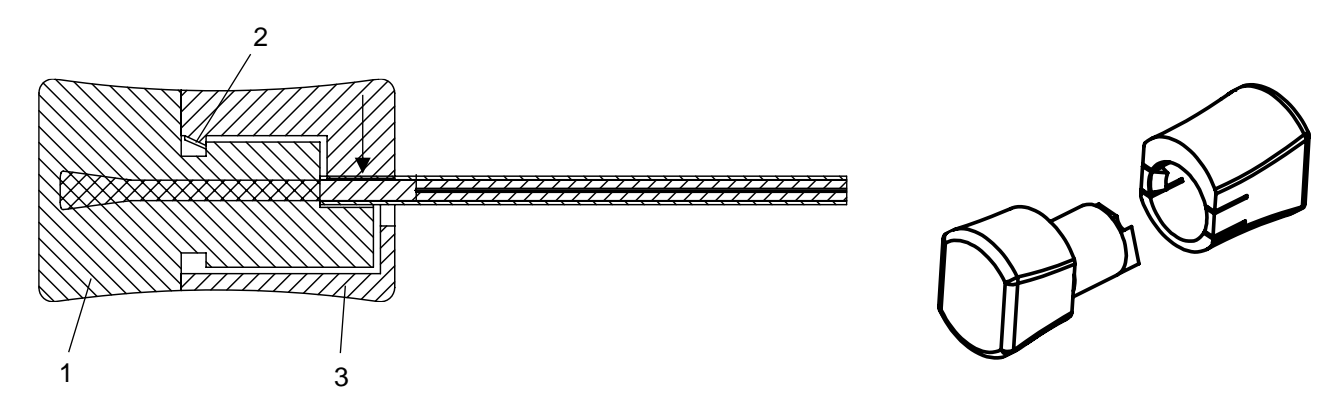


Figure 30 Eccentric lock. Left shows a section view, right shows an isometric view. Black arrows show clamping force. (1: base part injection molded over stylet, 2: snap hooks, 3: rotating clamp)

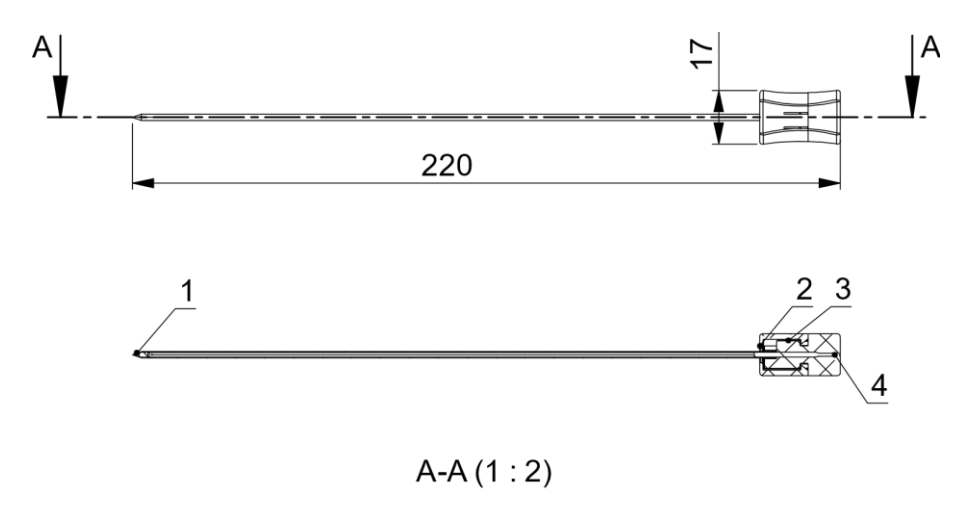


side of the handle (Figure 30 right) give the user grip to twist the handle and indicate if the sleeve is locked in place. When the flats do not align, the sleeve is not locked.

4.5. Final design

To be able to steer the needle comfortably, the user should be able to easily manipulate the needle. A secure fixation of sleeve to stylet is also necessary, to ensure the sleeve does not move in relation to the stylet which could result in kinks or breaks in the sleeve. We have therefore chosen to fit the stylet with the eccentric lock (Section 4.4.4). The handle gives the user a comfortable interface and strongly fixates the sleeve to the stylet, while still allowing the user to easily detach the sleeve after implantation. As for the material of the handle, there are a number of constrains. The material should be injection mouldable, medical grades should be available, the materials should be sufficiently stiff, and the material should be sterilisable, either through radiation, ethylene oxide or steam autoclave. With these constraints in place, the three materials with lowest price per kilogram found in CES, in ascending order are SMMA, ABS, and PC. Any of these three materials are suitable for the handle. ABS is ubiquitous in injection moulded parts due to its low cost, strength, and dimensional stability. SMMA and PC have the advantage of being transparent, enabling the surgeon to see if the sleeve is seated properly or if something inside the mechanism has broken. SMMA is chosen because of its transparency. For the handle there are multiple suitable materials, depending on the manufacturer's capabilities any of the above-mentioned materials should perform adequately.

Figure 31 shows an overview of the parts of the final SN design with some general dimensions. To assemble the system, the bottom handle (3) is injection moulded around the stylet (4). Finally, the top (2) is clicked into place. This assembly is then sterilised, packaged, and delivered sterile to its user. The physician opens the packaging and places a sleeve. The process of placing and locking a sleeve can be seen in Figure 32.



ITEM NO.	PART NUMBER	MATERIAL	AMOUNT	
1	Sleeve	-	1	
2	Handle Top	SMMA	1	
3	Handle Bottom	SMMA	1	
4	Stylet	AISI M42	1	

Figure 31 Final design SN overview with cross section and material overview



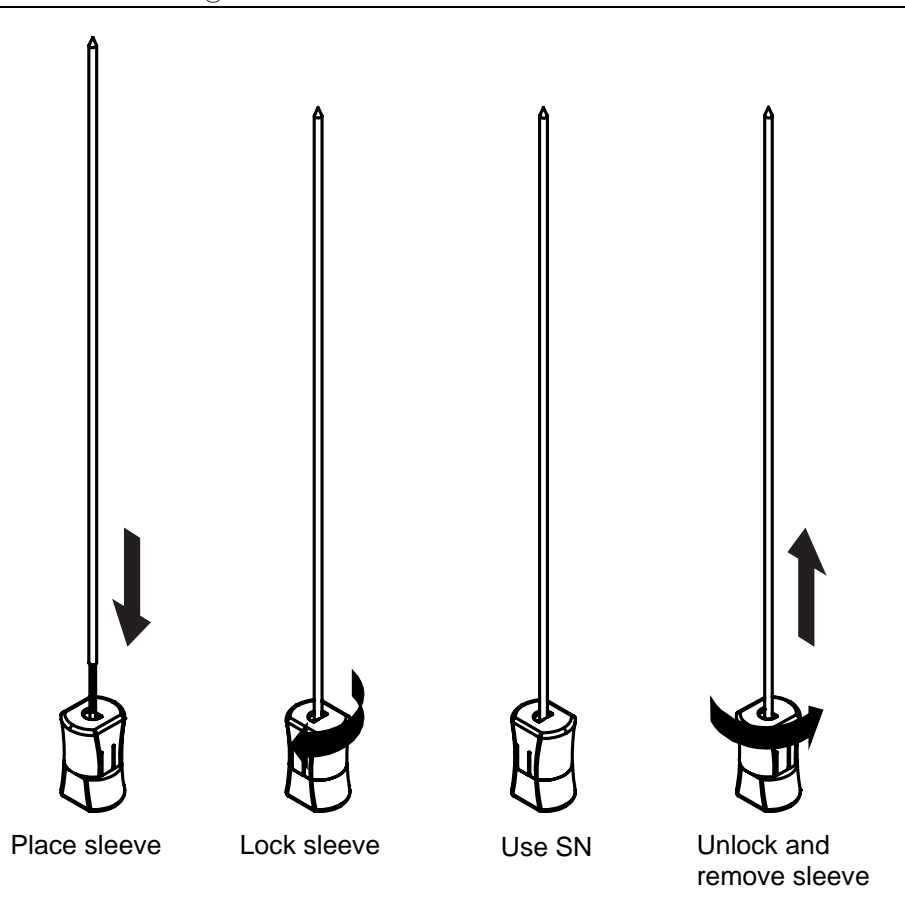


Figure 32 Mounting and dismounting of sleeve in order from left to right.

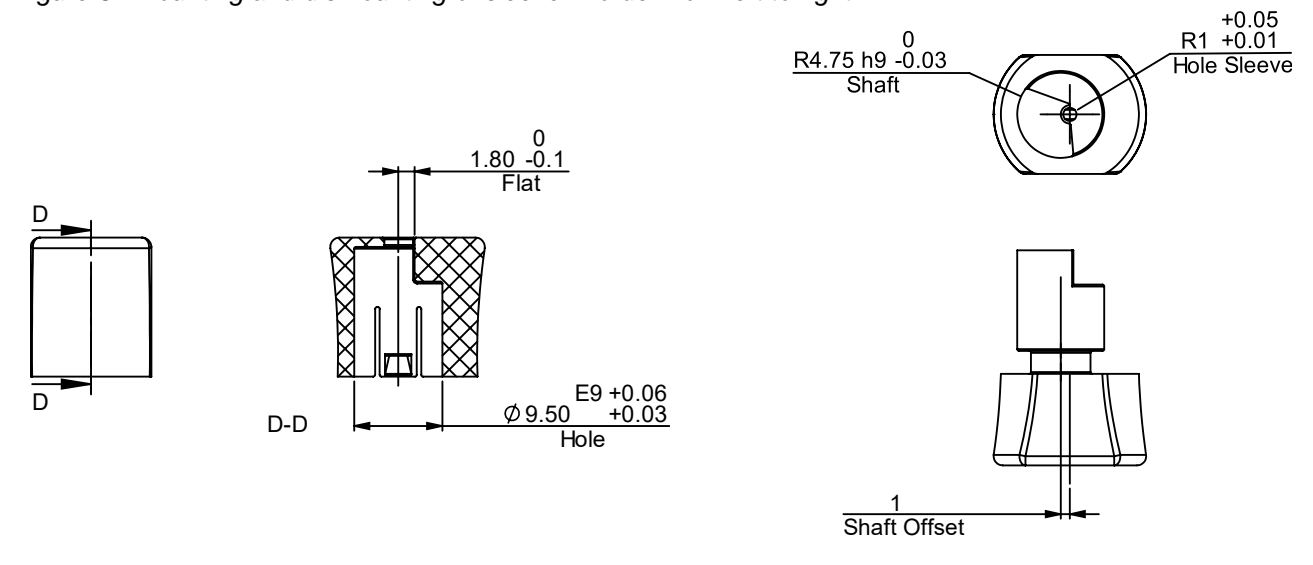


Figure 33 Critical dimensions handle. Left shows clamping section, right shows bottom section which is injection molded over the stylet.

The diameter of the stylet is the most critical dimension for the system to work. The diameter of the stylet should be 1.44 $\frac{+0.00}{-0.04}$ mm. Firstly, a stylet diameter smaller than specified would result in increased buckling risk as buckling is heavily dependent on the diameter of the stylet (Equation 10). Secondly, a stylet diameter smaller than specified could interfere with the locking mechanism of the handle. The length of the stylet should always be $\frac{-0.01}{-0.05}$ mm smaller than the inner length of the sleeve to ensure force is transferred to the sleeve and not he stylet. To ensure the locking system on the handle functions properly, there are a number of critical dimensions of which an estimation can be found in Figure 33. In the top section of the handle (left) the



dimension of the hole is critical to ensure smooth rotation and provide the right clamping force on the sleeve. A loose fit of E9/h9 should allow for smooth rotation while being accurate enough to provide sufficient clamping force. The distance of the flat to the centre of rotation is critical to produce the right amount of clamping force on the sleeve. Depending on material, surface roughness and manufacturing technique, this value will have to be re-evaluated in a later stage to provide the correct clamping force. In the bottom section of the handle (right) the critical dimensions are the shaft diameter and the diameter of the hole for the sleeve. The slop between the shaft and the hole needs to be added to the tolerance of the flat and sleeve hole to find the clamping interference. This comes to in the upper extreme to (0.06 - -0.03 + 0.05) 0.14mm and in the lower extreme to (0.03 + 0 + 0.01) 0.04mm. The diameter of a sleeve is approximately 2.00. We assume there to be very little variation between sleeves. The dimension of the flat, between 1.70mm and 1.80mm, will ensure an interference between the handle and the sleeve of (2.00 - 0.04 - 1.70) 0.26mm and (2.00 - 0.14 - 1.80) 0.06mm in the upper and lower extreme respectively. Dimensions and tolerances will heavily depend on material and manufacturing choices and will certainly need to be adjusted as the device is developed. Figure 33 only serves to indicate critical dimensions in the handle design.

Figure 34 gives an indication of what the instrument could look like. A QR code on the handle allows every instrument to be tracked through its lifecycle. The arrows on the handle provide a secondary indication of the locked position. Whether the symbols meet EN 15223 should be investigated in the further development of the SN. The bottom image in Figure 34 shows the way the disposable SN might be delivered to the medical staff, sterile and ready to be used. The tube and its lid are sealed together by melting a small notch at their interface. The tube should protect the SN against damage during transport. Further study is required to determine if the packaging meets ISO 11607. Whether this packaging provides sufficient protection during transit should be evaluated in future development of the SN.

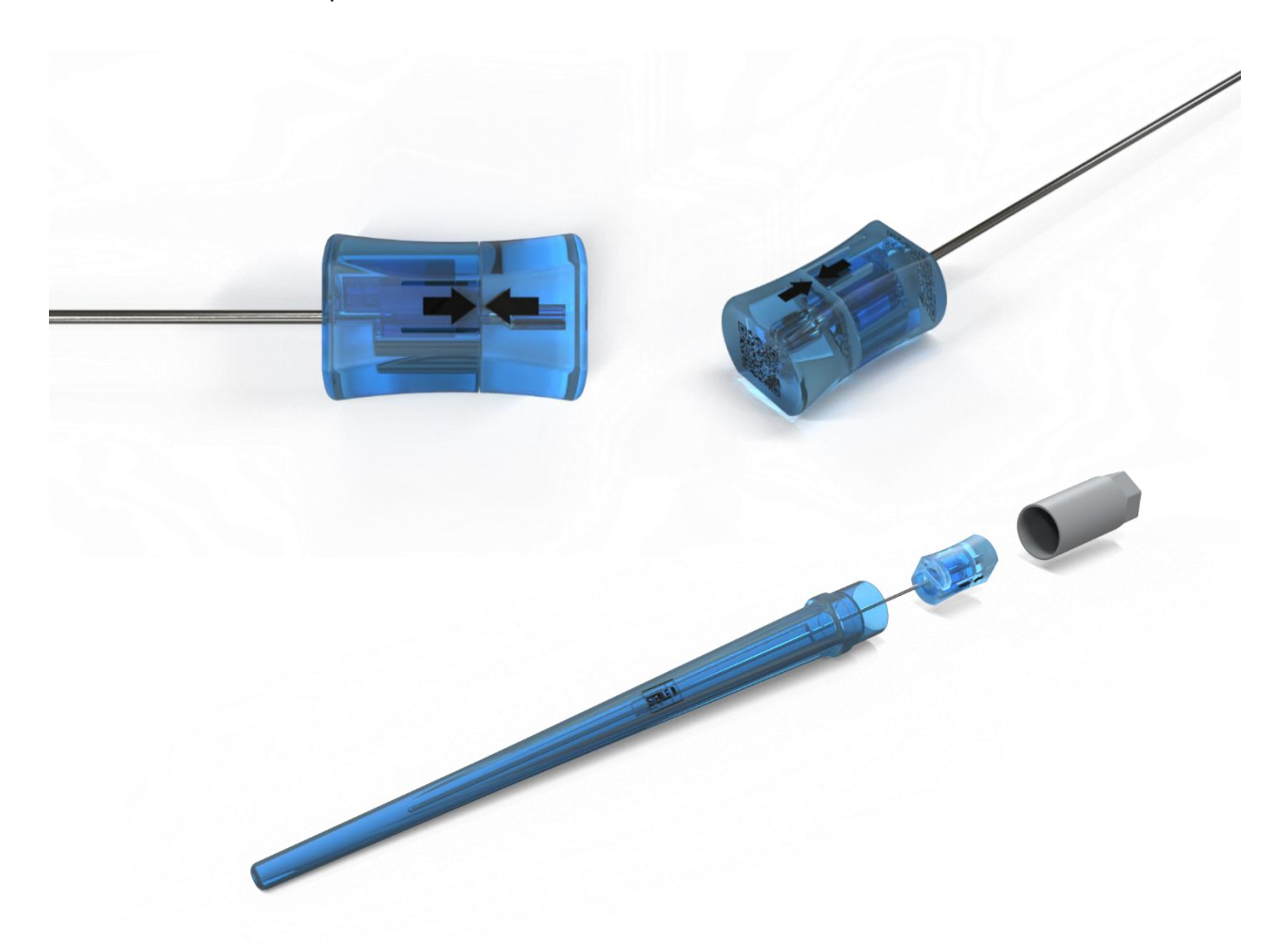


Figure 34 Visualisation of final design. Top shows the handle, bottom shows the complete needle and packaging.



Performance evaluation

Abstract

To be able to provide a verdict on the performance of the steerable needle, the system is tested against a commercially available needle. A PVA phantom is developed to better mimic the tissue in and around the prostate, and enable ultrasound visualisation. Using two PVA phantoms with different Young's moduli, the placement accuracy of the developed SN is compared to that of a commercially available needle both steered and un-steered. Active steering does significantly improve endpoint accuracy and gives an indication of the ability to outperform currently available systems in an experimental setting. The cost-effectiveness of the SN is evaluated by comparing the added cost of the developed system with the potential cost saving effects of the system.



The first two chapters have described the design process of the SN. Chapter 3 has described the steering capability of several prototypes. Chapter 4 has described the final design of the SN. This chapter will aim to evaluate the performance of this steerable needle in comparison to the rigid needles currently in use.

In the preceding literature review we found the needle placement accuracy to currently be of little importance in the outcome of HDR prostate BT. Mainly since the dose plan is generated after the needles are implanted. However, more accurate needle placement could reduce procedure time and reduce the number of needles necessary per implant. During observation of salvage HDR prostate BT (Appendix F.3), we learned needle placement to be more relevant in salvage BT as the target of the radio therapy is limited to the tumour and not the entire prostate. This means placing the needles accurately is much more important and difficult.

Another area of interest is the ability to negotiate anatomic interference (e.g. PAI) and avoid sensitive tissues (e.g. penile bulb). It is unfortunately difficult to evaluate the performance of the SN in this area as there is no instrument or procedure to make a direct comparison with. We can however, provide an evaluation of the steering capability of the needle and the accuracy of said steering. A more valuable evaluation would be to compare late toxicities with the current implantation technique and a technique aimed to avoid sensitive tissue. This would require research from a medical perspective to develop a procedure sparing sensitive tissues using the SN, this is beyond the scope of this thesis.

This chapter will aim to provide an evaluation of the placement accuracy of the SN in comparison to currently used needles and provide some information about ability of the SN to steer to a target.

5.1. Improved phantom

The experiment in Chapter 3.1 describes the development of a gelatine phantom of which the penetration force is matched with the in vivo penetration force found in the paper by Podder et al. (2006a). This phantom was suitable to compare buckling tendency and maximum steering capability of the prototypes. To be able to compare the performance of the SN to an existing device, and more specifically the steering accuracy of the SN in comparison to the deflection of existing devices, we need a more representative phantom. In practice the implantation is performed under ultrasound guidance. To make a fair comparison the SN should therefore be steered under ultrasound guidance. Unlike gelatine, human tissue is not isotropic, human tissue generally has an orientation influencing a needle path. This anisotropy is likely to influence the needle path (Webster, Kim, Cowan, Chirikjian, & Okamura, 2006). During insertion the needle also encounters the prostatic capsule in HDR BT of the prostate. Passing through multiple layers of tissue can influence needle deflection (Abolhassani, Patel, & Moallem, 2007). The stiffness of the phantom will also influence the needle deflection (van Veen, Jahya, & Misra, 2012).

A representative prostate phantom would consist of two regions, one with the stiffness of soft tissue (the perineal area) and one with the stiffness of prostatic tissue. The phantom should be anisotropic and behave similarly under ultrasound imaging compared to human tissue. A polyvinyl alcohol (PVA) phantom seems to be the most suitable candidate. PVA is a synthetic polymer which through freeze-thaw cycles can be crosslinked. This results in a polyvinyl alcohol cryogen also known as '*PVA-C*'. PVA-C can be used as a ultrasound phantom due to its similar mechanical properties to human tissue (Zell, Sperl, Vogel, Niessner, & Haisch, 2007). By varying concentrations and number for freeze-thaw cycles, the stiffness of the phantom can be manipulated. PVA-C has been used as a phantom for liver (de Jong et al., 2017) and prostate tissue (Li, Jiang, Yu, Yang, & Yang, 2015) and is regarded to be a suitable phantom for needle implantations.

Before the SN reaches the prostate, it must first pass through mostly muscular and adipose tissue. Farrer et al. (2015) provide an overview of mechanical characteristics of different tissues. Muscular tissue at rest is presented to have a Young's modulus of between 6 and 15kPa. Fat tissue (from the breast) is presented to have a Young's modulus between 12 and 26kPa. McAnearney et al. (2011) present several sources of prostate stiffness measurements. A tremendous range of Young's moduli are presented for diseased prostate tissue (between 5 and 200 kPa). A more recent study with a larger sample size by Rouvière et al. (2017) shows different Young's moduli for the different zones of the prostate. Prostate cancer generally starts in the peripheral zone (PZ) (Paulsen & Waschke, 2013). In the PZ the Young's modulus of cancerous prostate tissue was found to be 39 to 77kPa (Rouvière et al., 2017).



There is a large stiffness difference between the prostatic tissue and the tissue that surrounds it. To ensure the SN can perform in both extremes, instead of trying to develop a multi-material phantom, we will design two phantoms. One with a stiffness approximating muscular and adipose tissue (±15kPa) and the second approximating prostatic tissue (±50kPa). If the needle is able to steer accurately both in phantoms, it should show the ability to steer in a combination of those phantoms.

In the design of PVA-C phantom, the ratio of PVA to solvent and the amount of freeze-thaw cycles both influence the stiffness of the phantom. The paper by Jiang, Liu, and Feng (2011) describes a 3 wt.% PVA-C phantom that underwent a single freeze-thaw cycle to have a Young's modulus of 3.6 kPa and a 3 wt.% PVA-C phantom that underwent five freeze-thaw cycles to have a Young's modulus of 11.4 kPa. This paper also noted the phantom to have properties similar to porcine liver. The thesis by Repetti (2019) describes the Young's moduli of 5, 10 and 15wt.% PVA-C phantoms with 1 to 5 freeze-thaw cycles. While there seems to be a positive correlation between the young's modulus of the phantom, the concentration and the number of freeze cycles, the data indicates that an additional freeze cycle could have the effect of decreasing the young's modulus instead of increasing it. It is therefore difficult to predict what concentration and number of freeze cycles we will need to achieve our desired stiffness.

Duboeuf et al. (2009) present two 10wt.% PVA-C phantoms that underwent two and five freeze-thaw cycles to have Young's moduli of 65.4 ±3 kPa and 167.4 ±10 kPa respectively. Fromageau, Brusseau, Vray, Gimenez, and Delachartre (2003) previously showed phantoms that are practically the same, to have Young's moduli of 52.4 ±9.2 kPa and 89.1 ±6.3 kPa respectively. Duboeuf et al. (2009) stress the importance of verifying the stiffness of a PVA-C phantom before any experiment as not only PVA concentration and number of freeze-thaw cycles but also freezing, thawing, and degassing time and manufacturing methods could influence the stiffness of the phantom. Therefore, preparing a phantom simply from instructions found in literature is inadequate to ensure an accurate phantom. The strength and stiffness of PVA-C is also depended on the degree of hydrolysis of the PVA used to produce the phantom (Schindler & Hauser, 2004).

To produce the two phantoms with a stiffness of ±15 and ±50kPa, we will manufacture two 10wt% PVA-C phantoms. The PVA will be dissolved in a 60:40 mixture of water and antifreeze, the antifreeze will help to maintain dimensional accuracy. The phantoms will undergo successive freeze-thaw cycles with a mechanical test after each cycle to determine its stiffness. Once the appropriate stiffness for each phantom has been reached, the phantoms are ready for use. We expect the 15kPa phantom to require a single freeze-thaw cycle and the 50kPa phantom between 4 and 5 cycles.

5.1.1. Materials and methods

Two 10wt.% PVA-C phantoms of approximately 350x130x90mm were produced. After every freeze-thaw cycle, an approximately 40mm cube cut from the phantoms underwent a compression test. A 9N force sensor (Futek) was used to measure normal force. To calibrate the sensor, weights of a known mass were hung from the sensor and the corresponding voltage was measured. Formula 12 shows the formula to calculating the Young's modulus of a sample undergoing force 'F' being deformed ' Δ L'. L₀ is the original length of the sample, A is the area of the sample.

A gel can be difficult to measure accurately. The measured dimensions of the sample are critical in the determination of the stiffness of the sample (Formula 12). It is therefore critical to use a large enough sample, as a small measurement error in the size of the sample can skew the results significantly.

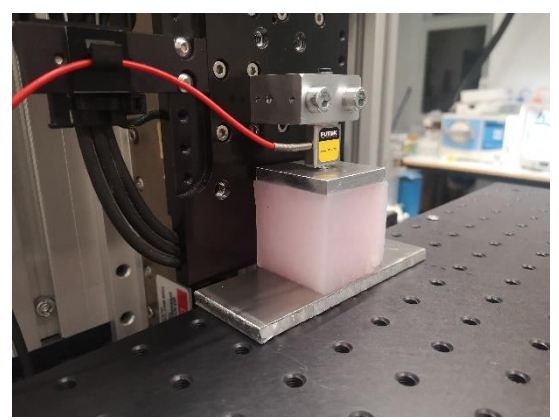


Figure 35 Phantom compression test using a linear stage and a 9N force sensor

Using a sample cube with ribs of 15mm, a measurement error of 2mm would skew the results $(\frac{15^2-13^2}{15^2}*100)$ 24.9%. In a 40mm cube by comparison, a 2mm measured error would only skew the results $(\frac{40^2-38^2}{40^2}*100)$ 9.8%.

$$E = \frac{FL_0}{A\Delta L}$$



The Young's modulus of PVA-C depends on the strain rate (Duboeuf et al., 2009; Repetti, 2019). In our experiment the phantom will be uncompressed. We assume the needle insertion does not generate particularly large strains rates in the phantom. To evaluate the stiffness, the cube will be compressed at a rate of 0.1mm per second to minimise strain-rate effects. The stiffness of our phantoms will be measured between 0% and 10% strain. Every sample is compressed to 10% strain ten times over the axis of eventual needle insertion by a linear stage. A force sensor reads the normal force of the sample with a frequency of 200hz. Figure 35 shows the setup used to measure the stiffness of the samples.

5.1.2. Results

The mean of the ten repetitions per sample was taken. Because a significant amount of noise was present in the measurements, a moving mean with a sample width of 100 samples was applied. Figure 36 shows the force over strain graph of per sample. The coloured lines are lines fitted to the data. From the slope of these lines the Young's moduli were calculated. As can be seen in Figure 36, the lines do not all start at 0N. Because the PVA-C cubes are never completely cubic, a small amount of precompression is necessary to ensure good contact between the stage and the sample. Since we are interested in the slope of the line a small difference in the origin of the slope should only slightly skew the measurements.

The results of the stiffness validation can be found in Table 8. In Appendix F.4 an example of the raw data and a force-time graph of the experiment can be found.

From Section 5.1.1 we concluded two phantoms with approximate Young's moduli of 15kPa and 50kPa are suitable for the performance evaluation. A 10 wt.% PVA that underwent 1 freeze-thaw cycle and another that underwent 5 freeze-thaw cycles correspond best to these values.

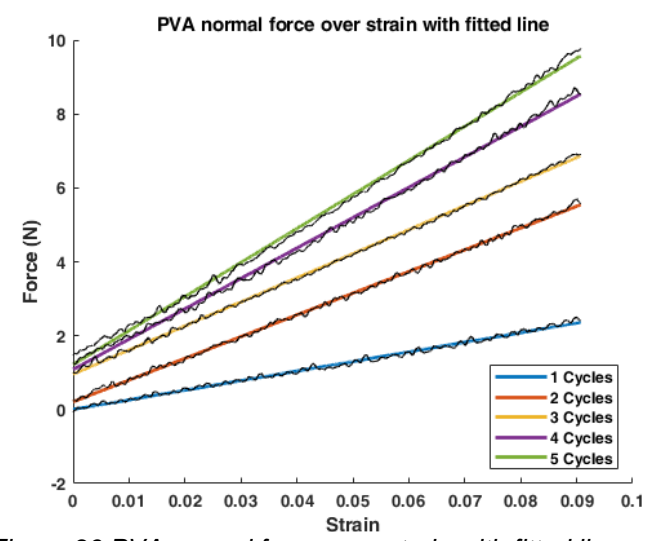


Figure 36 PVA normal force over strain with fitted line

Free-thaw cycles	Mean Young's modulus (kPa)
1	13.6
2	30.7
3	34.1
4	43.0
5	48.2

Table 8 Phantom stiffness verification n = 10



Materials and methods

Similar to the experiment described in Chapter 3, we will insert the needles approximately 90mm into a phantom. We define ten experimental conditions (EC) which can be seen in Table 9. The first two are the commercially available needle tested in both phantoms, these will not be steered. This will give us the error of currently available systems to compare with performance of our prototype. The second two EC's are the SN prototype inserted without active steering into both phantoms to find the average error of the prototype without steering. The next two EC's are actively correcting the prototype SN to minimise the endpoint error of the needle. EC₄₁ and EC₄₂ entail placing the target endpoint 15mm or 7.5mm out of the direct projected path of the SN (Figure 37). This situation mimics actively steering around anatomy. The last EC's are derived from a relevant question from physicians Table 9 Experimental conditions

n = 20	Muscular and adipose phantom	Prostatic phantom
Commercially available needle	EC ₁₁	EC ₁₂
Non-steered SN	EC ₂₁	EC ₂₂
Correcting	EC ₃₁	EC ₃₂
Active steering	EC ₄₁	EC ₄₂
Retracted then active steering	EC ₅₁	EC ₅₂

from the Erasmus medical centre (EMC). The question being: Is the needle able to leave a previous made pathway? It is imageable a physician is not satisfied with the position of a steerable needle and would like to retract the needle somewhat to subsequently reinsert the SN to improve its position. The last two EC's will entail driving the needle to end of the phantom without steering, retracting approximately 50mm and subsequently steering the needle to a predetermined target (Figure 38).

A digital microscope (Dino-Lite) will be aligned with the central template hole. After each insertion the microscope will take an image to evaluate the vertical deviation from the central line. Horizontal deflection will not be considered, as the ultrasound modality available to us (Phillips HD7 XE) is unable to provide threedimensional visualisation. A PETG wedge will be used as an ultrasound target. The wedge is mounted on rails so it can be removed before every image and accurately put back.

To ensure the needle paths do not intersect the phantom will be moved laterally 10mm between insertions in every experimental condition. To maximise the number of possible insertions in the developed phantoms, the phantom will be raised 25mm after one row of insertions is performed. Both phantoms will be allowed to come up to room temperate (20°). To negate any temporal or learning effects, all insertion will be randomised for each phantom. Randomisation between the phantoms would entail excessive manipulation of the phantom, likely resulting in damage to the phantoms. Therefore, all insertions in the lower stiffness phantoms will be performed first, followed by the higher stiffness insertions. This diminishes the value of comparison between EC's in different phantoms, as learning effects influence the results between phantoms. We are interested in the comparison between the commercially available needle and our SN prototype. To ensure the

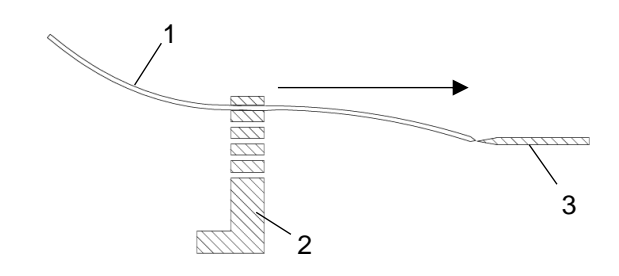


Figure 37 EC₄₁ and EC₄₂; Active steering (1: SN, 2: Template, 3: PETG wedge)

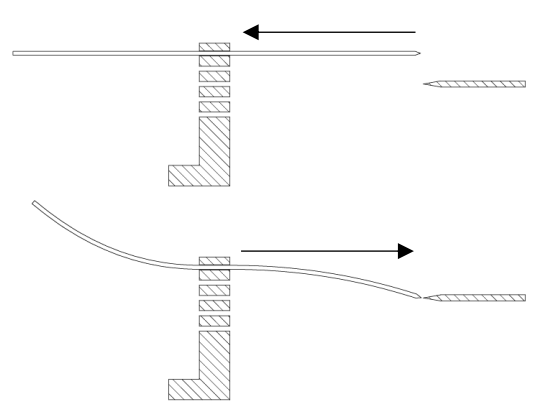


Figure 38 EC₅₁ and EC₅₂; Top shows retraction, bottom shows active steering.

validity of the experiment we use a 'best-case' and 'worst-case' phantom. The comparison of EC between phantoms is therefore of minor interest. Because needle tracks left by previous insertions make the ultrasound



visualisation more difficult, the correcting and active steering EC's will be performed before EC_{1x} and EC_{2x} . Because there is likely no learning effect in EC_{1x} and EC_{2x} , this should not skew any results.

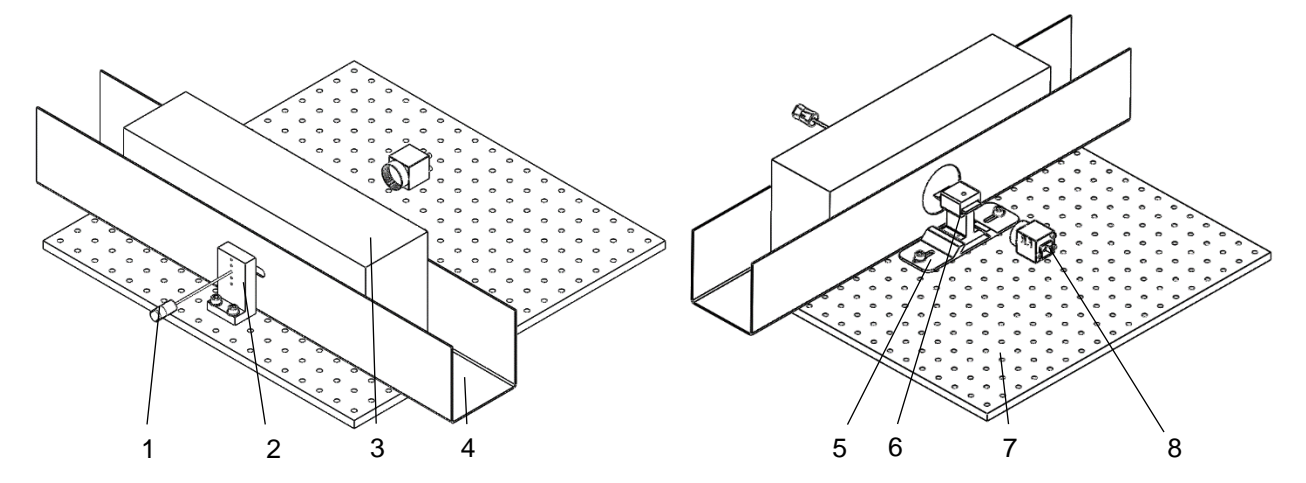


Figure 39 Experimental setup (1: SN, 2: Template, 3: Phantom, 4: Phantom shoot, 5: Target guide, 6: Target slide, 7: Mounting plate, 8: Camera)

Figure 39 shows the experimental setup. The phantom (3) is contained in a shoot (4). The SN (1) is inserted through a template (2) into the phantom. The top of the phantom is exposed to enable ultrasound visualisation. To give the SN a target, a PETG wedge in a slide is placed against the phantom (6), this slide moves along a guide (7). Before every run, the slide is placed in the guide and pressed into the phantom. The PETG wedge gives a clear target on the ultrasound. After every run, the slide is removed and an image is taken with the digital microscope (8). From the footage the deviation from the target will be determined. Only deflections in the vertical plane will be measured. For the non-steered EC's both horizontal and vertical deflection measurements will be taken as ultrasound guidance is unnecessary in these EC's. Horizontal deflections will not be discussed in this thesis.

The dimension of the holes in the template (Figure 39 (2)) and thickness of the template are critical in the amount of leeway a needle has in the hole and will likely impact the deviation of said needle. Elekta was kind enough to provide us with the dimensions of the holes in their template which were replicated. Our template is 15mm thick and has holes of $2.1\frac{+0.05}{-0.05}$ mm. Because we are only able to visualise horizontal displacement, our template only has vertical holes. The template has five holes. The middle one is used for all non-steering and correcting EC's. The holes used in EC₄₁, EC₄₂, EC₅₁, and EC₅₂ are located 7.5mm and 15mm above and below this central hole (Figure 38).

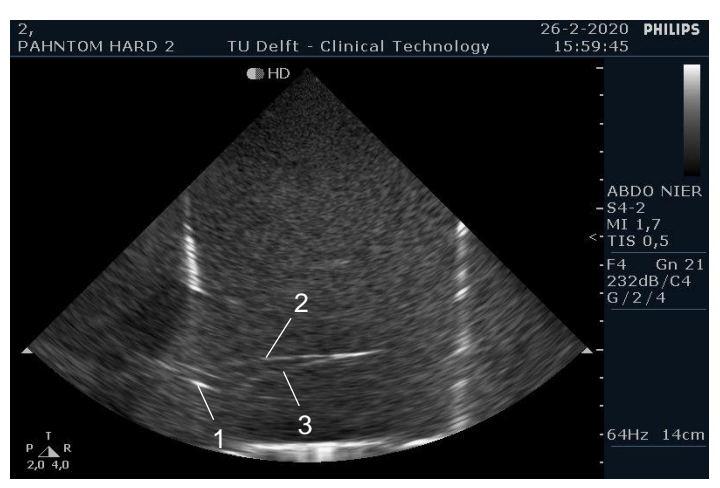


Figure 40 Example ultrasound visualisation EC10 (1: PETG target, 2: retracted needle path, 3: SN)



Figure 41 shows the final setup of the experiment. The left image shows the turned steel rod to calibrate the PETG target and digital microscope. The right image shows the phantom in the shoot and in the background the ultrasound equipment used to visualise the needle insertions. Figure 40 shows an example of the ultrasound visualisation. The PETG target can be seen as a bright spot on the left of the image (1). This image was taken during an insertion for EC₅₂, the needle path of the retraction (2) can clearly be seen above the current position of the SN (3). The null hypnosis is that there is no difference between the EC's. The alpha used is 0.05.



Figure 41 Final experimental setup (left: Steel calibration rod, right: phantom in shoot with ultrasound machine)

5.3. Results

Figure 42 shows a scatterplot of the error of all needle insertions performed. For the non-steered experimental conditions both the vertical and the horizontal error can be seen. Because we had no means to visualise the horizontal error in the steered experimental conditions, the horizontal error was not measured in these EC's. Table 10 shows the means of every EC. As can be seen in Figure 42 the mean of all insertions is around 0, to be able to extract a meaningful error, the absolute error will be used. When using the absolute error, the data collected fails normality tests. This is likely due to the skewedness resulting from taking the absolute error. Because the conditions are ranked and non-normal, a Kruskal-Wallis test is most appropriate to analyse the

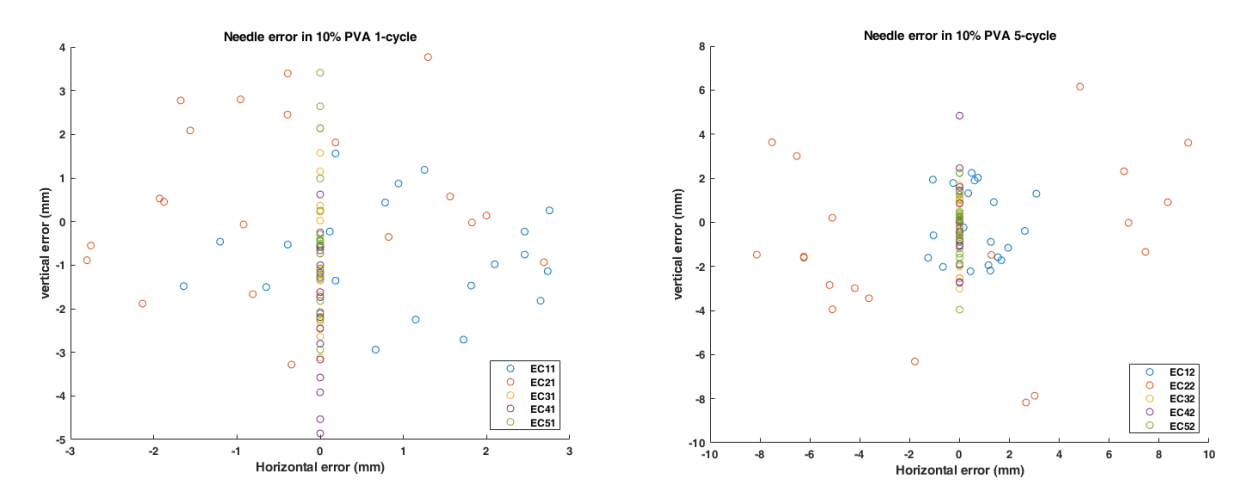


Figure 42 Scatterplot of error needle insertions. Left shows PVA phantom that underwent 1 freeze-thaw cycle, right shows phantom that underwent 5 freeze-thaw cycles



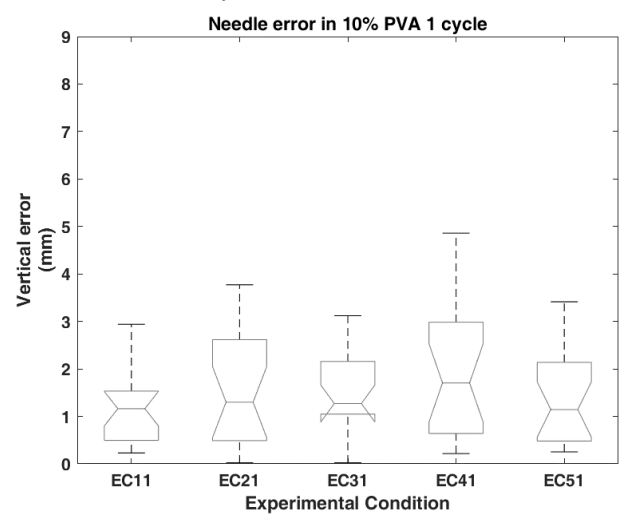
results. There was no randomisation between phantoms, this allows for the possibility that learning has a significant effect of the findings phantoms. It is therefore between both inappropriate to directly compare the correcting and active steering EC's from both phantom to one

Figure 43 shows a boxplot for the low stiffness phantom (left) and the high stiffness phantom (right). Noticeable is the difference in absolute error Table 10 Performance evaluation absolute mean error between EC11 and EC12 but also EC21 and EC22, (mm) (Light grey: lowest value, dark grey: highest which as expected indicates a stiffer phantom value)

N = 20	EC _{1x}	EC _{2x}	EC _{3x}	EC _{4x}	EC _{5x}
EC _{x1}	1.21	1.52	1.46	1.95	1.39
EC _{x2}	1.50	3.15	1.15	1.45	1.07

increases needle error. Conversely, the error found in the correcting and steering EC's seems to decrease with a stiffer phantom. Because we were unable to randomise between phantoms this effect could very well be due to the effect of learning, as the insertions on the stiffer phantom (right) were performed after the less stiff phantom (left). From comparing EC₂₂ with EC₃₂, EC₄₂, and EC₅₂ we can clearly see correcting and steering decreases endpoint error.

A Kruskal-Wallis test shows no statistically significant differences between the measured deflections of the insertions in the low-stiffness phantom (χ^2 _(4, N = 20) = 2.75, p = 0.60). The lack of effect is likely to be at least partially due to the low sample size (n=20). A Kruskal-Wallis test of the stiff phantom does show statically significant differences in mean ranks (χ^2 _(4, N = 20) = 17.22, p = 0.0018). The EC's that significantly differ from one another are EC_{22} and EC_{32} (p=0.0089), also EC_{22} and EC_{52} (p=0.0019). The mean ranks of EC_{22} and EC_{42} fall just shy of differing significantly (p=0.053). From these results can be concluded, that in the stiffer phantom correcting or active steering does increase needle endpoint accuracy. While not significant, the large difference in medians between EC22 and EC12 does seem to imply the developed SN performs worse when un-steered in stiff tissue compared to the much stiffer commercially available needle.



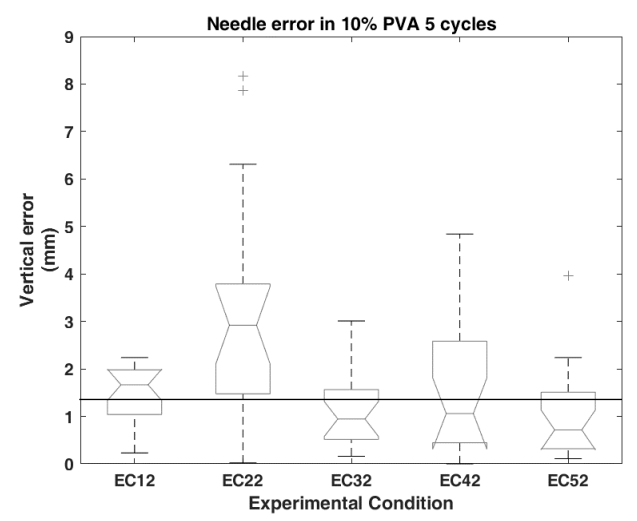


Figure 43 Boxplot absolute needle error performance evaluation. Left shows the insertions into the 1 cycle phantom, right shows the insertions into the 5 cycles phantom. The black horizontal line in the right figure shows the lower bound of the 95% confidence interval of EC₁₂.

When we draw a horizontal line at the lower limit of the 95% confidence interval of the median in EC₁₂, we find it does not intersect with the 95% confidence interval of both EC_{32} and EC_{52} . This would indicate the true median of EC₁₂ differs from EC₃₂ and EC₅₂. While not significant in a Kruskal-Wallis test, this does at minimum indicate non-inferiority.

The experiment was performed with a different type of ultrasound equipment used generically in HDR BT and without prior ultrasound experience. One issue that arose occasionally was the acquirement of a wrong target. Slight damage to the phantom can present a similar ultrasound signature as the PETG target. This, at least in part, explains the large variety in the steering EC's and the outliers (EC₅₂ for example). Because it is difficult to determine if an insertion with a particularly large error was due to acquiring a wrong target or simply poor



steering, no outliers were removed. The learning effect is one explanation for the large difference in correcting and active steering errors between the phantoms. To illustrate this effect, when combining the first half of the insertions of every correcting and steering EC and comparing those to the second half of insertions of every correcting and steering EC, we find a difference in means: 1.61 and 1.22 respectively. A Wilcoxon rank sum test shows a significant difference in mean ranks (Z = 1.98, p = 0.048). It should be noted that the end-user of the instrument is expected to have some degree of training and will therefore probably perform more like the insertions in the stiffer phantom.

The vertical distance from the neutral axis of the PETG target in the active steering EC's was either 7.5mm or 15mm. When combining the values from both phantoms the mean absolute errors between the 7.5mm and 15mm offset are 1.720mm and 1.719mm respectively (n=40). A Wilcoxon rank sum test shows no significant difference in mean ranks (Z=0.30, p=0.76). The results would indicate there is no difference in steering accuracy between 7.5mm and 15mm. This once again demonstrates the ability of the SN to steer 15mm of a 50mm insertion.

From the insertions in the low stiffness phantom Figure 43 (left) little conclusions can be drawn. From Figure 43 (right) we have found correcting and active steering increases the endpoint accuracy in comparison the SN inserted non-steered. There seems to be little evidence of significant difference in error between the correcting (EC_{3x}) , active steering (EC_{4x}) and (EC_{5x}) retracting then steering. When considering the experimenters lack of ultrasound experience, the absence of needle deflection due to patient movement and inhomogeneity of the tissue, and limited sample size we can conclude that at minimum this experiment provides evidence of the non-inferiority of this SN in HDR BT needle implantation. To provide definitive evidence of the efficacy of the SN in comparison to a commercially available needle, an experiment with a larger sample size should be performed by a medical profession with ultrasound aptitude in a more representative phantom.

5.4. Cost-effectiveness

Appendix A Section 3.2.4 describes the cost-effectiveness of a HDR BT procedure, HDR brachytherapy's popularity as a booster for EBRT is likely in part due its cost-effectiveness (Morris et al., 2017). To ensure adoption of the SN, it is of critical importance the system does not significantly decrease the cost-effectiveness of the procedure. By estimating the additional cost of the SN and take into account possible cost reductions resulting from its use, we hope to make an estimation of the systems cost-effectiveness.

5.4.1. Cost of the steerable needle

The paper by Ilg et al. (2016) reports 'Flexi Needles' used in HDR BT monotherapy to cost \$459.78,- per procedure. Establishing an exact cost of the needles the SN would be replacing is difficult as the manufacturers of these needle do not make their prices publicly available. One of the advantages of this SN is its striking similarity with systems currently in use. The Mick FlexiGuide® system also used a single use steel stylet with a polymer handle. The only significant difference between the developed SN and existing systems are the two wire-EDM slots that enable the steering. We can therefore say, the only added cost of the developed system is the machining of the slots.

We will assume an EDM wire diameter of 0.254mm (0.01 inch) and a length of cut of approximately 360mm. The two slots would take approximately 43 minutes ("High-Performance Wire EDM: Speed Isn't Everything," 2004) According to CES in an automated EDM process, an operating cost of \$50,- per hour is achievable. This would mean the production of the developed SN would cost approximately €32,- more than currently available systems. Increasing the production cost has a large impact on the final cost of the system. In consumer products, a multiplication of four is often used to roughly estimate the retail price from a production price. While the consumer and medical world are obviously very different, we will use the same conversion factor to give an indication of the retail price in absence of a better method. This would mean, the SN will be roughly €130,-more expensive per procedure then currently used systems.

The SN could possibly be manufactured by methods other than EDM, for example by using LASER cutting or micro machining. Soldering four extruded wire quadrants together might also be an option. These developments could decrease the production cost of the SN. For this cost-analysis we will assume EDM to be the manufacturing technique, in future development of the system this topic should be revisited.



5.4.2. Potential cost reductions

There are several potential cost reductions to be gained by using a steerable needle. The SN could enable more accurate needle placement resulting in less needle relocations. This in turn would reduce procedure time. A reduction in procedure time would reduce personnel costs and allow more procedures per day, reducing the overhead costs of the operation room and equipment. By reducing the amount of retraction and reinsertions, tissue trauma and related late toxicities could be reduced. Less late toxicity means less rehospitalisation and reduced lifetime cost. By actively steering around sensitive anatomy, late toxicities could possibly be further reduced. Finally, the SN could ensure more patients to be suitable for HDR BT, therefore reducing the need for more costly procedures.

Physicians from the Erasmus Medical Centre indicated a routine needle implantation for HDR BT to take approximately 30 to 45 minutes (Appendix D.4). Childers and Maggard-Gibbons (2018) found a Californian operating room to cost on average \$36,- to \$37,- per minute. That means a four-minute decrease in procedure time would make the SN cost-effective in California. While OR costs vary greatly between country and hospitals, a small reduction in operating time could make a significant impact on the cost-effectiveness of the developed system.

The rate of AUR in HDR BT is approximately 10% (Buskirk et al., 2004; Skouteris et al., 2018). In complicated cases AUR requires hospitalisation. A Belgian study by Lamotte et al. (2005) found the six month costs related to hospitalisation in the case of AUR to be \leq 4.722,- (SE= \leq 526,-). The SN could allow for less tissue trauma or the avoidance of sensitive tissue, reducing the instances of AUR. Even a small reduction in AUR significantly improves the cost-effectiveness of the SN.

Vu, Blas, Lanni, Gustafson, and Krauss (2018) showed IMRT with a HDR BT boost to be cost-effective in intermediate to high risk patients in comparison to IMRT only, with associated lifetime costs of \$68.696,- and \$114.944,- respectively. A patient with risk of PAI could be advised to undergo IMRT only. The SN could allow such patients to undergo IMRT with an HDR BT boost, the added cost of the SN would in this case be justifiable.

Improving the quality of an HDR BT implantation could naturally improve the outcome of the procedure. This would decrease the necessity of costly salvage treatments. The possible cost reductions listed above only serve to indicate the possibility of the developed SN being cost-effective. Unfortunately, in this stage we cannot make a substantiated claim about the cost-effectiveness of the developed system. We do however hope to have shown the possibility of its cost-effectiveness.





Abstract

The steerable needle developed shows promise in being able to steer a reasonable amount with respectable endpoint accuracy. The simplicity and compatibility of the system mean the compliant mechanism could be applied to a whole range of high dose-rate brachytherapy procedures. The main question remaining concerns the medical implications of the steerable needle. Possible advantages have been presented but should be quantified before allocating resources to the further development of the steerable needle. With the quantitative information about the medical advantages of the steerable needle, determining the potential cost-effectiveness of the system should be straightforward.



The literature study at the beginning of this document has provided the clinical relevance of a steerable needle in high dose-rate brachytherapy of the prostate. The previous chapters have presented the design process and evaluation of the steerable needle in question. This chapter will discuss the findings presented, critically examine the evidence, and provide recommendations for the further development of the steerable needle.

6.1. The big picture

The aim of this thesis was to develop a manually operated steerable needle for high dose-rate brachytherapy. To accomplish this goal several requirements were set, of which the most important were:

- The ability to steer a minimum of 15mm over an insertion of 50mm;
- The ability to increase endpoint accuracy;
- The compatibility with existing equipment;
- Retaining the cost-effetiveness of HDR BT of the prostate.

Every experiment performed has shown the ability to steer a minimum of 15mm over an insertion of 50mm. While an insertion in vivo will certainly present new challenges, all evidence suggests sufficient steering capability. Endpoint accuracy was described mostly in the previous chapter. While most results were non-significant, likely due to small sample size and an inexperienced experimenter, the SN showed, at minimum, evidence of non-inferiority compared to a commercially available stylet. The simplicity of the design means it can be a drop-in replacement for existing stylets. And the relative low cost of the system could make the SN a cost-effective instrument.

The ability to steer around obstacles can be useful in HDR BT, for example to treat patients with PAI, or access the area of the prostate occluded by the urethra. This thesis also presents one of the advantages of a SN to be the ability to avoid sensitive tissues. While there is evidence of needle trauma being related to late toxicities in HDR BT of the prostate, reducing this trauma requires the development of a new insertion technique. Which, unfortunately, is outside the scope of this thesis. A 'curvilinear implantation' has been theorised to improve prostate HDR BT outcome. The 15mm steering over a 50mm insertion has been treated as a minimum. From concept evaluation experiment we can see the developed system is able to steer more then this minimum. With the available amount of steering a large part of the sensitive tissues mentioned could be avoided by steering.

This thesis does not provide conclusive evidence of increase endpoint accuracy compared to commercially available systems. It does however show the possibility of increasing endpoint accuracy is with a SN in a phantom. The presented performance evaluation suffers from a small sample size, a homogeneous non-moving phantom, an inexperienced experimenter, and only evaluating steering in one plane. In non-homogeneous moving tissue, the amount of noodle deflection to compensate for will likely be larger. In these conditions, a more experienced experimenter with a larger sample size could possibly achieve statistical significance. Despite its flaws, the performance evaluation experiment shows the means and medians of every correcting and actively steered EC in the stiffer phantom to be lower than those of the non-steerable commercially available needle. In the case of HDR BT of the prostate the main advantage of increased endpoint accuracy should be the decrease in retractions and procedure time. Whether the use of an SN does in fact decrease procedure time and needle retractions should be investigated in future development.

By ensuring the system is compatible with existing equipment (sleeves, templates, and visualisation modalities) the steps needed for adoption are greatly reduced. Additionally, this means the system can easily be adapted for use in other HDR BT procedures. For example, in breast HDR BT, needles are passed through a template, through the breast and are expected to emerge through the same hole in an opposite template. In this procedure, the same stylets and sleeves are used as in HDR BT. If the developed SN can provide value in HDR BT of the prostate it is imaginable it can do the same in other HDR BT procedures.

The cost-effectiveness of the developed system remains unsubstantiated. The effect the developed steerable needle will have on the outcome of an HDR BT procedure is simply too complex to predict. As presented in the previous chapter, the developed SN is to cost approximately €130,- more than currently available systems. While this might seem costly for a disposable instrument, when lifetime costs of a prostate HDR BT procedure exceed \$50,000,- in the United States, even a small improvement in procedure outcome can make the



instrument cost-effective. The further development of the SN might decrease the unit cost increasing the chances of the system's cost-effectiveness.

6.2. Challenges

The preceding literature review presents evidence of steering capability and increased endpoint accuracy potentially improving the outcome of HDR BT prostate procedures. This thesis provides preliminary evidence of the steering and endpoint accuracy potential of this SN. The main question now becomes if increased accuracy and steering potential does in fact positively influence the outcome of an HDR BT procedure. This piece of evidence is required in providing conclusive evidence of the benefit of the developed SN in HDR BT of the prostate. An answer to this question would legitimise the further development of the system. Answering this question would also provide the crucial information required to make an informed estimation of the cost-effectiveness of the system.

A statistically significant learning effect was uncovered in the performance evaluation experiment. This speaks to the probability that medical staff will require some training to effectively use the SN. Like many surgical instruments, the efficacy of the instrument will largely depend on the aptitude of the surgeon. This means providing high-quality training becomes as important as providing a well-designed instrument. Steering in this thesis has only been studied in a single plane due to visualisation constraints. Whether a trained surgeon will be able to steer in two planes with similar accuracy as can be achieved in a single plane, will have to be examined.

There is evidence to support the need for steerable needles in HDR BT and evidence of the desire of medical personnel to have access to the instrument. To be adopted, using a SN will have to be cost-effective. This means, firstly, quantitatively determining the effects of the developed SN on an HDR BT prostate procedure. Secondly, developing the SN further to formulate a more accurate estimation of the system's cost. The value of this design is in its simplicity and therefor low-cost. Should this system turn out not to be cost-effectiveness, it is unlikely any SN will be cost-effective for an HDR BT procedure of the prostate

6.3. Recommendations

The current manufacturing cost is an estimation based on literature. The simplest way to determine a more accurate cost would be to approach manufacturers and have them advise on the manufacturing process and associated costs. In this stage it could prove fruitful to explore the availability of a superelastic material with a similar Young's modulus compared to the steel used in the prototype. We were unable to find such a material. The main cost of producing the stylet are the EDM'ed slots. This issue was previously addressed by soldering four wires together. However, four round wires have the tendency to slip which results in decreased steering potential. By joining four extruded quadrants this issue should not arise. Because extruded steel quadrants in the required dimensions are not readily available, we were unable to test this theory. In further development this manufacturing technique should be explored.

All evidence of steering and endpoint accuracy in this thesis is provided in artificial phantoms. To provide a more valuable comparison, the developed SN should be compared to commercially available systems in biological tissue. The experiment should be performed by someone experienced with ultrasound visualisation. The experiment should also involve the appropriate equipment and setting. Lastly a larger number of repetitions should be performed to increase the power of the experiment. Whether the phantom is porcine, canine or cadaver, the increased realism from having non-homogeneous anisotropic tissue and the appropriate target to steer towards should make for a more valuable comparison.

From literature and consultation with experts we uncovered several possible advantages and disadvantages of using a steerable needle in high dose-rate brachytherapy of the prostate. Based on these advantages and disadvantages the steerable needle was developed. In reality, the exact way the steerable needle will be used and what advantages it can have will have to be determined by its end-user, the surgeon. It is imaginable that there are use-case for the steerable needle that have not been discussed in this thesis. Just as likely there are disadvantages of using a steerable needle that have not been discussed. We therefore believe it is imperative to closely involve the end-user of the system, the surgeon, in the further development of the steerable needle.



The mechanical properties and design requirements of the SN have been reported in this thesis. The literature study warrants the further investigation of using a SN in HDR BT. To show the medical benefit of using an SN for HDR BT, a quantitative study should be performed preferably by someone with a medical background. With this information a verdict on the value and cost-effectiveness of the SN can be made. Once the above mentioned is available, there would be a working prototype, evidence of its efficacy in biological tissue and quantitative information of the medical advantages of said prototype. This should be everything needed to make a well-grounded ruling on the further development of the SN.



Conclusion

This thesis presents the first evidence of the value of this compliant mechanism steerable needle for high dose-rate brachytherapy of the prostate. By minimising complexity and maximising compatibility an effort is made to design a steerable needle that not only allows the surgeon to perform a new set of manoeuvres but can also easily be adopted into the existing workflow. The compatibility with existing sleeve designs mean the concept is not limited to high dose-rate brachytherapy of the prostate but could be used in numerous high dose-rate brachytherapy procedures.

The amount of steering the needle has shown should be sufficient to help the surgeon in dealing with pubic arch interference and steering to sections of the prostate occluded by the urethra. The amount of steering could also allow for the development of a novel implantation method sparing sensitive tissues. This thesis fails to reach the significance threshold when comparing the endpoint accuracy of the developed steerable needle to a commercially available needle. However, with a more representative phantom an more power statistical significance could likely be achievable in further research.

By improving the production process the manufacturing cost of the system could be decreased. By involving the end-user of the system in the early development, new advantages and disadvantages of the steerable needle could be uncovered. The next steps in the development of this system should include quantifying the possible advantages of the steerable needle to be able to make an informed decision about its added benefit to the field of high dose-rate brachytherapy.



Bibliography

- Abolhassani, N., Patel, R., & Moallem, M. (2007). Needle insertion into soft tissue: A survey. *Medical Engineering & Physics*, 29(4), 413-431. doi:10.1016/j.medengphy.2006.07.003
- Adebar, T. K., Greer, J. D., Laeseke, P. F., Hwang, G. L., & Okamura, A. M. (2016). Methods for Improving the Curvature of Steerable Needles in Biological Tissue. *IEEE transactions on bio-medical engineering*, 63(6), 1167-1177. doi:10.1109/TBME.2015.2484262
- Aluwini, S., Busser, W. M., Baartman, L. E., Bhawanie, A., Alemayehu, W. G., Boormans, J. L., & Kolkman-Deurloo, I. K. (2016). Fractionated high-dose-rate brachytherapy as monotherapy in prostate cancer: Does implant displacement and its correction influence acute and late toxicity? *Brachytherapy*, *15*(6), 707-713. doi:10.1016/j.brachy.2016.05.008
- Andersson, K.-E., & Michel, M. C. (2011). Urinary Tract. Heidelberg: Springer.
- AprioMed. (2019). Morrison Your first choice for deep-seated targets. In AprioMed (Ed.).
- Arredondo, S. A., Downs, T. M., Lubeck, D. P., Pasta, D. J., Silva, S. J., Wallace, K. L., & Carroll, P. R. (2008). Watchful waiting and health related quality of life for patients with localized prostate cancer: data from CaPSURE. *J Urol*, 179(5 Suppl), S14-18. doi:10.1016/j.juro.2008.03.132
- ASM. (2020). ASM Materials Information. Retrieved from https://matdata.asminternational.org/mmd/index.aspx?history=114190&dbKey=grantami_mmd
- Astrom, L., Sandin, F., & Holmberg, L. (2018). Good prognosis following a PSA bounce after high dose rate brachytherapy and external radiotherapy in prostate cancer. *Radiother Oncol, 129*(3), 561-566. doi:10.1016/j.radonc.2018.08.011
- Balgobind, B. V., Koedooder, K., Ordonez Zuniga, D., Davila Fajardo, R., Rasch, C. R., & Pieters, B. R. (2015). A review of the clinical experience in pulsed dose rate brachytherapy. *Br J Radiol, 88*(1055), 20150310. doi:10.1259/bjr.20150310
- Bellon, J., Wallner, K., Ellis, W., Russell, K., Cavanagh, W., & Blasko, J. (1999). Use of pelvic CT scanning to evaluate pubic arch interference of transperineal prostate brachytherapy. *International Journal of Radiation Oncology Biology Physics*, *43*(3), 579-581. doi:10.1016/S0360-3016(98)00466-0
- Bhattacharya, K., & Kohn, R. V. (1996). Symmetry, texture and the recoverable strain of shape-memory polycrystals. *Acta Materialia*, *44*(2), 529-542. doi:10.1016/1359-6454(95)00198-0
- Blumenfeld, P., Hata, N., DiMaio, S., Zou, K., Haker, S., Fichtinger, G., & Tempany, C. M. (2007). Transperineal prostate biopsy under magnetic resonance image guidance: a needle placement accuracy study. *J Magn Reson Imaging*, *26*(3), 688-694. doi:10.1002/jmri.21067
- Burdette, E. C., Rucker, D. C., Prakash, P., Diederich, C. J., Croom, J. M., Clarke, C., . . . Webster III, R. J. (2010). *The ACUSITT ultrasonic ablator: the first steerable needle with an integrated interventional tool* (Vol. 7629): SPIE.
- Burgner, J., Swaney, P. J., Bruns, T. L., Clark, M. S., Rucker, D. C., Burdette, E. C., & Webster, R. J. (2012). An Autoclavable Steerable Cannula Manual Deployment Device: Design and Accuracy Analysis. *J Med Device*, 6(4), 410071-410077. doi:10.1115/1.4007944
- Buskirk, S. J., Pinkstaff, D. M., Petrou, S. P., Wehle, M. J., Broderick, G. A., Young, P. R., . . . Igel, T. C. (2004). Acute urinary retention after transperineal template-guided prostate biopsy. *International Journal of Radiation Oncology*Biology*Physics*, *59*(5), 1360-1366. doi:10.1016/j.ijrobp.2004.01.045 Buus, S., Lizondo, M., Hokland, S., Rylander, S., Pedersen, E. M., Tanderup, K., & Bentzen, L. (2018). Needle
- Buus, S., Lizondo, M., Hokland, S., Rylander, S., Pedersen, E. M., Tanderup, K., & Bentzen, L. (2018). Needle migration and dosimetric impact in high-dose-rate brachytherapy for prostate cancer evaluated by repeated MRI. *Brachytherapy*, 17(1), 50-58. doi:10.1016/j.brachy.2017.08.005
- Cancer Facts & Figures. (2019). Retrieved from American Cancer Society: https://www.cancer.org/research/cancer-facts-statistics/all-cancer-facts-figures/cancer-facts-figures-2019.html



- Chao, M., Bolton, D., Lim Joon, D., Chan, Y., Lawrentschuk, N., Ho, H., . . . Khoo, V. (2019a). High dose rate brachytherapy boost for prostate cancer: Biochemical control and the impact of transurethral resection of the prostate and hydrogel spacer insertion on toxicity outcomes. *J Med Imaging Radiat Oncol, 63*(3), 415-421. doi:10.1111/1754-9485.12882
- Chao, M., Ow, D., Ho, H., Chan, Y., Joon, D. L., Spencer, S., . . . Bolton, D. (2019b). Improving rectal dosimetry for patients with intermediate and high-risk prostate cancer undergoing combined high-dose-rate brachytherapy and external beam radiotherapy with hydrogel space. *J Contemp Brachytherapy*, 11(1), 8-13. doi:10.5114/jcb.2019.82836
- Chatzikonstantinou, G., Zamboglou, N., Rodel, C., Zoga, E., Strouthos, I., Butt, S. A., & Tselis, N. (2017). High-dose-rate brachytherapy as salvage modality for locally recurrent prostate cancer after definitive radiotherapy: A systematic review. *Strahlenther Onkol, 193*(9), 683-691. doi:10.1007/s00066-017-1157-2
- Chiang, P. H., & Liu, Y. Y. (2016). Comparisons of oncological and functional outcomes among radical retropubic prostatectomy, high dose rate brachytherapy, cryoablation and high-intensity focused ultrasound for localized prostate cancer. *Springerplus*, *5*(1), 1905. doi:10.1186/s40064-016-3584-4
- Childers, C. P., & Maggard-Gibbons, M. (2018). Understanding Costs of Care in the Operating Room. *JAMA Surg*, 153(4), e176233. doi:10.1001/jamasurg.2017.6233
- Chin, J., Rumble, R. B., Kollmeier, M., Heath, E., Efstathiou, J., Dorff, T., . . . Loblaw, D. A. (2017). Brachytherapy for Patients With Prostate Cancer: American Society of Clinical Oncology/Cancer Care Ontario Joint Guideline Update. *Journal of Clinical Oncology*, 35(15), 1737-1743. doi:10.1200/jco.2016.72.0466
- Chong, J. J., Van Hemelrijck, M., Cahill, D., & Kinsella, J. (2016). Serial transperineal sector prostate biopsies: impact on long-term erectile dysfunction. *Ecancermedicalscience*, 10, 643. doi:10.3332/ecancer.2016.643
- CIRS. (2019). TISSUE EQUIVALENT ULTRASOUND PROSTATE PHANTOM. Retrieved from https://www.cirsinc.com/products/ultrasound/zerdine-hydrogel/tissue-equivalent-ultrasound-prostate-phantom/
- Compliant mechanisms explained. (2019). Retrieved from https://www.compliantmechanisms.byu.edu/about-compliant-mechanisms
- Cook Medical. (2019). Choose from our extensive inventory of biopsy and breast lesion devices. In C. Medical (Ed.).
- COUNCIL DIRECTIVE 93/42/EEC, (1993).
- Cowan, N. J., Goldberg, K., Chirikjian, G. S., Fichtinger, G., Alterovitz, R., Reed, K. B., . . . Okamura, A. M. (2011). Robotic Needle Steering: Design, Modeling, Planning, and Image Guidance. In J. Rosen, B. Hannaford, & R. M. Satava (Eds.), *Surgical Robotics: Systems Applications and Visions* (pp. 557-582). Boston, MA: Springer US.
- Datla, N. V., Konh, B., Honarvar, M., Podder, T., Dicker, A. P., Yu, Y., & Hutapea, P. (2014). A model to predict deflection of bevel-tipped active needle advancing in soft tissue. *Medical Engineering & Physics*, *36*(3), 285-293. doi:10.1016/j.medengphy.2013.11.006
- de Jong, T. L., Pluymen, L. H., van Gerwen, D. J., Kleinrensink, G. J., Dankelman, J., & van den Dobbelsteen, J. J. (2017). PVA matches human liver in needle-tissue interaction. *J Mech Behav Biomed Mater, 69*, 223-228. doi:10.1016/j.jmbbm.2017.01.014
- de Jong, T. L., van de Berg, N. J., Tas, L., Moelker, A., Dankelman, J., & van den Dobbelsteen, J. J. (2018). Needle placement errors: do we need steerable needles in interventional radiology? *Med Devices* (Auckl), 11, 259-265. doi:10.2147/mder.S160444
- DEMCON. (2019). Needle positioning system MIRIAM. Retrieved from https://www.demcon.nl/en/showcase/miriam/
- Denmeade, S. R., & Isaacs, J. T. (2002). A history of prostate cancer treatment. *Nat Rev Cancer*, 2(5), 389-396. doi:10.1038/nrc801
- Design of shape memory alloy (SMA) actuators. (2015). New York, NY: Springer Berlin Heidelberg.
- Dilibal, S., Sehitoglu, H., Hamilton, R. F., Maier, H. J., & Chumlyakov, Y. (2011). On the volume change in Co-Ni-Al during pseudoelasticity. *Materials Science and Engineering a-Structural Materials Properties Microstructure and Processing, 528*(6), 2875-2881. doi:10.1016/j.msea.2010.12.056
- DiMaio, S. P., & Salcudean, S. E. (2003). *Needle Steering and Model-Based Trajectory Planning*, Berlin, Heidelberg.
- Duboeuf, F., Basarab, A., Liebgott, H., Brusseau, E., Delachartre, P., & Vray, D. (2009). Investigation of PVA cryogel Young's modulus stability with time, controlled by a simple reliable technique. *Med Phys*, *36*(2), 656-661. doi:10.1118/1.3065031



- Duerig, T. W., Melton, K. N., Stöckel, D., & Wayman, C. M. (1990). *Engineering Aspects of Shape Memory Alloys*: Butterworth-Heinemann.
- Dupont, P. É., Lock, J., Itkowitz, B., & Butler, E. (2010). Design and Control of Concentric-Tube Robots. *IEEE Transactions on Robotics*, 26(2), 209-225. doi:10.1109/TRO.2009.2035740
- Dutta, S. W., Alonso, C. E., Libby, B., & Showalter, T. N. (2018). Prostate cancer high dose-rate brachytherapy: review of evidence and current perspectives. *Expert Rev Med Devices*, *15*(1), 71-79. doi:10.1080/17434440.2018.1419058
- Eapen, L., Kayser C Fau Deshaies, Y., Deshaies Y Fau Perry, G., Perry G Fau E, C., E C Fau Morash, C., Morash C Fau Cygler, J. E., . . . Dahrouge, S. (2014). Correlating the degree of needle trauma during prostate brachytherapy and the development of acute urinary toxicity. *Int. J. Radiation Oncology Biol. Phys.*, *59*(0360-3016 (Print)), 1392–1394. doi:10.1016/j.ijrobp.2004.01.041
- Fact Sheet: Targeted Radionuclide Therapy and Prostate Cancer. (2019, 2019). Society of nuclear medicine & molecular imaging.
- Falk, A. T., Demontoy, S., Chamorey, E., Chand, M. E., Gautier, M., Azria, D., . . . Hannoun-Levi, J. M. (2017). High-dose-rate brachytherapy boost for prostate cancer: Comparison of three different fractionation schemes. *Brachytherapy*, *16*(5), 993-999. doi:10.1016/j.brachy.2017.06.013
- Farrer, A. I., Odeen, H., de Bever, J., Coats, B., Parker, D. L., Payne, A., & Christensen, D. A. (2015). Characterization and evaluation of tissue-mimicking gelatin phantoms for use with MRgFUS. *J Ther Ultrasound*, *3*, 9. doi:10.1186/s40349-015-0030-y
- Fisch, B. M., Pickett, B., Weinberg, V., & Roach, M. (2001). Dose of radiation received by the bulb of the penis correlates with risk of impotence after three-dimensional conformal radiotherapy for prostate cancer. *Urology, 57*(5), 955-959. Retrieved from https://www.goldjournal.net/article/S0090-4295(01)00940-2/fulltext
- Fröhlich, G., Ágoston, P., Lövey, J., Polgár, C., & Major, T. (2010). The Effect of Needle Number on the Quality of High-dose-rate Prostate Brachytherapy Implants. *Pathology & Oncology Research*, *16*(4), 593-599. doi:10.1007/s12253-010-9252-z
- Fromageau, J., Brusseau, E., Vray, D., Gimenez, G., & Delachartre, P. (2003). Characterization of PVA cryogel for intravascular ultrasound elasticity imaging. *IEEE Trans Ultrason Ferroelectr Freq Control*, *50*(10), 1318-1324. doi:10.1109/tuffc.2003.1244748
- Fukada, J., Shigematsu, N., Nakashima, J., Ohashi, T., Kawaguchi, O., & Oya, M. (2012). Predicting pubic arch interference in prostate brachytherapy on transrectal ultrasonography-computed tomography fusion images. *J Radiat Res*, *53*(5), 753-759. doi:10.1093/jrr/rrs020
- Fukui, Y., Inamura, T., Hosoda, H., Wakashima, K., & Miyazaki, S. (2004). Mechanical Properties of a Ti-Nb-Al Shape Memory Alloy. *MATERIALS TRANSACTIONS*, *45*(4), 1077-1082. doi:10.2320/matertrans.45.1077
- Gibbons, E. P., Smith, R. P., Beriwal, S., Krishna, K., & Benoit, R. M. (2009). Overcoming pubic arch interference with free-hand needle placement in men undergoing prostate brachytherapy. *Brachytherapy*, *8*(1), 74-78. doi:10.1016/j.brachy.2008.04.007
- Goksel, O., Dehghan, E., & Salcudean, S. E. (2009). Modeling and simulation of flexible needles. *Medical Engineering & Physics*, 31(9), 1069-1078. doi:10.1016/j.medengphy.2009.07.007
- Grills, I. S., Martinez, A. A., Hollander, M., Huang, R., Goldman, K., Chen, P. Y., & Gustafson, G. S. (2004). High dose rate brachytherapy as prostate cancer monotherapy reduces toxicity compared to low dose rate palladium seeds. *J Urol*, 171(3), 1098-1104. doi:10.1097/01.ju.0000113299.34404.22
- Grummet, J., Pepdjonovic, L., Huang, S., Anderson, E., & Hadaschik, B. (2017). Transperineal vs. transrectal biopsy in MRI targeting. *Transl Androl Urol, 6*(3), 368-375. doi:10.21037/tau.2017.03.58
- Halpern, J. A., Sedrakyan, A., Hsu, W.-C., Mao, J., Daskivich, T. J., Nguyen, P. L., . . . Hu, J. C. (2016). Use, complications, and costs of stereotactic body radiotherapy for localized prostate cancer. *Cancer*, 122(16), 2496-2504. doi:10.1002/cncr.30101
- Hamilton, R. F., Dilibal, S., Sehitoglu, H., & Maier, H. J. (2011). Underlying mechanism of dual hysteresis in NiMnGa single crystals. *Materials Science and Engineering: A, 528*(3), 1877-1881. doi:10.1016/j.msea.2010.10.042
- Hannoun-Levi, J. M. (2017). Brachytherapy for prostate cancer: Present and future. *Cancer Radiother, 21*(6-7), 469-472. doi:10.1016/j.canrad.2017.06.009
- Hauck, C. R., Ye, H., Chen, P. Y., Gustafson, G. S., Limbacher, A., & Krauss, D. J. (2017). Increasing Fractional Doses Increases the Probability of Benign PSA Bounce in Patients Undergoing Definitive HDR Brachytherapy for Prostate Cancer. *Int J Radiat Oncol Biol Phys*, *98*(1), 108-114. doi:10.1016/j.ijrobp.2017.01.025
- Hegde, J. V., Collins, S. P., Fuller, D. B., King, C. R., Demanes, D. J., Wang, P. C., . . . Kamrava, M. (2018). A Pooled Analysis of Biochemical Failure in Intermediate-risk Prostate Cancer Following Definitive



- Stereotactic Body Radiotherapy (SBRT) or High-Dose-Rate Brachytherapy (HDR-B) Monotherapy. *Am J Clin Oncol*, *41*(5), 502-507. doi:10.1097/coc.00000000000311
- Henken, K. R., Seevinck, P. R., Dankelman, J., & van den Dobbelsteen, J. J. (2017). Manually controlled steerable needle for MRI-guided percutaneous interventions. *Med Biol Eng Comput, 55*(2), 235-244. doi:10.1007/s11517-016-1490-0
- Hepp, R., Eggert, T., Schabl, G., Herberholz, L., Petry, T., & Galalae, R. (2018). Salvage high-dose-rate brachytherapy for prostate cancer persistence after brachytherapy: repeated use of a polyethylene glycol hydrogel spacer. *J Contemp Brachytherapy*, 10(2), 169-173. doi:10.5114/jcb.2018.75602
- Hibbeler, R. C., & Fan, S. C. (2011). Mechanics of Materials: Prentice Hall.
- High-Performance Wire EDM: Speed Isn't Everything. (2004). Retrieved from https://www.moldmakingtechnology.com/articles/high-performance-wire-edm-speed-isn't-everything
- Hirsch, L., Gibney, M., Berube, J., & Manocchio, J. (2012). Impact of a modified needle tip geometry on penetration force as well as acceptability, preference, and perceived pain in subjects with diabetes. *Journal of diabetes science and technology*, *6*(2), 328-335. doi:10.1177/193229681200600216
- Hoskin, P., Rojas, A., Ostler, P., Hughes, R., Alonzi, R., & Lowe, G. (2017). Single-dose high-dose-rate brachytherapy compared to two and three fractions for locally advanced prostate cancer. *Radiother Oncol*, 124(1), 56-60. doi:10.1016/j.radonc.2017.06.014
- Hoskin, P. J., Rojas, A. M., Bownes, P. J., Lowe, G. J., Ostler, P. J., & Bryant, L. (2012). Randomised trial of external beam radiotherapy alone or combined with high-dose-rate brachytherapy boost for localised prostate cancer. *Radiotherapy and Oncology, 103*(2), 217-222. doi:10.1016/j.radonc.2012.01.007
- Huang, W. (2002). On the selection of shape memory alloys for actuators. *Materials & Design*, 23(1), 11-19. doi:10.1016/S0261-3069(01)00039-5
- Ilg, A. M., Laviana, A. A., Kamrava, M., Veruttipong, D., Steinberg, M., Park, S. J., . . . Saigal, C. (2016). Time-driven activity-based costing of low-dose-rate and high-dose-rate brachytherapy for low-risk prostate cancer. *Brachytherapy*, *15*(6), 760-767. doi:10.1016/j.brachy.2016.08.008
- Ishiyama, H., Kamitani, N., Kawamura, H., Kato, S., Aoki, M., Kariya, S., . . . Hayakawa, K. (2017). Nationwide multi-institutional retrospective analysis of high-dose-rate brachytherapy combined with external beam radiotherapy for localized prostate cancer: An Asian Prostate HDR-BT Consortium. *Brachytherapy*, 16(3), 503-510. doi:10.1016/j.brachy.2017.01.006
- Ittmann, M. (2018). Anatomy and Histology of the Human and Murine Prostate. *Cold Spring Harb Perspect Med, 8*(5). doi:10.1101/cshperspect.a030346
- Jamaluddin, M. F., Ghosh, S., Waine, M. P., Tavakoli, M., Amanie, J., Murtha, A. D., . . . Usmani, N. (2017). Intraoperative factors associated with stranded source placement accuracy in low-dose-rate prostate brachytherapy. *Brachytherapy*, *16*(3), 497-502. doi:10.1016/j.brachy.2017.01.007
- Jawad, M. S., Dilworth, J. T., Gustafson, G. S., Ye, H., Wallace, M., Martinez, A., . . . Krauss, D. J. (2016). Outcomes Associated With 3 Treatment Schedules of High-Dose-Rate Brachytherapy Monotherapy for Favorable-Risk Prostate Cancer. *Int J Radiat Oncol Biol Phys*, *94*(4), 657-666. doi:10.1016/j.ijrobp.2015.10.011
- Jayachandran, S., Akash, K., Mani Prabu, S. S., Manikandan, M., Muralidharan, M., Brolin, A., & Palani, I. A. (2019). Investigations on performance viability of NiTi, NiTiCu, CuAlNi and CuAlNiMn shape memory alloy/Kapton composite thin film for actuator application. *Composites Part B: Engineering, 176*, 107182. doi:10.1016/j.compositesb.2019.107182
- Jiang, P., van der Horst, C., Kimmig, B., Zinsser, F., Poppe, B., Luetzen, U., . . . Siebert, F. A. (2017). Interstitial high-dose-rate brachytherapy as salvage treatment for locally recurrent prostate cancer after definitive radiation therapy: Toxicity and 5-year outcome. *Brachytherapy*, 16(1), 186-192. doi:10.1016/j.brachy.2016.09.008
- Jiang, S., Liu, S., & Feng, W. (2011). PVA hydrogel properties for biomedical application. *J Mech Behav Biomed Mater, 4*(7), 1228-1233. doi:10.1016/j.jmbbm.2011.04.005
- Jun, C., Lim, S., Petrisor, D., Chirikjian, G., Kim, J. S., & Stoianovici, D. (2019). A simple insertion technique to reduce the bending of thinbevel-point needles. *Minim Invasive Ther Allied Technol*, 1-7. doi:10.1080/13645706.2018.1505758
- Jung, J., Ahn, H. K., & Huh, Y. (2012). Clinical and functional anatomy of the urethral sphincter. *Int Neurourol J*, *16*(3), 102-106. doi:10.5213/inj.2012.16.3.102
- Kamali, K., Nabizadeh, M., Ameli, M., Emami, M., Mahvari-Habibabadi, M., & Amirpoor, M. (2019). Impact of prostate needle biopsy on erectile function: A prospective study. *Urologia Journal*, 0391560319834488. doi:10.1177/0391560319834488
- Kent, A. R., Matheson, B., & Millar, J. L. (2019). Improved survival for patients with prostate cancer receiving high-dose-rate brachytherapy boost to EBRT compared with EBRT alone. *Brachytherapy*, *18*(3), 313-321. doi:10.1016/j.brachy.2019.01.013



- Key Statistics for Prostate Cancer. (2019). *cancer.org*. Retrieved from https://www.cancer.org/cancer/prostate-cancer/about/key-statistics.html
- Khadem, M., Rossa, C., Usmani, N., Sloboda, R. S., & Tavakoli, M. (2016, 12-15 July 2016). *Introducing notched flexible needles with increased deflection curvature in soft tissue*. Paper presented at the 2016 IEEE International Conference on Advanced Intelligent Mechatronics (AIM).
- Khadem, M., Rossa, C., Usmani, N., Sloboda, R. S., & Tavakoli, M. (2018). Robotic-Assisted Needle Steering Around Anatomical Obstacles Using Notched Steerable Needles. *IEEE Journal of Biomedical and Health Informatics*, 22(6), 1917-1928. doi:10.1109/JBHI.2017.2780192
- Ko, S. Y., Frasson, L., & Rodriguez y Baena, F. (2011). Closed-Loop Planar Motion Control of a Steerable Probe With a "Programmable Bevel" Inspired by Nature. *IEEE Transactions on Robotics*, 27(5), 970-983. doi:10.1109/TRO.2011.2159411
- Kollmeier, M. A., McBride, S., Taggar, A., Anderson, E., Lin, M., Pei, X., . . . Zelefsky, M. J. (2017). Salvage brachytherapy for recurrent prostate cancer after definitive radiation therapy: A comparison of low-dose-rate and high-dose-rate brachytherapy and the importance of prostate-specific antigen doubling time. *Brachytherapy*, *16*(6), 1091-1098. doi:10.1016/j.brachy.2017.07.013
- Kragelj, B. (2016). Obstructive urination problems after high-dose-rate brachytherapy boost treatment for prostate cancer are avoidable. *Radiol Oncol*, *50*(1), 94-103. doi:10.1515/raon-2015-0010
- Kragelj, B., Zlatic, J., & Zaletel-Kragelj, L. (2017). Avoidance of late rectal toxicity after high-dose-rate brachytherapy boost treatment for prostate cancer. *Brachytherapy*, *16*(1), 193-200. doi:10.1016/j.brachy.2016.10.008
- Krauss, D. J., Ye, H., Martinez, A. A., Mitchell, B., Sebastian, E., Limbacher, A., & Gustafson, G. S. (2017). Favorable Preliminary Outcomes for Men With Low- and Intermediate-risk Prostate Cancer Treated With 19-Gy Single-fraction High-dose-rate Brachytherapy. *Int J Radiat Oncol Biol Phys*, *97*(1), 98-106. doi:10.1016/j.ijrobp.2016.08.011
- Kukielka, A. M., Hetnal, M., & Bereza, K. (2016). Evaluation of tolerance and toxicity of high-dose-rate brachytherapy boost combined with interstitial hyperthermia for prostate cancer. *Int J Hyperthermia*, 32(3), 324-330. doi:10.3109/02656736.2015.1132339
- Kundu, S. D., Roehl, K. A., Eggener, S. E., Antenor, J. A., Han, M., & Catalona, W. J. (2004). Potency, continence and complications in 3,477 consecutive radical retropubic prostatectomies. *J Urol*, 172(6 Pt 1), 2227-2231. doi:10.1097/01.ju.0000145222.94455.73
- Lamotte, M., Annemans, L., Lamberts, G., Michielsen, D., Nicolas, H., Van Cangh, P., . . . Vranckx, K. (2005). [The cost of complicated acute urinary retention: a patient chart analysis in Belgium]. *Rev Med Liege, 60*(11), 875-881.
- Lee, J. Y., Spratt, D. E., Liss, A. L., & McLaughlin, P. W. (2016). Vessel-sparing radiation and functional anatomy-based preservation for erectile function after prostate radiotherapy. *Lancet Oncol, 17*(5), e198-208. doi:10.1016/s1470-2045(16)00063-2
- Lee, N., Wuu, C.-S., Brody, R., Laguna, J. L., Katz, A. E., Bagiella, E., & Ennis, R. D. (2000). Factors predicting for postimplantation urinary retention after permanent prostate brachytherapy. *International Journal of Radiation Oncology*Biology*Physics*, 48(5), 1457-1460. doi:10.1016/S0360-3016(00)00784-7
- Lei, S., Piel, N., Oermann, E. K., Chen, V., Ju, A. W., Dahal, K. N., . . . Collins, S. P. (2011). Six-Dimensional Correction of Intra-Fractional Prostate Motion with CyberKnife Stereotactic Body Radiation Therapy. *Front Oncol, 1,* 48. doi:10.3389/fonc.2011.00048
- Leissner, K. H., & Tisell, L. E. (1979). The Weight of the Human Prostate. *Scandinavian Journal of Urology and Nephrology, 13*(2), 137-142. doi:10.3109/00365597909181168
- Li, P., Jiang, S., Yu, Y., Yang, J., & Yang, Z. (2015). Biomaterial characteristics and application of silicone rubber and PVA hydrogels mimicked in organ groups for prostate brachytherapy. *Journal of the Mechanical Behavior of Biomedical Materials, 49.* doi:10.1016/j.jmbbm.2015.05.012
- Li, Q., Niinomi, M., Nakai, M., Cui, Z., Zhu, S., & Yang, X. (2012). Effect of Zr on super-elasticity and mechanical properties of Ti–24at% Nb–(0, 2, 4)at% Zr alloy subjected to aging treatment. *Materials Science and Engineering: A, 536*, 197-206. doi:10.1016/j.msea.2011.12.103
- Liu, J., Kaidu, M., Sasamoto, R., Ayukawa, F., Yamana, N., Sato, H., . . . Aoyama, H. (2016). Two-fraction high-dose-rate brachytherapy within a single day combined with external beam radiotherapy for prostate cancer: single institution experience and outcomes. *J Radiat Res, 57*(3), 280-287. doi:10.1093/jrr/rrw003
- Macdonald, A. G., Keyes, M., Kruk, A., Duncan, G., Moravan, V., & Morris, W. J. (2005). Predictive factors for erectile dysfunction in men with prostate cancer after brachytherapy: Is dose to the penile bulb important? *International Journal of Radiation Oncology*Biology*Physics*, 63(1), 155-163. doi:10.1016/j.ijrobp.2004.12.056



- Maenhout, M., Peters, M., van Vulpen, M., Moerland, M. A., Meijer, R. P., van den Bosch, M., . . . van der Voort van Zyp, J. R. N. (2017a). Focal MRI-Guided Salvage High-Dose-Rate Brachytherapy in Patients With Radiorecurrent Prostate Cancer. *Technol Cancer Res Treat, 16*(6), 1194-1201. doi:10.1177/1533034617741797
- Maenhout, M., van der Voort van Zyp, J. R. N., Borot de Battisti, M., Peters, M., van Vulpen, M., van den Bosch, M., & Moerland, M. A. (2018). The effect of catheter displacement and anatomical variations on the dose distribution in MRI-guided focal HDR brachytherapy for prostate cancer. *Brachytherapy*, 17(1), 68-77. doi:10.1016/j.brachy.2017.04.239
- Maenhout, M., van Vulpen, M., Moerland, M., Peters, M., Meijer, R., van den Bosch, M., . . . van der Voort van Zyp, J. (2017b). Second salvage high-dose-rate brachytherapy for radiorecurrent prostate cancer. *J Contemp Brachytherapy*, *9*(2), 161-166. doi:10.5114/jcb.2017.67015
- Majewicz, A., Marra, S. P., van Vledder, M. G., Lin, M., Choti, M. A., Song, D. Y., & Okamura, A. M. (2012). Behavior of tip-steerable needles in ex vivo and in vivo tissue. *IEEE transactions on bio-medical engineering*, *59*(10), 2705-2715. doi:10.1109/TBME.2012.2204749
- Mavroidis, P., Milickovic, N., Cruz, W. F., Tselis, N., Karabis, A., Stathakis, S., . . . Baltas, D. (2014). Comparison of Different Fractionation Schedules Toward a Single Fraction in High-Dose-Rate Brachytherapy as Monotherapy for Low-Risk Prostate Cancer Using 3-Dimensional Radiobiological Models. *International Journal of Radiation Oncology*Biology*Physics*, 88(1), 216-223. doi:10.1016/j.ijrobp.2013.10.016
- McAnearney, S., Fedorov, A., Joldes, G., Hata, N., Tempany, C., Miller, K., & Wittek, A. (2011). The Effects of Young's Modulus on Predicting Prostate Deformation for MRI-Guided Interventions. In (pp. 39-49).
- Medical, M. (2017). Osseoflex® SN. In M. Medical (Ed.).
- Mendez, L. C., & Morton, G. C. (2018). High dose-rate brachytherapy in the treatment of prostate cancer. *Transl Androl Urol, 7*(3), 357-370. doi:10.21037/tau.2017.12.08
- Minhas, D. S., Engh, J. A., Fenske, M. M., & Riviere, C. N. (2007). Modeling of needle steering via duty-cycled spinning. *Conf Proc IEEE Eng Med Biol Soc, 2007*, 2756-2759. doi:10.1109/iembs.2007.4352899
- Misra, S., Reed, K. B., Douglas, A. S., Ramesh, K. T., & Okamura, A. M. (2008, 19-22 Oct. 2008). *Needle-tissue interaction forces for bevel-tip steerable needles*. Paper presented at the 2008 2nd IEEE RAS & EMBS International Conference on Biomedical Robotics and Biomechatronics.
- Monroe, A. T., Faricy, P. O., Jennings, S. B., Biggers, R. D., Gibbs, G. L., & Peddada, A. V. (2008). High-dose-rate brachytherapy for large prostate volumes (≥50cc)—Uncompromised dosimetric coverage and acceptable toxicity. *Brachytherapy*, 7(1), 7-11. doi:10.1016/j.brachy.2007.10.005
- Moon, D. H., Efstathiou, J. A., & Chen, R. C. (2017). What is the best way to radiate the prostate in 2016? *Urol Oncol*, 35(2), 59-68. doi:10.1016/j.urolonc.2016.06.002
- Moreira, P., Patel, N., Wartenberg, M., Li, G., Tuncali, K., Heffter, T., . . . Tokuda, J. (2018). Evaluation of robot-assisted MRI-guided prostate biopsy: needle path analysis during clinical trials. *Phys Med Biol*, 63(20). doi:10.1088/1361-6560/aae214
- Morris, W. J., Tyldesley, S., Rodda, S., Halperin, R., Pai, H., McKenzie, M., . . . Murray, N. (2017). Androgen Suppression Combined with Elective Nodal and Dose Escalated Radiation Therapy (the ASCENDE-RT Trial): An Analysis of Survival Endpoints for a Randomized Trial Comparing a Low-Dose-Rate Brachytherapy Boost to a Dose-Escalated External Beam Boost for High- and Intermediate-risk Prostate Cancer. *International Journal of Radiation Oncology*Biology*Physics*, *98*(2), 275-285. doi:10.1016/j.ijrobp.2016.11.026
- Morton, G., Chung, H. T., McGuffin, M., Helou, J., D'Alimonte, L., Ravi, A., . . . Loblaw, A. (2017). Prostate high dose-rate brachytherapy as monotherapy for low and intermediate risk prostate cancer: Early toxicity and quality-of life results from a randomized phase II clinical trial of one fraction of 19Gy or two fractions of 13.5Gy. *Radiother Oncol*, 122(1), 87-92. doi:10.1016/j.radonc.2016.10.019
- Murgic, J., Chung, P., Berlin, A., Bayley, A., Warde, P., Catton, C., . . . Menard, C. (2016). Lessons learned using an MRI-only workflow during high-dose-rate brachytherapy for prostate cancer. *Brachytherapy*, 15(2), 147-155. doi:10.1016/j.brachy.2015.12.004
- Nagore, G., Lopez Guerra, J. L., Krumina, E., Lagos, M., Ovalles, B., Miro, A., . . . Gomez-Iturriaga, A. (2018). High dose rate brachytherapy for prostate cancer: A prospective toxicity evaluation of a one day schedule including two 13.5Gy fractions. *Radiother Oncol*, 127(2), 219-224. doi:10.1016/j.radonc.2018.03.022
- Ng, I. W. S., Tey, J. C. S., Soon, Y. Y., Tseng, M. S. F., Chen, D., & Lim, K. H. C. (2018). Outcomes of Asian patients with localized prostate cancer treated with combined intensity modulated radiation therapy (IMRT) and high dose rate (HDR) brachytherapy: A single institution experience. *Asia Pac J Clin Oncol*, 14(5), e386-e391. doi:10.1111/ajco.12819



- Ng, K. W., Goh, J. Q., Foo, S. L., Ting, P. H., & Lee, T. K. (2013). *Needle Insertion Forces Studies for Optimal Surgical Modeling*.
- O' Leary, M. D., Simone, C., Washio, T., Yoshinaka, K., & Okamura, A. M. (2003, 14-19 Sept. 2003). *Robotic needle insertion: effects of friction and needle geometry.* Paper presented at the 2003 IEEE International Conference on Robotics and Automation (Cat. No.03CH37422).
- Okazawa, S., Ebrahimi, R., Chuang, J., Salcudean, S. E., & Rohling, R. (2005). Hand-held steerable needle device. *IEEE/ASME Transactions on Mechatronics*, 10(3), 285-296. doi:10.1109/TMECH.2005.848300
- Olarte, A., Cambeiro, M., Moreno-Jimenez, M., Arbea, L., Perez-Gracia, J. L., Gil-Bazo, I., . . . Martinez-Monge, R. (2016). Dose escalation with external beam radiation therapy and high-dose-rate brachytherapy combined with long-term androgen deprivation therapy in high and very high risk prostate cancer: Comparison of two consecutive high-dose-rate schemes. *Brachytherapy*, 15(2), 127-135. doi:10.1016/j.brachy.2015.12.008
- Patel, S., Demanes, D. J., Ragab, O., Zhang, M., Veruttipong, D., Nguyen, K., . . . Kamrava, M. (2017). High-dose-rate brachytherapy monotherapy without androgen deprivation therapy for intermediate-risk prostate cancer. *Brachytherapy*, *16*(2), 299-305. doi:10.1016/j.brachy.2016.11.002
- Paulsen, A. F., & Waschke, J. (2013). Sobotta Atlas of Human Anatomy: Volume 2, 15th ed., English/Latin (15 ed.): [S.I.] Elsevier Health Sciences Germany
- Peeters, S. T. H., Heemsbergen, W. D., Koper, P. C. M., van Putten, W. L. J., Slot, A., Dielwart, M. F. H., . . . Lebesque, J. V. (2006). Dose-Response in Radiotherapy for Localized Prostate Cancer: Results of the Dutch Multicenter Randomized Phase III Trial Comparing 68 Gy of Radiotherapy With 78 Gy. *Journal of Clinical Oncology*, 24(13), 1990-1996. doi:10.1200/jco.2005.05.2530
- Pepe, P., & Pennisi, M. (2015). Erectile dysfunction in 1050 men following extended (18 cores) vs saturation (28 cores) vs saturation plus MRI-targeted prostate biopsy (32 cores). *International Journal Of Impotence Research*, 28, 1. doi:10.1038/ijir.2015.18
- Pepe, P., Pietropaolo, F., Dibenedetto, G., & Aragona, F. (2013). Erectile function after repeat saturation prostate biopsy: Our experience in 100 patients. *Arch Ital Urol Androl, 85*, 130-132. doi:10.4081/aiua.2013.3.130
- Peters, M., van Son, M. J., Moerland, M. A., Kerkmeijer, L. G. W., Eppinga, W. S. C., Meijer, R. P., . . . van der Voort van Zijp, J. R. N. (2019). MRI-Guided Ultrafocal HDR Brachytherapy for Localized Prostate Cancer: Median 4-Year Results of a feasibility study. *Int J Radiat Oncol Biol Phys.* doi:10.1016/j.ijrobp.2019.03.032
- Podder, T., Clark, D., Sherman, J., Fuller, D., Messing, E., Rubens, D., . . . Ng, W. S. (2006a). In vivo motion and force measurement of surgical needle intervention during prostate brachytherapy. *Med Phys*, 33(8), 2915-2922. doi:10.1118/1.2218061
- Podder, T., Dicker, A. P., Hutapea, P., Darvish, K., & Yu, Y. (2012). A novel curvilinear approach for prostate seed implantation. *Med Phys*, *39*(4), 1887-1892. doi:10.1118/1.3694110
- Podder, T., Sherman, J., Fuller, D., Messing, E. M., Rubens, D. J., Strang, J. G., . . . Yu, Y. (2006b, 30 Aug. 3 Sept. 2006). *In-vivo Measurement of Surgical Needle Intervention Parameters: A Pilot Study.* Paper presented at the 2006 International Conference of the IEEE Engineering in Medicine and Biology Society.
- Poulin, E., Varfalvy, N., Aubin, S., & Beaulieu, L. (2016). Comparison of dose and catheter optimization algorithms in prostate high-dose-rate brachytherapy. *Brachytherapy*, *15*(1), 102-111. doi:10.1016/j.brachy.2015.09.010
- Prada, P. J., Cardenal, J., Blanco, A. G., Anchuelo, J., Ferri, M., Fernández, G., . . . Fernández, J. (2016). High-dose-rate interstitial brachytherapy as monotherapy in one fraction for the treatment of favorable stage prostate cancer: Toxicity and long-term biochemical results. *Radiotherapy and Oncology,* 119(3), 411-416. doi:10.1016/j.radonc.2016.04.006
- Prostate cancer statistics. (2019). cancerresearchuk.org. Retrieved from https://www.cancerresearchuk.org/health-professional/cancer-statistics/statistics-by-cancer-type/prostate-cancer#heading-One
- Prostate Cancer Treatment. (2019). cancer.gov. Retrieved from https://www.cancer.gov/types/prostate/patient/prostate-treatment-pdg
- Prostate HDR Brachytherapy. (2019). Retrieved from https://www.micknuclear.com/home/products/hdr_brachytherapy/prostate_applications/
- Raychaudhuri, B., & Cahill, D. (2008). Pelvic Fasciae in Urology (Vol. 90).
- Rebeka, R., & Ferčec, J. (2013). Force measurements on teeth using fixed orthodontic systems. *Military Technical Courier*, *61*, 105-122. doi:10.5937/vojtehg61-2960



- Repetti, E. (2019). Design and develop a 3D printed medical phantom able to replicate lungs and bronchial tree geometrical and mechanical characteristics as human tissue. (Master of Science in Biomedical Engineering). TU Delft,
- Romero, F. R., Romero, A. W., Filho, T. B., Kulysz, D., Oliveira, F. C., & Filho, R. T. (2012). The prostate exam. *Health Education Journal*, *71*(2), 239-250. doi:10.1177/0017896911398234
- Rouvière, O., Melodelima, C., Hoang Dinh, A., Bratan, F., Pagnoux, G., Sanzalone, T., . . . Souchon, R. (2017). Stiffness of benign and malignant prostate tissue measured by shear-wave elastography: a preliminary study. *European Radiology*, *27*(5), 1858-1866. doi:10.1007/s00330-016-4534-9
- Royce, T. J., & Efstathiou, J. A. (2018). Proton therapy for prostate cancer: A review of the rationale, evidence, and current state. *Urol Oncol.* doi:10.1016/j.urolonc.2018.11.012
- Rutigliano, S., Abraham, J. A., Kenneally, B. E., Zoga, A. C., Nevalainen, M., & Roedl, J. B. (2017). Analysis of a Steerable Needle for Fine Needle Aspiration and Biopsy: Efficiency and Radiation Dose Compared With a Conventional Straight Needle. *J Comput Assist Tomogr, 41*(6), 957-961. doi:10.1097/RCT.0000000000000616
- Ryoichi Oyasu, X. J. Y., Osamu Yoshida. (2008). Does a prostatic capsule exist? Pathologists and urologists use the word "capsule" when evaluating the extent of prostatic cancer in prostatectomy specimens. In *Questions in Daily Urologic Practice: Updates for Urologists and Diagnostic Pathologists* (pp. 3-6). Tokyo: Springer Japan.
- Ryu, S. C., Quek, Z. F., Koh, J., Renaud, P., Black, R. J., Moslehi, B., . . . Cutkosky, M. R. (2015). Design of an Optically Controlled MR-Compatible Active Needle. *IEEE Transactions on Robotics*, *31*(1), 1-11. doi:10.1109/TRO.2014.2367351
- Sadjadi, H., Hashtrudi-Zaad, K., & Fichtinger, G. (2014). Needle deflection estimation: prostate brachytherapy phantom experiments. *International Journal of Computer Assisted Radiology and Surgery*, *9*(6), 921-929. doi:10.1007/s11548-014-0985-0
- Sahlabadi, M., & Hutapea, P. (2018). Novel design of honeybee-inspired needles for percutaneous procedure. *Bioinspir Biomim*, 13(3), 036013. doi:10.1088/1748-3190/aaa348
- Saigal, K., All, S., Potrebko, P., Feranec, N., Keller, A., Lizaso, M., . . . Biagioli, M. (2019). Incorporating Routine Magnetic Resonance Imaging-based Planning for the Delivery of High-dose-rate Brachytherapy for Prostate Cancer: An Evaluation of Clinical Feasibility and Dosimetric Outcomes. *Cureus*, 11(2), e4085. doi:10.7759/cureus.4085
- Sakes, A., Dodou, D., & Breedveld, P. (2016). Buckling prevention strategies in nature as inspiration for improving percutaneous instruments: a review. *Bioinspir Biomim, 11*(2), 021001. doi:10.1088/1748-3190/11/2/021001
- Sanchez-Gomez, L. M., Polo-deSantos, M., Rodriguez-Melcon, J. I., Angulo, J. C., & Luengo-Matos, S. (2017). High-dose rate brachytherapy as monotherapy in prostate cancer: A systematic review of its safety and efficacy. *Actas Urol Esp.*, *41*(2), 71-81. doi:10.1016/j.acuro.2016.06.001
- Scali, M., Kreeft, D., Breedveld, P., & Dodou, D. (2017a). *Design and evaluation of a wasp-inspired steerable needle* (Vol. 10162): SPIE.
- Scali, M., Pusch, T. P., Breedveld, P., & Dodou, D. (2017b). Needle-like instruments for steering through solid organs: A review of the scientific and patent literature. *Proc Inst Mech Eng H, 231*(3), 250-265. doi:10.1177/0954411916672149
- Scali, M., Pusch, T. P., Breedveld, P., & Dodou, D. (2017c). Ovipositor-inspired steerable needle: design and preliminary experimental evaluation. *Bioinspir Biomim, 13*(1), 016006. doi:10.1088/1748-3190/aa92b9
- Schindler, W. D., & Hauser, P. J. (2004). 4 Hand building finishes. In W. D. Schindler & P. J. Hauser (Eds.), Chemical Finishing of Textiles (pp. 43-50): Woodhead Publishing.
- Sears, P., & Dupont, P. (2006, 9-15 Oct. 2006). A Steerable Needle Technology Using Curved Concentric Tubes. Paper presented at the 2006 IEEE/RSJ International Conference on Intelligent Robots and Systems.
- Siddiqui, Z. A., Gustafson, G. S., Ye, H., Martinez, A. A., Mitchell, B., Sebastian, E., . . . Krauss, D. J. (2019). Five-Year Outcomes of a Single-Institution Prospective Trial of 19-Gy Single-Fraction High-Dose-Rate Brachytherapy for Low- and Intermediate-Risk Prostate Cancer. *Int J Radiat Oncol Biol Phys.* doi:10.1016/j.ijrobp.2019.02.010
- Skouteris, V. M., Crawford, E. D., Mouraviev, V., Arangua, P., Metsinis, M. P., Skouteris, M., . . . Stone, N. N. (2018). Transrectal Ultrasound-guided Versus Transperineal Mapping Prostate Biopsy: Complication Comparison. *Rev Urol*, *20*(1), 19-25. doi:10.3909/riu0785
- Skowronek, J. (2017). Current status of brachytherapy in cancer treatment short overview. *J Contemp Brachytherapy*, *9*(6), 581-589. doi:10.5114/jcb.2017.72607



- Spratt, D. E., Lee, J. Y., Dess, R. T., Narayana, V., Evans, C., Liss, A., . . . McLaughlin, P. W. (2017). Vessel-sparing Radiotherapy for Localized Prostate Cancer to Preserve Erectile Function: A Single-arm Phase 2 Trial. *Eur Urol*, 72(4), 617-624. doi:10.1016/j.eururo.2017.02.007
- Steggerda, M. J., van der Poel, H. G., & Moonen, L. M. F. (2008). An analysis of the relation between physical characteristics of prostate I-125 seed implants and lower urinary tract symptoms: Bladder hotspot dose and prostate size are significant predictors. *Radiotherapy and Oncology, 88*(1), 108-114. doi:10.1016/j.radonc.2007.10.030
- Steggerda, M. J., van der Poel, H. G., & Moonen, L. M. F. (2010). Minimizing the number of implantation needles for prostate 125I brachytherapy: An investigation of possibilities and implications. *Brachytherapy*, *9*(4), 319-327. doi:10.1016/j.brachy.2009.07.010
- Strassmann, G., Olbert, P., Hegele, A., Richter, D., Fokas, E., Timmesfeld, N., . . . Engenhart-Cabillic, R. (2011). Advantage of robotic needle placement on a prostate model in HDR brachytherapy. *Strahlentherapie und Onkologie, 187*(6), 367-372. doi:10.1007/s00066-011-2185-y
- Strouthos, I., Chatzikonstantinou, G., Zamboglou, N., Milickovic, N., Papaioannou, S., Bon, D., . . . Tselis, N. (2018a). Combined high dose rate brachytherapy and external beam radiotherapy for clinically localised prostate cancer. *Radiother Oncol*, *128*(2), 301-307. doi:10.1016/j.radonc.2018.04.031
- Strouthos, I., Tselis, N., Chatzikonstantinou, G., Butt, S., Baltas, D., Bon, D., . . . Zamboglou, N. (2018b). High dose rate brachytherapy as monotherapy for localised prostate cancer. *Radiother Oncol, 126*(2), 270-277. doi:10.1016/j.radonc.2017.09.038
- Swaney, P. J., Burgner, J., Gilbert, H. B., & Webster, R. J. (2013). A Flexure-Based Steerable Needle: High Curvature With Reduced Tissue Damage. *IEEE Transactions on Biomedical Engineering, 60*(4), 906-909. doi:10.1109/TBME.2012.2230001
- Thiruthaneeswaran, N., & Hoskin, P. J. (2016). High dose rate brachytherapy for prostate cancer: Standard of care and future direction. *Cancer Radiother*, 20(1), 66-72. doi:10.1016/j.canrad.2016.01.001
- Torabi, M., Gupta, R., & Walsh, C. J. (2014). Compact Robotically Steerable Image-Guided Instrument for Multi-Adjacent-Point (MAP) Targeting. *IEEE Transactions on Robotics*, 30(4), 802-815. doi:10.1109/TRO.2014.2304773
- Tselis, N., Hoskin, P., Baltas, D., Strnad, V., Zamboglou, N., Rodel, C., & Chatzikonstantinou, G. (2017). High Dose Rate Brachytherapy as Monotherapy for Localised Prostate Cancer: Review of the Current Status. *Clin Oncol (R Coll Radiol)*, 29(7), 401-411. doi:10.1016/j.clon.2017.02.015
- van de Berg, N. J., Dankelman, J., & van den Dobbelsteen, J. J. (2017). Endpoint Accuracy in Manual Control of a Steerable Needle. *Journal of Vascular and Interventional Radiology*, 28(2), 276-283.e272. doi:10.1016/j.jvir.2016.07.018
- van de Berg, N. J. P. (2016). *Needle steering mechanics and design cases.* (Doctural Thesis). Delft University of Technology,
- van Gerwen, D. J., Dankelman, J., & van den Dobbelsteen, J. J. (2012). Needle-tissue interaction forces A survey of experimental data. *Medical Engineering & Physics*, 34(6), 665-680. doi:10.1016/j.medengphy.2012.04.007
- Van Meter, M. M., & Adam, R. A. (2016). Costs associated with instrument sterilization in gynecologic surgery. *Am J Obstet Gynecol*(1097-6868 (Electronic)). doi:10.1016/j.ajog.2016.06.019
- van Veen, Y. R., Jahya, A., & Misra, S. (2012). Macroscopic and microscopic observations of needle insertion into gels. *Proc Inst Mech Eng H*, 226(6), 441-449. doi:10.1177/0954411912443207
- Vargas, C., Ghilezan, M., Hollander, M., Gustafson, G., Korman, H., Gonzalez, J., & Martinez, A. (2005). A NEW MODEL USING NUMBER OF NEEDLES AND ANDROGEN DEPRIVATION TO PREDICT CHRONIC URINARY TOXICITY FOR HIGH OR LOW DOSE RATE PROSTATE BRACHYTHERAPY. *The Journal of Urology, 174*(3), 882-887. doi:10.1097/01.ju.0000169136.55891.21
- Vigneault, E., Mbodji, K., Magnan, S., Despres, P., Lavallee, M. C., Aubin, S., . . . Martin, A. G. (2017). High-dose-rate brachytherapy boost for prostate cancer treatment: Different combinations of hypofractionated regimens and clinical outcomes. *Radiother Oncol, 124*(1), 49-55. doi:10.1016/j.radonc.2017.06.012
- Vigneault, E., Morton, G., Parulekar, W. R., Niazi, T. M., Springer, C. W., Barkati, M., . . . Loblaw, A. (2018). Randomised Phase II Feasibility Trial of Image-guided External Beam Radiotherapy With or Without High Dose Rate Brachytherapy Boost in Men with Intermediate-risk Prostate Cancer (CCTG PR15/NCT01982786). Clin Oncol (R Coll Radiol), 30(9), 527-533. doi:10.1016/j.clon.2018.05.007
- Vu, C. C., Blas, K. G., Lanni, T. B., Gustafson, G. S., & Krauss, D. J. (2018). Cost-effectiveness of prostate boost with high-dose-rate brachytherapy versus intensity-modulated radiation therapy in the treatment of intermediate-high risk prostate cancer. *Brachytherapy*, 17(6), 852-857. doi:10.1016/j.brachy.2018.07.009



- Wallner, K. E., Merrick, G. S., Benson, M. L., Butler, W. M., Maki, J., & Tollenaar, B. G. (2002). Penile bulb imaging. *Int J Radiat Oncol Biol Phys*, *53*(4), 928-933. doi:10.1016/s0360-3016(02)02805-5
- Wang, C. P., Su, Y., Yang, S. Y., Shi, Z., & Liu, X. J. (2014). A new type of Cu-Al-Ta shape memory alloy with high martensitic transformation temperature. *Smart Materials and Structures*, *23*(2). doi:Artn 025018 10.1088/0964-1726/23/2/025018
- Webster, R. J., Kim, J. S., Cowan, N. J., Chirikjian, G. S., & Okamura, A. M. (2006). Nonholonomic Modeling of Needle Steering. *The International Journal of Robotics Research*, 25(5-6), 509-525. doi:10.1177/0278364906065388
- Wedde, T. B., Smastuen, M. C., Brabrand, S., Fossa, S. D., Kaasa, S., Tafjord, G., . . . Lilleby, W. (2019). Tenyear survival after High-Dose-Rate Brachytherapy combined with External Beam Radiation Therapy in high-risk prostate cancer: A comparison with the Norwegian SPCG-7 cohort. *Radiother Oncol, 132*, 211-217. doi:10.1016/j.radonc.2018.10.013
- Wilkin, R., & Hamm, R. (2010). How to make a cheap and simple prostate phantom. *J Ultrasound Med*, *29*(7), 1151-1152. doi:10.7863/jum.2010.29.7.1151
- Wojcieszek, P., Szlag, M., Glowacki, G., Cholewka, A., Gawkowska-Suwinska, M., Kellas-Sleczka, S., . . . Fijalkowski, M. (2016). Salvage high-dose-rate brachytherapy for locally recurrent prostate cancer after primary radiotherapy failure. *Radiother Oncol, 119*(3), 405-410. doi:10.1016/j.radonc.2016.04.032
- Wust, P., von Borczyskowski, D. W., Henkel, T., Rosner, C., Graf, R., Tilly, W., . . . Kahmann, F. (2004). Clinical and physical determinants for toxicity of 125-I seed prostate brachytherapy. *Radiotherapy and Oncology, 73*(1), 39-48. doi:10.1016/j.radonc.2004.08.003
- Xu, J., Duindam, V., Alterovitz, R., Pouliot, J., Cunha, J. A. M., Hsu, I., & Goldberg, K. (2009, 10-15 Oct. 2009). Planning fireworks trajectories for steerable medical needles to reduce patient trauma. Paper presented at the 2009 IEEE/RSJ International Conference on Intelligent Robots and Systems.
- Yamauchi, K., Ohkata, I., Tsuchiya, K., & Miyazaki, S. (2011). Shape memory and superelastic alloys: Woodhead Publishing Limited.
- Yamazaki, H., Masui, K., Suzuki, G., Nakamura, S., Shimizu, D., Nishikawa, T., . . . Ogawa, K. (2018a). High-Dose-Rate Brachytherapy Monotherapy versus Image-Guided Intensity-Modulated Radiotherapy with Helical Tomotherapy for Patients with Localized Prostate Cancer. *Cancers (Basel), 10*(9). doi:10.3390/cancers10090322
- Yamazaki, H., Masui, K., Suzuki, G., Nakamura, S., Yamada, K., Okihara, K., . . . Ogawa, K. (2019). High-dose-rate brachytherapy monotherapy versus low-dose-rate brachytherapy with or without external beam radiotherapy for clinically localized prostate cancer. *Radiother Oncol, 132*, 162-170. doi:10.1016/j.radonc.2018.10.020
- Yamazaki, H., Masui, K., Suzuki, G., Nakamura, S., Yoshida, K., Kotsuma, T., . . . Ogawa, K. (2018b). Comparison of three moderate fractionated schedules employed in high-dose-rate brachytherapy monotherapy for clinically localized prostate cancer. *Radiother Oncol,* 129(2), 370-376. doi:10.1016/j.radonc.2018.07.026
- Yang, X., Rossi, P. J., Jani, A. B., Mao, H., Zhou, Z., Curran, W. J., & Liu, T. (2017). Improved prostate delineation in prostate HDR brachytherapy with TRUS-CT deformable registration technology: A pilot study with MRI validation. *J Appl Clin Med Phys*, *18*(1), 202-210. doi:10.1002/acm2.12040
- Yaxley, J. W., Lah, K., Yaxley, J. P., Gardiner, R. A., Samaratunga, H., & MacKean, J. (2017). Long-term outcomes of high-dose-rate brachytherapy for intermediate- and high-risk prostate cancer with a median follow-up of 10 years. *BJU Int*, 120(1), 56-60. doi:10.1111/bju.13659
- Yoshioka, D. Y., Itami, D. J., Oguchi, D. M., & Nakano, D. T. (2019). *Brachytherapy Techniques and Evidences*: Springer.
- Yoshioka, Y., Kotsuma, T., Komiya, A., Kariya, S., Konishi, K., Nonomura, N., . . . Itami, J. (2017). Nationwide, Multicenter, Retrospective Study on High-Dose-Rate Brachytherapy as Monotherapy for Prostate Cancer. *Int J Radiat Oncol Biol Phys*, *97*(5), 952-961. doi:10.1016/j.ijrobp.2016.12.013
- Zell, K., Sperl, J. I., Vogel, M. W., Niessner, R., & Haisch, C. (2007). Acoustical properties of selected tissue phantom materials for ultrasound imaging. *Phys Med Biol*, *52*(20), N475-484. doi:10.1088/0031-9155/52/20/N02



Abbreviations

Below abbreviations used in this thesis and literate review can be found in alphabetical order:

BT - BrachyTherapy

CT - Computer Tomography

EC - Experimental Condition

EDM – Electrical Discharge Machining

EMC - Erasmus Medical Centre

ER – External Radiation

HDR - High Dose-Rate

IMRT - Intensity-Modulated Radiation Therapy

LDR - Low Dose-Rate

LUMC - Leiden University Medical Centre

MRR - Metal Removal Rate

NiTi - Nickel Titanium (Nitinol)

OR – Operating Room

PAI - Pubic Arch Interreference

PDR - Pulse Bose Bate

PVA - PolyVinyl Alcohol

PZ – Peripheral Zone

SN - Steerable Needle

TRUS - Trans-Rectal Ultrasound

UMCU - University Medical Centre Utrecht



Appendix A — Literature review



The usefulness of a steerable needle in high dose-rate prostate brachytherapy
A Literature Review





The usefulness of a steerable needle in high dose-rate prostate brachytherapy

A Literature Review

Ву

M.M. Nobel

in partial fulfilment of the requirements for the degree of

Master of Science in Biomedical Engineering

at the Delft University of Technology.

Supervisor: dr. J.J. van den Dobbelsteen





Abstract

Prostate cancer is the most common cancer in men and third in terms of mortality. High dose rate brachytherapy is a commonly used and effective treatment to combat this cancer. High dose rate brachytherapy requires the implantation of several needles into the prostate trough which a radiation source is introduced. This implantation can present a number of difficulties. Steerable needles have been proposed to address some of these difficulties. This literature review aims to determine the usefulness of steerable needles in high dose rate brachytherapy of the prostate.

By reviewing literature on high dose rate brachytherapy, needle complications, and steerable needles separately a large body of literature was compiled. Combining this literature resulted in the findings presented in this literature review.

This paper identifies several advantages a steerable needle could have over a conventional needle, these include:

- The ability to steer around sensitive tissues, thereby reducing implant related toxicities;
- Avoiding anatomical obstructions, increasing the number of patients eligible for high dose rate brachytherapy, and possibly simplifying the procedure for the surgeon;
- Decreasing the number of required needle implants, decreasing implant related toxicity;
- Increasing needle positioning accuracy, reducing the number of required needle implants.

Possible disadvantages include increased system complexity and decreased cost-effectiveness. The design of a steerable needle for high dose rate brachytherapy should take these disadvantages into account.

Evidence of the usefulness of a steerable needle in prostate high dose rate brachytherapy is far from definitive. However, the possible advantages of the technique warrant the development of a manual controlled steerable needle for high-dose rate brachytherapy of the prostate. This paper provides a foundation of information for the development of this needle.





Introduction

Prostate cancer is the most common cancer in men and third in terms of mortality. In high dose rate radiotherapy, needles are implanted into the prostate, through which an afterloader inserts a radioactive source. One of this procedure's benefits is its ability to deliver local doses of radiations, sparing surrounding tissue.

The implantation of needles in high dose rate brachytherapy can be challenging, especially in the case of the prostate. The target is deep inside the body and access is limited by other anatomies. To aid in accurately and safely implanting these needles, the use of steerable needles has been proposed. The goal of this literature review is to deliver a verdict on the usefulness of a steerable needle in high dose rate brachytherapy of the prostate.

To answer this question, I will provide some background on prostate cancer and radiation therapies in the first chapter. In chapter two I will define the methods I used to find relevant literature on the subject of high dose rate brachytherapy in the treatment of prostate cancer and the influence of needles and their accuracy on this procedure. In the third chapter I will describe the state of the art in high dose rate prostate brachytherapy and its future directions. The fourth chapter discusses prostate anatomy and needle related complications in high dose rate brachytherapy of the prostate. The fifth chapter presents an overview of literature available on steerable needles and their performance. The sixth and final chapter combines the previous chapters into a discussion about the place of steerable needles in high dose rate prostate brachytherapy.



Contents

1. PROSTATE CANCER	75
1.1 THE DISEASE	76
1.2,1 External beam radiotherapy 1.2.2 Brachytherapy 1.2.3 Radionuclide therapy	77
2 METHODS	
3 HIGH DOSE RATE BRACHYTHERAPY PROSTATE CANCER THERAPY	8C
3.1 METHODS AND PRACTICES 3.2 CLINICAL OUTCOMES	
4 PROSTATE ANATOMY AND NEEDLE POSITIONING DIFFICULTIES	
4.1 GENERAL PROSTATE ANATOMY	88 88 89 90 90 91 91 91 92
5.1 COMMERCIALLY AVAILABLE STEERABLE NEEDLES 5.2 STEERING MECHANISMS 5.2.1 BASE MANIPULATION 5.2.2 BEVEL-TIP 5.2.3 PRE-CURVED STYLET 5.2.4 ACTIVE CANNULA 5.2.5 PROGRAMMABLE BEVEL-TIP	94 92 95 95 95
5.2.6 ARTICULATED-TIP STEERING	
5.3.1 TIP GEOMETRY	96



5.3.3 Coating	96
5.4 PERFORMANCE EVALUATION OF STEERABLE NEEDLES FOUND IN LITERATURE	
5.5 PROSPECTS	
5.6 CONCLUSION	98
6 THE PLACE OF STEERABLE NEEDLES IN PROSTATE HDR-BT	99
6.1 ADVANTAGES	100
6.1 ADVANTAGES	100
6.1.2 AVOIDANCE OF SENSITIVE TISSUES	
6.1.3 INCREASED NEEDLE POSITIONING ACCURACY	100
6.1.4 Decreased needle insertions	
6.2 Drawbacks	101
6.2.1 System complexity	101
6.2.2 Intervention costs	101
6.3 CONCLUSION	
CONCLUSION	103



Prostate Cancer

Abstract

Prostate cancer is the most common cancer in men and third in terms of mortality. Treatments include pharmacotherapy, radiation therapies, and hormonal therapies depending on the stage of the cancer and condition of the patient. External beam radiotherapy, brachytherapy, and radio nucleotide therapy are examples of radiation therapies. In high dose-rate brachytherapy, a high dose rate radiation source is placed through polymer sleeves into the tumour for a short period of time. Possible advantages include decreased hospitalisation time and more precise radiation control over other radiotherapy modalities.



This chapter provides some rudimentary information about prostate cancer and available treatments. Readers familiar with radiation treatments are advised to move on to the next chapter.

1.1. The disease

Prostate cancer is the most common cancer found in men. After lung and bronchus cancer it claims more of men's lives than any other cancer (*Cancer Facts & Figures*, 2019). The American Cancer Society estimates 1 in 9 men will be diagnosed with prostate cancer during their lifetime and 1 in 41 men will die of prostate cancer ("Key Statistics for Prostate Cancer," 2019). Cancer Research UK estimates 1 in 6 males born after 1960 will be diagnosed with prostate cancer in their lifetime and that prostate cancer is responsible for 7% of all male cancer mortality ("Prostate cancer statistics," 2019). Men with African ancestry and/or a family history of the disease are especially susceptible to the disease. The 'western lifestyle' also seems to increase the risk of developing prostate cancer (Denmeade & Isaacs, 2002).

Prostate cancer has a mean onset age of 66. This, combined with the fact that 90% of the cases are discovered at the local or regional stage, means that the 10-year survival rate for all stages combined is 98%. Cancer Research UK reports the 10-year survival rate in England and Wales between 2010 and 2011 for prostate cancer was 84%.

In early stages, prostate cancer has no symptoms. The first symptoms that appear usually are difficulty urinating, blood in the urine or pain with urination. More advanced symptoms are pain in the bones of the hips, spine, or ribs. Screening can be a good way to detect early stage prostate cancer. By doing a prostate-specific antigen (PSA) test, performing a rectal exam, using transrectal ultrasound or using magnetic resonance imaging, the disease can be detected before symptoms arise ("Prostate Cancer Treatment," 2019).

Treatments include surgery, pharmacotherapy, radiation therapies, and hormonal therapies depending on the stage of the cancer and condition of the patient. Treatment can have a negative impact on the quality of life of the patient. Urinary or erectile difficulties are common side-effects. The next section discusses radiotherapy in more detail.

1.2. Radiotherapy

Radiation therapy employs ionising radiation to stunt the growth of, or kill malignant cells. What radiotherapy is preferred, depends on factors such as the stage of the disease, the age of the patient and the risk-factor of the patient (Moon, Efstathiou, & Chen, 2017). Radiation therapy is mostly used in localised prostate cancer. Combinations of radiation therapy with other radiation therapies or with hormonal or surgical interventions are common.

1.2.1. External-beam radiotherapy

There are several therapies in which a radiation source irradiates the patient from outside of the body. These therapies will be called external radiation (ER) when the specific radiation modality is not mentioned in literature. External-beam radiation therapy (EBRT) is the most common form of ER. In EBRT an ionising beam is pointed at the tumour from outside the patient. A linear accelerator produces megavoltage photon beams that penetrate the tissue and deliver their ionising payload. The major disadvantage of EBRT is the fact the radiation is not contained to the tumour. Instead a portion of the radiation ends up in the surrounding tissues. The adverse effects of this access radiation can be decreased by spreading the treatment over a longer period, usually weeks or months, giving the healthy tissue time to recover. Additionally, using techniques such as intensity-modulated radiotherapy (IMRT) or stereotactic body radiotherapy (SBRT) can reduce the dose to surrounding healthy tissue, while delivering a therapeutic dose to the malignancy (Moon et al., 2017).

A recent addition to the field of EBRT for prostate cancer treatment is proton therapy. Instead of using photon-beams, protons beams are used to irradiate the tumour. Proton therapy potentially offers to reduce the side effects of photon therapy while maintaining its efficacy. However, the superiority of this technique is still a matter of debate (Royce & Efstathiou, 2018).



1.2.2. Brachytherapy

In brachytherapy (BT), instead of using an external source of radiation that radiates inward, a radiation source is placed directly in the malignant tissue. This is done in an effort to minimise radiation exposure to surrounding healthy tissues and increase dose accuracy. Brachytherapy has for a long time been a standard treatment for low risk prostate cancer (Moon et al., 2017). In 2017, the American Society of Clinical Oncology and Cancer Care Ontario recommended that medium to high risk prostate cancer patients should also be offered BT (Chin et al., 2017).

Low dose rate brachytherapy

LDR BT is especially suitable for low-intermediate risk prostate cancer (Hannoun-Levi, 2017). In low dose rate brachytherapy (LDR BT), a multitude of radioactive 'seeds' are implanted in the tumour. These seeds slowly release their radiation, killing malignant cells. The main advantage of this therapy is the concentration of radiation, sparing healthy tissues. Another advantage of this therapy is the reduced number of required hospital visits.

High dose rate brachytherapy

In high dose rate brachytherapy (HDR BT) instead of implanting long-term low radiation sources, a high dose rate radiation source is placed in the tumour for a short period of time. During the procedure a series of needles are placed and fixated in the prostate. These needles are later populated with high dose rate radiation sources with the help of an afterloader. By using high rate radiation sources, the exposure time can be reduced to minutes.

Some advantages of this technique are accelerated treatment and the possibility of more accurate dose distribution by using inverse treatment planning to adjust dwell positions and times (Skowronek, 2017). Disadvantages are greater late tissue effects, the need for shielded rooms and afterloading equipment.

Pulsed dose rate brachytherapy

Pulse dose rate brachytherapy (PDR BT) aims to offer the accurate dose shaping and expeditious treatment of high dose radiation with the low late tissue effects of LDR BT. The procedure is comparable to HDR BT, but instead of using high-dose rate radiation for a few minutes to treat the tumour, it uses pulses of a lower dose rate radiation source over a period of hours (Balgobind et al., 2015). A possible disadvantage of this therapy is the increased treatment duration and therefore diminished cost-effectiveness.

1.2.3. Radionuclide therapy

Radionuclide therapy, or nuclear medicine, uses radioactive pharmaceuticals that are designed to accumulate in the malignant growth to deliver ionising radiation to the tumour. Researchers are looking for specific markers to bind the radiopharmaceutical to the growth. This therapy is currently limited to certain types of prostate tumours, generally castrate resistant tumours ("Fact Sheet: Targeted Radionuclide Therapy and Prostate Cancer," 2019).



Methods

Quality literature on steerable needles for HDR BT in prostate cancer treatment is scarce. Therefore, I decided to split my research in three parts. Firstly, to find literature on the state of the art in HDR BT, I searched PubMed with the search terms: "HDR Brachytherapy[Title]" OR "High Dose Rate Brachytherapy[Title]" AND "Prostate[Title]" AND "2016"[PDAT]: "2019"[PDAT].

This search yielded 110 papers. 18 Additional sources were identified mainly in the bibliography of previously found papers. After removing duplicates, the papers were screened for access to full-text availability. The remaining paper were then assessed on their relevance, this resulted in a total of 63 papers. The study section process can be seen in Figure 44.

The second part of my research was into the anatomy and characteristics of the prostate and its surroundings and the difficulties experienced in implanting

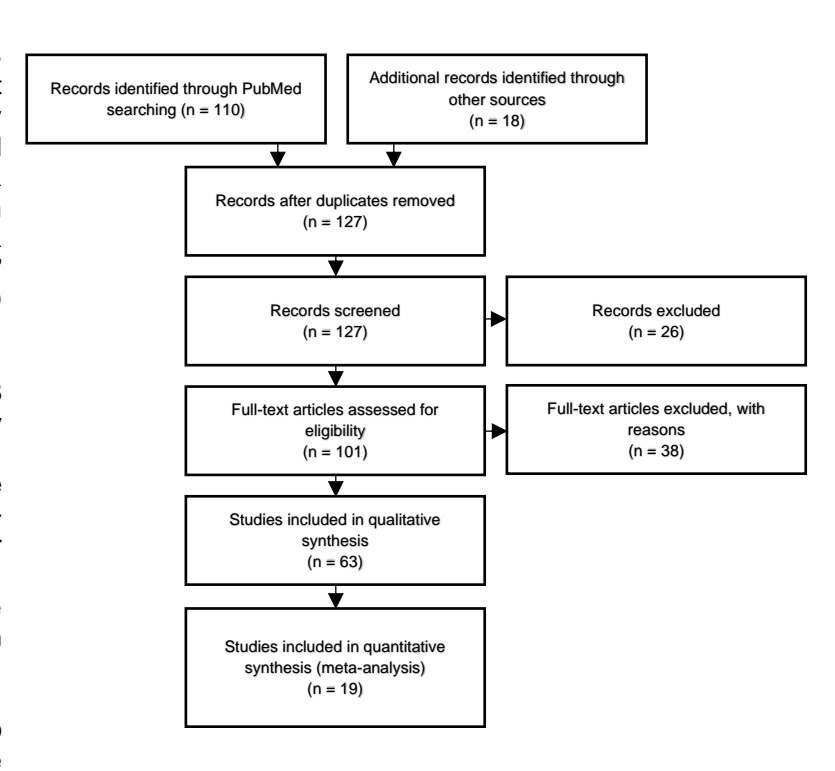


Figure 44 Study Selection Process HDR BT

HDR BT implants. Because the information I was after was quite specific, a systematic approach such as in the preceding chapter would be unsuccessful. Instead I searched for papers pertaining to implantation related toxicities in prostate cancer and used their references to build a comprehensive overview of the field. Additionally, I used the book Sabotta; Atlas of Human Anatomy (Paulsen & Waschke, 2013) for addition information on anatomy. In total I collected 43 sources. 32 Of those paper were determined to be relevant and were included in this literature review.



The third part of my literature review pertains to steerable needles used for the treatment of the prostate. I searched PubMed, the journal Medical Engineering & Physics and Google Scholar with the terms 'Steerable' and 'Prostate'. This yielded a limited number of papers. Using the bibliographies of the previously found papers I collected a total of 50 papers, of which 42 were deemed to be relevant and were included in this literary review.



High dose rate brachytherapy orostate cancer therapy

Abstract

In high dose-rate brachytherapy of the prostate, multiple sleeves are placed transperineally into the prostate under transrectal ultrasound guidance. High dose-rate brachytherapy is often used as monotherapy for low to intermediate risk prostate cancer patients. In high risk patients a combination of high dose-rate brachytherapy and external beam radiotherapy is common. In recent years, the field has seen a shift to less fractions with higher doses.



The advantage of BT over EBRT is the localised radiation and thereby supposed diminished adverse side effects. Through the ability to adjust dwell times to the 3d geometry of the tumour, HDR BT has the ability to reduce radiation to surrounding tissue and reduce adverse effects over LDR BT (Dutta, Alonso, Libby, & Showalter, 2018). It has been shown HDR BT can be advantageous in the treatments of low, medium and high risk prostate cancer (Dutta et al., 2018; Grills et al., 2004; Skowronek, 2017). This chapter aims to determine the state of the art in HDR brachytherapy, the clinical outcomes of these methods and possible future innovations in the field.

3.1. Methods and practices

The HDR BT procedure can be divided into four general steps:

- 1. **Needle implantation –** While the patient is in a dorsal lithotomy or lateral decubitus position (Tselis et al., 2017), under real-time transrectal ultrasonography (TRUS) or magnetic resonance imaging (MRI)-based guidance, needles are inserted through a template into the perineum. approximately 15 needles are placed throughout the prostate. Depending on the cancer, needle positions can vary (Yoshioka, Itami, Oguchi, & Nakano, 2019);
- 2. Treatment planning Inverse treatment planning is common, using computer tomography (CT), MRI or TRUS to map the position of every needle. Geometric optimisation is used to calculate dose distribution according to the prescribed dose and the planning target volume (PTV);
- 3. Afterloading An afterloader is used to populate the needles in the prostate. The afterloader populates the needle according to the treatment plan generated in the previous step. By modulating dwell times, the afterloader can deliver ionising radiation to the required sites while sparing healthy tissue. Common dose prescriptions are 54Gy in six fractions and 38Gy in four fractions (Tselis et al., 2017);
- Patient management Depending on the number of fractions per implant, the patient might need to remain in bed for hours or days. During this time, measures are taken to minimise complications and discomfort.

While the general steps in modern HDR BT are constant, there is discussion about the specifics of the procedure. One of these discussions pertains to the dosimetry. The field currently is moving towards higher dose rates with lower fractions. Therapies with doses of up to 19Gy in a single fraction have been described (Hoskin et al., 2017; Prada et al., 2016; Siddiqui et al., 2019). It should be noted that some of the authors warn about 19Gy being a suboptimal dose for HDR BT.

A recent trend in the treatment of prostate cancer has been the decrease in screening and curative treatment. Because of the nature of this cancer, it is often advantageous for the quality of life of the patient to implement watchful waiting instead of radical treatment (Arredondo et al., 2008).

3.2. Clinical outcomes

To be able to evaluate the clinical outcome of different studies I will where possible use 5-year biochemical non-evidence of disease (bNED) rates. These rates are the most widely reported and allow best for comparison. Late gastrointestinal toxicity (GI) and late genitourinary toxicity (GU) rates above grade 3 will be used to describe toxicity of the treatment. For the classification of risk-groups the widely used D'Amico classification will be used.

Please note that the inclusion criteria for toxicity statistics can vary between studies, complicating direct comparison. Secondly, the occurrence of these late toxicities is relatively rare which makes the power of most studies insufficient.



3.2.1. HDR BT as monotherapy, a comparison with other radiological interventions

HDR BT has widely been accepted as a monotherapy for low and intermediate risk localised prostate cancer (Yoshioka et al., 2019). However, also for high-risk patients, HDR BT might be non-inferior to other radiological therapies. Table 11 shows the result of studies specifically into the use of HDR BT as a monotherapy for prostate cancer.

Study	Patients	Risk Group	5-year bNED	Treatment (Total dose Gy/ fractions)	Late GI toxicity (grade 3 or above)	Late GU toxicity (grade 3 or above)
	73	Low	95%	27 Gy/2, 45.5		
Yoshioka et al. (2017)	207	Intermediate	94%	Gy/7, 49 Gy/7,	1%	0.2%
(2011)	244	High	89%	54 Gy/9		
	198	Low	96.1%			
Strouthos et al. (2018b)	135	Intermediate	96.1%	34.5/3	0%	18.7%**
(20100)	117	High	92.1%			
	48	Low	100%		2%	0%
Yamazaki et al.	75	Intermediate	95.6%	45.5/7, 54/9.		
(2018a)	128	High	90.4%	49/7,		
	19	Very High	89.2%			
Patel et al. (2017)	190	Intermediate	97%	43.5/6*	0%	3.7%
Nagore et al.	84	Low		07/0		
(2018)	35	Intermediate	96%	27/2	1%	2%

Table 11 HDR BT Monotherapy, only significant values (*median values ** including erectile disfunction)

Patel et al. (2017) report HDR BT to be a safe and highly effective treatment for localized prostate cancer in intermediate-risk patients. This study also highlights the difficulty in comparing different studies A 3.7% genitourinary toxicity is reported, while also stating 32% erectile dysfunction under previously non-symptomatic patients.

Yamazaki et al. (2018a) showed no statistically significant difference for HDR BT monotherapy versus image-guided intensity-modulated radiotherapy (IG-IMRT) for localized prostate cancer. The 5-year bNED after patient selection bias adjustments were 92.9% and 89.1% (p=0.18) for HDR BT and IG-IMRT respectively. They did find increased genitourinary toxicity in patients treated with HDR BT.

Yamazaki et al. (2019) showed an equivalent outcome of HDR BT compared to LDR BT with or without EBRT. Kollmeier et al. (2017) found no significant difference in outcomes for LDR and HDR salvage BT for selected patients. Hegde et al. (2018) showed stereotactic body radiotherapy as well as HDR BT can provide excellent bNED rates for intermediate risk prostate cancer.

The ASCENDE-RT trial found dose-escalated EBRT as a monotherapy to result in a 62% five year disease free survival rate (Morris et al., 2017). The studies listed in Table 11, show higher 5-year bNED rates in high-risk patient who underwent HDR BT as monotherapy. The excellent 5-year bNED rates of HDR BT for high-risk prostate cancer treatment seem to indicate non-inferiority to other radiological modalities. Despite these 5-year bNED rates, high-risk prostate cancer is recommended to be treated with EBRT with a HDR-BT booster (Morris et al., 2017).

3.2.2. HDR BT as booster, a comparison with other radiological Interventions

For intermediate and high-risk patients an HDR BT boost is often used in combination with external radiation. Table 12 describes studies into HDR BT as a booster for external radiation radiotherapy. The type of ER varies among studies and is not always disclosed. Often external beam radiation therapy (ERBT) is used.



Study	Patients	Risk Group	Treatment (Total dose (Gy)/ fractions)	5-year bNED	Late GI toxicity (grade 3 or above)	Late GU toxicity (grade 3 or above)	ER treatment
Yaxley et al. (2017)	169	Intermediate	16.5/3, 18/3,	93.3%			46Gy/ 23
Taxley et al. (2017)	338	High	19.5/3	74.2%			40Gy/ 23
	57	Low	18/3, 19.5/3, 19/2,	94.8%			
Vigneault et al. (2017)	640	Intermediate	20/2, 21/2 and	95%			36-45Gy/ 15-22
	135	High	15/1	93.5%			10 22
Strouthos et al. (2018a)	303	High	21/2	85.7% **	0%	23.3%***	45Gy
	5	Low		100%*			
Liu et al. (2016)	36	Intermediate	18/2	100%*		2.6%	39Gy/13
	115	High		96.9%*			
	163	Low		98.1			
labinaria et al. (2047)	1058	Intermediate	Median 19/7	95.5	0,6%	6.2%	Median
Ishiyama et al. (2017)	1689	High		89.5			39Gy/ 13
	490	Very-high		80.4			
Ob 1 - 1 (0040-)	42	Intermediate	40/0.40/0	92%	00/	5.00/	50.4Gy/
Chao et al. (2019a)	53	High	18/3,16/2	88%	0%	5.3%	28
	65	Intermediate					
Olarte et al. (2016)	100	High	19/4	88.7%**	2.2%	7.6%	54Gy
	18	Very High					
Ng et al. (2018)	20	Intermediate	0.1/0.10/0.15	100%	221	407	45 Gy (median)
	55	High	21/2, 19/2, 15/1	80.3%	0%	4%	
	7	Low		75% 26%			
Hoskin et al. (2012)	43	Intermediate	17/2		26%	7%	35,75Gy/ 13
	56	High					13

Table 12 HDR BT booster studies, only significant values (* 3 years bNED ** 7 years bNED *** including erectile disfunction)

A Norwegian cohort study showed the efficacy of HDR BT+ EBRT over EBRT only for high-risk patients. Patients undergoing EBRT only had a 1.6 times higher overall mortality rate over ten years then the HDR BT+EBRT cohort (95% CI 1.08–2.44) (Wedde et al., 2019).

Kent, Matheson, and Millar (2019) showed an overall survival and cause-specific survival increase for all risk-groups in their cohort when comparing EBRT with an HDR BT boost with EBRT alone.

Chiang and Liu (2016) showed HDR BT as boost to ER performed significantly worse in biochemical control then radical retropubic prostatectomy, cryoablation and high-intensity focused ultrasound. To be noted is this result is at least partially due to the lack of recommended androgen deprivation therapy.

The ASCENDE-RT trial (Morris et al., 2017) has shown that a LDR BT boost in external radiation therapy is effective for intermediate to high-risk prostate cancer. The conclusion of the paper stated; 'Compared with 78 Gy EBRT, men randomized to the LDR BT boost were twice as likely to be free of biochemical failure at a median follow-up of 6.5 years.' Hoskin et al. (2012). Found a statistically significant bNED rate increase for HDR BT boosted EBRT versus EBRT alone.

Older phase III trials puts the 5 year bNED rates of EBRT alone at 64% and 54% for 78-Gy and 68-Gy treatments respectively for high risk prostate cancer patients (Peeters et al., 2006). The data in Table 12 and the previously cited works lead me to believe in the definite advantages to an HDR BT boost in ER therapy in comparison to ER therapy alone, makes it highly likely HDR BT boost for EBRT therapy is effective.



3.2.3. Dosimetry

A recent development in HDR BT is research into hypo-fractioned treatments. It is known cancerous prostate cells should respond favourably to higher doses of ionising radiation. Additionally, increasing doses and decreasing fractions could reduce costs and hospitalisations. Table 13 describes the studies specifically into the dosimetry of HDR BT.

Study	Patients	Treatment (Total dose (Gy)/ fractions)	Risk Group	5-year bNED	Late Gastrointestinal toxicity (grade 3 or above)	Genitourinary toxicity (grade 3 or above)	Combined With
	0		Low	-			
	26	45.5/7	Intermediate	100%	1%	-	
	2		High	100%			
	48		Low	90%			
Yamazaki et al. (2018b)	52	49/7	Intermediate	100%	5%	-	-
(20105)	39		High	97.4%			
	38		Low	86.8%			
	71	54/9	Intermediate	94.1%	3%	-	
	71		High	88.5%			
Prada et al.	44	40/4	Low Intermediate	66% (6 years)	0%	0%	
(2016)	16	19/1		60% (6 years)	0%	0%	-
Nagore et al.	84	07/0	Low Intermediate	96%	0%	1%	-
(2018)	35	27/2					
	319	38/4	Low,	97%			
Jawad et al. (2016)	79	24/2		87%	0%	<1%	-
(2010)	96	27/2	memediate	90%			
	49	20/1, 19/2		94%*	0%	2.6%	
Hoskin et al. (2017)	139	26/2	Intermediate, high	93%*	0%	1%	
(2017)	106	31.5/3		91%*	0%	1.1%	
	30	18/3	Low,	86.5%		<5%	46Gy EBRT
Falk et al. (2017)	55	18/2	Intermediate,	86.6%	0%		
(2011)	74	14/1	High	87.2%			

Table 13 Dosimetry Studies, only significant values (* 4-years)

The discussion pertaining to dosimetry in HDR BT stems from the finding of low alfa/beta ration of prostate cancer cells. This effectively means the malignancy should respond more favourably to higher doses of radiation per fraction (Thiruthaneeswaran & Hoskin, 2016). A lot of interest has been shown in single fraction HDR BT after Mavroidis et al. (2014) showed that, theoretically, a single fraction of 19.2 to 19.7 Gy should result in comparable biological control to current practices, while significantly decreasing complication rate.

A number of studies investigated the efficacy of single fraction 19Gy HDR BT (Krauss et al., 2017; Morton et al., 2017; Siddiqui et al., 2019; Vigneault et al., 2018). In the authors opinion, the only study with a sufficient sample size and a meaningful was conclusion is the paper by Prada et al. (2016) of which the results can be found in Table 13. This study shows promising late toxicity rates, but shows rather disappointing biochemical control rates at 5 years. A finding supported by the paper from Siddiqui et al. (2019). Contradictory, Hoskin et al. (2017) reported 5-year bNED rates of 96% and 85% for intermediate and high-risk patients respectively. These results were achieved with a single implantation and up to a single fraction. Falk et al. (2017) showed respectable bNED rates with a single fraction of 14Gy.

Hauck et al. (2017) showed that patients receiving single-fraction HDR-BR have a higher chance of presenting a benign elevated PSA, also known as a 'bounce'. This could in part be an explanation for the discrepancy between the theoretical efficacy of single fraction HDR BT and its clinical outcomes. Astrom, Sandin, and Holmberg (2018) also found this 'bounce' and associated it with a good clinical outcome. Vigneault et al. (2017)



concluded that hypo fractioned therapies with a higher biologically effective dose (BED) resulted in improved biochemical control at the cost of a small but acceptable increase in urinary toxicity.

The discussion about the dosimetry in HDR BT for prostate cancer is far from over. There does however seem to be evidence that a hypo fractionated therapy with a higher BED has the potential to be non-inferior to current methods in terms of bNED rates while possibly decreasing costs and required hospitalisations.

3,2,4. Cost-effectiveness

A study from Vu et al. (2018), using the data from the ASCENDE-RT trial, showed EBRT with a HDR BT boost to be cost-effective in comparison to EBRT alone due to the lower expected lifetime treatment costs. Halpern et al. (2016) shows brachytherapy to have significantly lower costs than all the EBRT and proton beam treatments. The same study also shows a decrease in utilization of brachytherapy between 2005 and 2011. Ilg et al. (2016) showed HDR to be less economical of a procedure than LDR BT for low-risk localized prostate cancer. The main cost increased# comes from the prolonged hospitalization due to multiple fractions and the personnel costs this entails.

Assuming equivalent clinical outcomes, HDR BT seems to only be more cost-effective then LDR BT in low to intermediate-risk patients if hypo fractionated regimes are adopted. As a boost or monotherapy for intermediate to high-risk patients, HDR BT is cost-effective even with the current fractionations.

3.3. Prospects

HDR BT is largely accepted as an adequate treatment for low and intermediate risk prostate cancer treatment (Sanchez-Gomez, Polo-deSantos, Rodriguez-Melcon, Angulo, & Luengo-Matos, 2017). A randomised trial showed the effectiveness and safety of a HDR BT boost for EBRT (Hoskin et al., 2012) Studies into the HDR BT of high-risk prostate cancer are becoming more frequent. Multiple studies have shown the safety, advantages and cost-effectiveness of HDR BT as monotherapy or as boost for EBRT for patients in all risk groups (Hannoun-Levi, 2017; Mendez & Morton, 2018).

Studies into the use of HDR BT in salvage prostate cancer treatment are appearing (Chatzikonstantinou et al., 2017; Hepp et al., 2018; Jiang et al., 2017; Maenhout et al., 2017a; Maenhout et al., 2017b; Wojcieszek et al., 2016). and show promising results. Studies into dose planning algorithms and parameters continue to improve survival rates as well decrease late toxicity (Kragelj, 2016; Kragelj, Zlatic, & Zaletel-Kragelj, 2017; Poulin, Varfalvy, Aubin, & Beaulieu, 2016).

One often described complication in HDR BT is the post-implantation displacement of needles and anatomical changes during the procedure (Maenhout et al., 2018). With multiple fractions per implantation the chance of this occurring increases. Using MRI or CT to do the treatment planning also increases the chance of displacement of equipment or anatomical variations, because the patient must be moved and repositioned. This effect could be minimised by using TRUS for treatment planning and single fraction implantations (Tselis et al., 2017). However, with high dose rate hypofractionated regimes, the adverse effect of a displaced needle would theoretically be more severe than in a treatment with more implants.

Some of the recently appearing practises, using hydrogel spacers to distance the rectum from the prostate during radiation, have shown significant dose reduction to the rectum, thereby decreasing acute GI toxicity and possibly late GI toxicity (Chao et al., 2019b). Another novel approach is inducing hyperthermia to sensitize the malignant cells to radiation before radiotherapy (Kukielka, Hetnal, & Bereza, 2016). Another topic that is frequently studied is imaging of the prostate. With better imaging modalities, a more accurate and valuable treatment plan can be synthesised (Murgic et al., 2016; Peters et al., 2019; Saigal et al., 2019; Yang et al., 2017).

To summarise, the field of HDR BT is moving toward hypo fractionated high BED therapies for all risk-patients. Imaging modalities and assistive techniques are being developed to make the process more effective, faster, more economical, and safer.



3.4. Conclusion

In HDR BT several needles are implanted in the prostate through which radiotherapy can be applied locally. This allows for a more targeted radiotherapy, sparing surrounding tissue. HDR BT has been accepted as an adequate, safe, and cost-effective monotherapy for low- and medium-risk prostate cancer and as a booster for all-risk prostate cancer in combination with EBRT. The field is moving toward hypofractionated treatments, promising reduced hospitalization time, increased patient comfort and decreased costs.



4

Prostate anatomy and needle positioning difficulties

Abstract

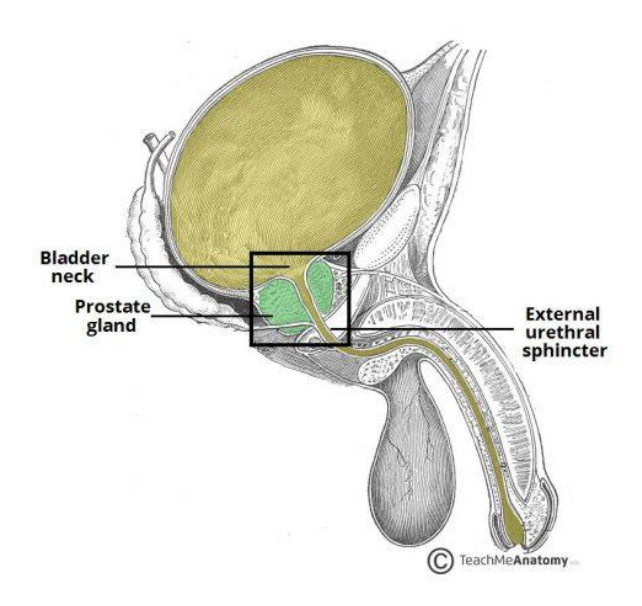
The prostate is located between the penis and bladder and surrounds the urethra. Needle positioning can be hindered by unwanted needle bending and tissue movement. The urethra and pubic arch can occlude the surgeons target. Placed needles cause trauma to the surrounding tissue. Research suggests there could be a link between needle related trauma and late toxicities such as acute urinary retention and erectile dysfunction.



Inserting needles through the perineum into the prostate causes trauma. This chapter aims to elaborate on the difficulties of needle placement in HDR BT and the toxicities due to implantation trauma. Because literature on needle accuracy and needle related trauma in the prostate is scarce, where appropriate, literature on prostate biopsies and LDR BT are cited.

4.1. General prostate anatomy

A normal prostate is about 3 cm high, 4 cm wide, 2 cm deep and weighs 11 grams (Leissner & Tisell, 1979). The prostate consists of three histological zones, the central, transitional, and peripheral zones (Figure 45) (Ittmann, 2018). The fibromuscular stroma is a result of developmental interactions with the urethra and has little glandular function. The prostate does not have a capsule surrounding it but a tough fibromuscular band that hinders needle insertions (Ryoichi Oyasu, 2008).



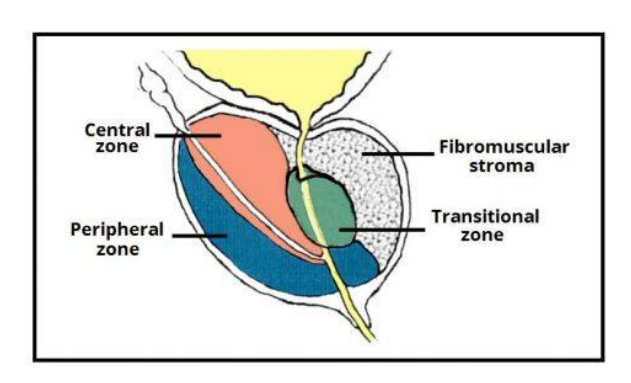


Figure 45 Prostate Anatomy and Histological Zones. (teachmeanatomy.info) Left figure shows the position of the prostate within the urinary system. Right figure shows the zones of the prostate.

The main function of the prostate is to produce prostatic fluid that in several ways aids the sperm in thriving in the vaginal environment. Prostate cancer often starts in the peripheral zone (Paulsen & Waschke, 2013). The fact the prostate surrounds the urethra explains the urinatory symptoms of prostate cancer.

To implant needles into the prostate through the perineum, the following tissues must be passed, from superficial do deep:

- Perineal membrane or corpus spongiosum;
- Transverse perineal muscles or Urethral sphincters;
- fibromuscular band of the prostate (Raychaudhuri & Cahill, 2008).

4.2. needle insertion force

To better understand the process of needle insertion, this section will discuss needle forces involved and required accuracy.

Podder et al. (2006b) used 6 DOF force sensor to record needle insertion data for 25 patients. They presented force and velocity data for 17g and 18g needles of which a summery can be found in Table 14. They also note needle velocity has little impact on the maximum needle force. Podder et al.

Needle	Max Force in the Perineum (N) (Avg./SD)	Max Force in the Prostate (N) (Avg./SD)	Max Velocity (m/s) (Avg./SD)
17G (1.47mm)	13.75/3.40	9.20/3.70	1.43/0.69
18G (1.27mm)	7.79/3.45	6.21/1.74	1.20/0.71

Table 14 Needle insertion forces and velocities (Podder et al., 2006b).



(2006b) states: "It is intuitive that lower force will cause less deformation and displacement of internal tissue/organ, and create less trauma and oedema to the patients. Thus, use of 18G needle (1.27mm in diameter) is more logical from a clinical point of view."

The number of needles required for a good quality HDR BT implant in most cases is 15-17 (Fröhlich, Ágoston, Lövey, Polgár, & Major, 2010). Evidence of a relation between toxicity and needle trauma is present and will be discussed later in this paper.

4.3. Needle insertion accuracy

In the placement of 1197 LDR seeds, Jamaluddin et al. (2017) found an average misplacement of 0.49 cm (95% CI [0.47-0.51]) at an average penetration distance of 6.46 cm (95% CI [6.24-6.68]). In 414 (34.6%) of seed placements, needle manipulation was observed. However, manual manipulation of the needle did not show statistically significant correlation with seed misplacement. Jamaluddin et al. (2017) also found a lower maximum velocity of the needle insertion increases the seed placement accuracy for LDR BT.

Blumenfeld et al. (2007) found the main deviation from target in prostate biopsies to be 6.5mm (*SD* 3.5mm). Large deviations were witnessed in asymmetrical needle tips and smaller deviations in symmetrical needle tips. Needle displacement error due to deflection was found to be a significant cause of diagnostic error. Sadjadi et al. (2014) found a 5 to 8mm needle deflection when inserting 18g bevel-tipped brachytherapy needles into a prostate phantom, corroborating the earlier finding.

In LDR BT the misplacement of seeds leads to a disturbance in the treatment plan. In HDR BT the treatment plan is determined after implantation and can account for needle inaccuracies. Due to this fact needle accuracy in HDR BT is less of an issue. Needle displacement after treatment planning however is critical, evident by the sheer amount of literature on post treatment planning needle displacement in HDR BT. Needle displacement regularly leads to post-implantation correction. Aluwini et al. (2016) found that correcting greater than 3mm displacements of HDR implants between fractions does not lead to increased acute or late GU or GI toxicity.

Buus et al. (2018) states that the threshold for acceptable needle migration should be 3mm. Buus et al. (2018) also states in lower fraction HDR therapies, this threshold should be reduced. Buus et al. (2018) proposes 2mm for doses ≥15 Gy. The necessity for a decreased threshold can be explained by the lack of the averaging effect of multiple fractions on the total dose of radiation a tissue receives.

While needle accuracy is not as critical in HDR BT as it is in prostate biopsies or LDR BT. Being able to implant needles more accurately could reduce needle manipulation and required number of needles to achieve adequate coverage of the prostate. Why this is of importance will be discussed in Section 4.5.

4.4. Unwanted needle bending

Sadjadi et al. (2014) found needle deflections in a bevel-tipped needle of 5 to 8mm at an insertion depth of 76mm in a prostate phantom. Moreira et al. (2018) found, in robot assisted trans-perineal biopsies, the mean targeting error to be 6.3mm. They concluded most of this error was due to contact between the skin and the needle. Methods are being investigated to partially mitigate needle bending in bevel-tip needles (Jun et al., 2019).

Needle bending is a serious and unpredictable issue complicating many fields including prostate BT. While needle accuracy is not as critical in HDR BT as it is in LDR BT or prostate biopsies, large inaccuracies are undesirable. In a questionnaire filled out by interventional radiologists, de Jong et al. (2018) found 85% of respondents experienced 'significant unwanted needle bending' in their practise. The respondents indicated a mean acceptable needle tip accuracy error of 2.7mm and a mean maximal encountered unwanted needle bending of 5.3mm. 95% of respondents agreed that that the needles used in interventional radiology needed improvement and 94% of respondents agreed that steerable needles would help in correcting for needle bending.



4.5. Evidence of implant related toxicities and responsible tissues

In HDR BT several needles are introduced through the perineum into the prostate. These needles damage surrounding tissues and structures. Quantifiable evidence of this trauma is hard to come by. This section will try to determine structures at risk and the complications that trauma to these structures' entails. Due to the similar nature of HDR and LDR brachytherapy needle implantation and the lack of literature, both papers on HDR BT and LDR BT will be included in this section to quantify needle implantation trauma.

The paper by Steggerda, van der Poel, and Moonen (2010) states that structures particularly at risk of damage by needle implantation of the prostate in LDR BT are: "penile bulb, neurovascular bundles, bladder neck, and bladder trigone". This paper subsequently states: "Acute and very early toxic reactions after the implantation, such as acute urinary retention (AUR), are most likely to be caused by the needle insertions because the delivered dose shortly after the procedure will be too small to cause these symptoms."

It speaks to reason that the implantation of needles through the perineum damages tissue which results in toxicities. This could explain evidence of increased toxicity in BT compared to IMBT, when BT should theoretically be tissue sparing. The subsequent question would be: what are these structures and can they be avoided? The following three sections discuss the three main categories of toxicity associated with HDR BT of the prostate: genitourinary, gastrointestinal and sexual.

4.5.1. Genitourinary

Tissues at risk of implant related trauma were identified using the Sabotta Atlas of Human Anatomy (Paulsen & Waschke, 2013) and the articles cited in the following section.

- Urethra: Responsible for transporting and controlling the flow of urine for removal from the body, also transports semen. Eapen et al. (2014) hypothesizes periurethral needle placement contributes to urinary toxicity;
- **Urethral sphincters:** a set of muscles inferiorly to the bladder responsible for controlling the flow of urine from the bladder. Only the external sphincter can be controlled voluntarily (Andersson & Michel, 2011);
- **Pudendal nerves:** innervates the urethral sphincters amongst other things (Jung, Ahn, & Huh, 2012).

Eapen et al. (2014) provided low level evidence that there is a link between periurethral needle manipulations and acute urinary toxicity. This finding is corroborated by findings from other papers linking the number of needle implantations to acute toxicities (Buskirk et al., 2004; Lee et al., 2000; Steggerda, van der Poel, & Moonen, 2008; Wust et al., 2004).

Buskirk et al. (2004) stated that all cases of acute urinary retention (AUR) after LDR brachytherapy could be due to the trauma related to needle implantation. This was concluded after trans-perineal template guided prostate biopsies showed a 11.5% incidence of AUR (95% CI [6.9–17.5]), rates similar to AUR rates in LDR brachytherapy. Skouteris et al. (2018) found 30 of 379 (7.9%) men developed urinary retention after transperineal template guided biopsy. The elevated risk of AUR in trans-perineal prostate biopsies in relation to transrectal prostate biopsies indicates AUR is presumably due to needle trauma (Grummet, Pepdjonovic, Huang, Anderson, & Hadaschik, 2017).

Vargas et al. (2005) found the an increased number of needles implanted to increase the risk of chronic grades 2 or greater and grade 3 urinary toxicity. The paper stated; 'Patients treated with 14 or greater needles had a 30% increase in grade 2 or greater and a 7% increase in grade 3 chronic urinary toxicity at 4 years (p < 0.001 and 0.05, respectively...'

In LDR BT the therapeutic dose of radiation is released over a period of months. This means that in the first 48 hours after implantation it is unlikely side effects are due to the radiation (Steggerda et al., 2010). The two studies mentioned previously indicate the same. The similarity in HDR and LDR brachytherapy implantation makes it likely that a significant portion of the acute urinary toxicity is due to needle trauma in HDR BT.



There is evidence of acute urinary toxicity due to needle trauma and even more evidence of AUR due to needle trauma. The mechanisms behind these toxicities are largely unknown. Trauma to the urethra, urethral sphincters, nerves, or blood supply are possibly causes. With the external urethral sphincter and urethra being of additional concern, as they are directly in the path of an HDR BT needle implantation.

4.5.2. Gastrointestinal

I was unable to find a link between implantation trauma and Gastrointestinal (GI) toxicity. GI toxicity does occur in HDR BT however it seems to be solely due to the radiation. Additionally, there are to my knowledge no nervous or vascular pathways through the perineum that serve the GI tract.

4.5.3. Sexual

To identify structures at risk of trauma in trans-perineal needle implantations responsible for sexual toxicities, I used the Sabotta Atlas of Human Anatomy (Paulsen & Waschke, 2013) and the paper by Lee et al. (2016) on vessel sparing in radiotherapy. Structures possibly susceptible to implant trauma are:

- **Bulbus penis:** enlarged proximal part of the corpus spongiosum. Radiation to this structure correlates with erectile dysfunction (Fisch, Pickett, Weinberg, & Roach, 2001);
- Corpus cavernosum: A sponge-like structure that engorges with blood to maintain an erection;
- Internal pudendal arteries: These arteries supply blood to the sex organs;
- Cavernous nerves: Responsible for facilitating erections, known to cause erectile dysfunction when damaged (Kundu et al., 2004; Paulsen & Waschke, 2013). These nerves can be highly variable in anatomy;
- Bulbourethral gland: responsible for producing pre-ejaculate. In close proximity to cavernous nerves:
- Prostatic plexus: Innervation of the prostate, known to cause erectile dysfunction when damaged.

The paper on vessel sparing radiotherapy and functional anatomy by Lee et al. (2016) provides an overview on the current knowledge of the structures that are responsible erectile function. The subsequent paper by the same authors (Spratt et al., 2017) shows a significantly higher percentage of patients undergoing radiotherapy maintained erectile function when these structures were spared. Macdonald et al. (2005) identified number of needle implantations in LDR BT to be one of the indicators of erectile dysfunction.

Erectile dysfunction of transient nature is relatively well reported in trans-perineal biopsies (Pepe & Pennisi, 2015; Pepe, Pietropaolo, Dibenedetto, & Aragona, 2013). Pepe and Pennisi (2015) concluded there to be no long-term effect of trans-perineal biopsies on erectile function. Contradictory, Chong, Van Hemelrijck, Cahill, and Kinsella (2016) found a long-term effect of trans-perineal biopsies on erectile dysfunction alongside a transient effect. A recent finding by Kamali et al. (2019) indicates that transrectal biopsies also could have an negative effect on erectile function.

Lee et al. (2016) identified tissues responsible for erectile dysfunction at risk of access ionising radiation. It stands to reason these tissues would not respond favourably to needle trauma. The paper states; "Radiation dose to the penile bulb is widely believed to be a surrogate to dose to adjacent essential structures such as the corpus cavernosa, internal pudendal arteries, or terminal branches of the cavernous nerves that drape over the penile bulb as these nerves approach the corpus cavernosa."

In the case of erectile dysfunction, the mechanisms behind the symptoms are better understood. Damage to any of the nerves or the vasculature listed above is known to play a role in erectile dysfunction. However due to the small size and complexity of these structures, minimising trauma can be a daunting task. Trauma to the bulbus penis is of especial concern as this tissue is known to be adjacent to the vasculature and neural pathways that serve the penis.



4.6. Anatomy limiting access to the prostate

Anatomy can limit access to the prostate. Some anatomical obstructions are always present, such as the urethra running through the prostate, and others are patient specific.

4.6.1. Urethra

The urethra runs through the prostate. During ejaculation prostate fluid is added to the semen in the prostatic urethra. To deliver a satisfactory dose distribution, needles must be placed conformally throughout the prostate. It is desirable to avoid the urethra when possible, as periurethral needle placement can increase the chance of urinary toxicity (Eapen et al., 2014). The anterior-medial area of the prostate can be hard to reach with a conventional template, because it is occluded by the urethra (Figure 46).

Prostate gland Implant catheters Template Ultrasound probe

Figure 46 Needle implantation in HDR BT. (www.prostate.org.au) Red arrow shows the prostate.

4.6.2. Pubic arch interference

Large prostate glands can result in an overlap between the pubic arch and the prostate, resulting in pubic arch interference (PAI). In PAI, a

part of the prostate is occluded by the pubic arch making implantation more difficult. Typically, patients with prostates larger than 50-60cc present a significant risk of PAI. Moreover, greatly enlarged prostate volume are considered a contraindicatory for HDR BT (Monroe et al., 2008). Several methods are available to decrease PAI, which are:

- Hormone therapy to decrease prostate size;
- Obliquely or freehand placed needles;
- · Repositioning the patient.

Gibbons, Smith, Beriwal, Krishna, and Benoit (2009) found using a free-hand perineal template yielded acceptable results for prostates larger than 50cc. Due to the post implantation treatment planning, a small amount of PAI can be accounted for in HDR BT.

4.7. Conclusion

The prostate is a difficult tissue to treat with radiotherapy, both due to its location in the human body and its makeup. Gaining access means passing through sensitive tissues. The damage needle implantation does to the tissues surrounding the prostate is largely unknown. By comparing HDR BT to trans-perineal biopsies and LDR BT, we find some of the urinary and sexual toxicities associated with HDR BT that are likely attributable to implant trauma. Minimising implant related trauma could be achieved by minimising the number of implantations in a given treatment, minimising the number of needles per implantation, or sparing some of the tissues likely involved in these toxicities. Tissue likely susceptible to needle implantation trauma related toxicities are; urethra, urethral sphincters, penile bulb, internal pudendal arteries, cavernous nerves, and prostatic plexus.



Steerable needles

Abstract

Steerable needles allow the user to correct the path of the needle after insertion. This gives the user the possibility to avoid sensitive tissues and place the needle more precisely. Several steerable needles are commercially available. None of these needles are suitable for use in high dose-rate brachytherapy of the prostate. There are multiple steering mechanisms including bevel-tip steering, pre-curved stylet, and articulated tip steering. Bevel-tip steering is becoming less prominent while biomimicry is gaining popularity.



Whilst the majority of the field calls the device implanted to deliver the radiotherapy in HDR BT, 'needles', there are some that use the term 'catheter'. The general association with steerable catheters are the steerable catheters used in cardiology. For the sake of simplicity and conformity with the field I will maintain the term 'steerable needle'.

There are a few possible advantages a steerable needle could have. Two of those being increased positioning accuracy and the ability to manoeuvre around sensitive tissues. This chapter aims to reveal currently available steerable needles for prostate procedures, research into the topic and prospects regarding steerable needles.

5.1. Commercially available steerable needles

Several steerable needles are commercially available for a variety of interventions. Some of these are:

- **Morrison** 21g (0.8mm), 1-way steerable stylet and needle. Intended uses percutaneous injection, aspiration and tissue sampling of musculature (AprioMed, 2019);
- Osseoflex® 8g-10g (4.0-3.5mm) 1-way steerable stylet and needle. Intended for vertebral augmentation (Medical, 2017);
- Pakter Curved Needle 21g (0.8), 1-way steerable stylet and needle. Intended for discography, diagnostic sampling, aspiration, and injection (Cook Medical, 2019).

Systems such as the MIRIAM, a robot designed to take prostate biopsies trans-perennially (DEMCON, 2019), are currently being developed. None of the available devices or devices being developed mentioned above are intended to be used in HDR BT of the prostate.

5.2. Steering mechanisms

The comprehensive paper by van de Berg (2016) classifies six steering techniques, which can be found in Figure 47. The steering mechanisms the paper identifies are discussed in the following sections

5.2.1. Base manipulation

Base manipulation was one of the earlier needle steering approaches. By manipulating the base of the needle after the tip is inserted, a curvature can be induced in the needle. Controlling this curvature according to a known model can result in steering (DiMaio & Salcudean, 2003). The practical complexity of this approach generally necessitates robotic closed loop control. A second disadvantage is that the amount of control over the needle tip decreases the deeper the needle penetrates.

5.2.2. Bevel-tip

A bevel-tipped needle has the tendency to veer off-course, by rotating the needle this effect is supressed. Using a duty-cycle can allow for steering (Minhas, Engh, Fenske, & Riviere, 2007). This approach has received the majority of attention which has resulted in the a relatively large volume of work on the subject. There are several relevant downsides to this technique:

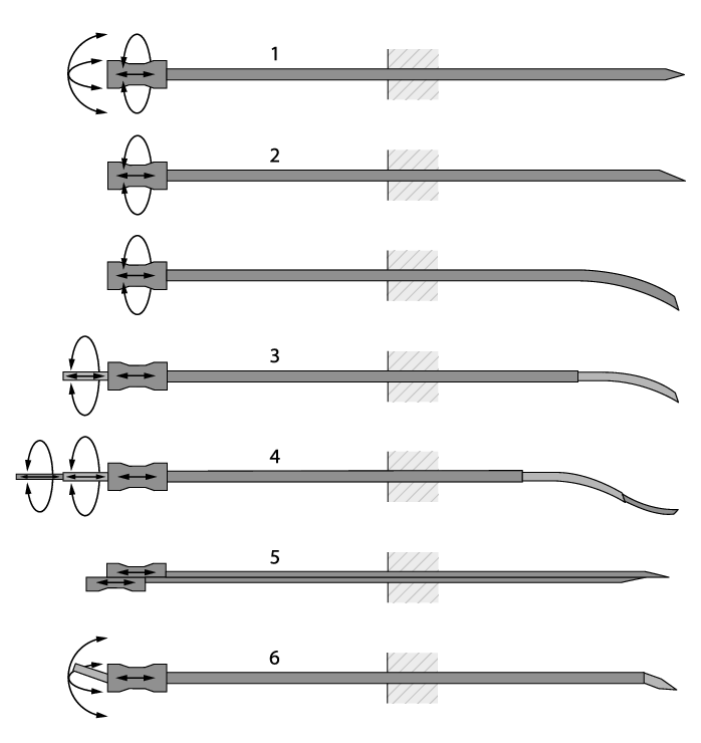


Figure 47 Six Needle Steering Mechanisms (van de Berg, 2016) (1: Base manipulation, 2: Bevel-tip, 3: Pre-curved stylet, 4: Active cannula, 5: Programmable bevel-tip, 6: Articulated-tip steering)



- Due to the constant rotation of the needle a helical path is cut in the tissue during insertion, this
 could be an indication of increased in-vivo trauma. This effect is especially present when using a
 pre-bent tip in concert with a bevel-tip to increase steering potential;
- Smaller bevelled needles tend to steer better. Unfortunately smaller needles are also more likely to buckle when inserted into stiff organs such as the prostate;
- Tissue interaction, needle torsion and other factors generally necessitates the use of a closed loop robotic approach and real-time MRI to achieve accurate duty-cycle steering.

Multiple papers present the steering capabilities of bevel-tipped needles and factors influencing steering are relatively well known (Adebar, Greer, Laeseke, Hwang, & Okamura, 2016; Cowan et al., 2011; Datla et al., 2014; Goksel, Dehghan, & Salcudean, 2009; Majewicz et al., 2012; Minhas et al., 2007; Swaney et al., 2013). However, to my knowledge this type of steerable needle has never been used or tested in-vivo. This leads me to believe the the complexity of the closed-loop MR-guided system poses technical challenges and monetary limitations that presently make the technique unappealing.

5.2.3. Pre-curved stylet

A pre-curved stylet is housed within a cannula, exposing more of the pre-curved styled results in more steering. This technique is best known from the paper of Okazawa, Ebrahimi, Chuang, Salcudean, and Rohling (2005), rotating the stylet in the cannula and concurrently exposing a porting of said styled, steering in all directions can be realised. Okazawa et al. (2005) reported 30mm of steering over a 100mm insertion in a tissue phantom. The system would lend itself for either manual of computer control. Torabi, Gupta, and Walsh (2014) presented a robotic system based on this technique for the implantation of LDR BT seeds.

5,2,4. Active cannula

Multiple concentric cannulas are placed within another. By exposing more or rotating a particular cannula steering can be achieved. This technique was first covered in detail in the paper by Sears and Dupont (2006) and later Dupont, Lock, Itkowitz, and Butler (2010). Burgner et al. (2012) presented a manually controllable device based on this technique. Some disadvantaged associated with this technique are:

- Lack of robustness against environment variables, making active cannulas best suited for open or fluid-filled environments;
- The complexity associated with steering is a non-cartesian manner;
- The risk of hard to predict instability due to local minima.

5.2.5. Programmable bevel-tip

A sectioned needle tip in which, by sliding sections in respect to each other, the geometry of the needle tip is changed and induces steering through tissue force interactions. The paper by Ko, Frasson, and Rodriguez y Baena (2011) first introduced the concepts based on the ovipositor of a wasp. The concept uses the asymmetric tip force generated by a bevel-tipped needle to induce steering. The papers Scali, Kreeft, Breedveld, and Dodou (2017a); Scali, Pusch, Breedveld, and Dodou (2017c) present a continuation on the concept by miniaturising the needle.

5.2.6. Articulated-tip steering

A needle with an articulated tip that can be controlled remotely. This type of mechanisms is common in other fields of medicine but has received relatively little attention. The size constraint of the needle likely makes the design and manufacturing of a tip-articulation mechanism for a needle challenging. The paper by van de Berg (2016) presents the design of a articulated-tip steering needle the sixth chapter. The Morrison steerable needle and Osseoflex® are both articulated-tip designs.

5.3. Needle characteristics

There are a number of needle characteristics relevant for the development of a needle. In Chapter 4.2 the needle insertion force for prostate BT was discussed. The following section will discuss how needle tip geometry, pre-bend and coatings affect among other things insertion force.



5.3.1. Tip geometry

In the implantation involved in HDR BT, there are generally three types of needle-tip geometries mentioned: conical, bevel and triangular geometries. Other geometries such as blunt or multi-faceted do exist but are mentioned infrequently.

O' Leary, Simone, Washio, Yoshinaka, and Okamura (2003) published a comprehensive paper on the relationship between insertion force, needle-tip geometry, and needle diameter using bovine liver as a phantom. A linear relationship was found between the insertion depth and insertion force. The slope of this relation for 1.55mm needles was -0.496, -0.552 and -0.360 for a 14° bevel-tipped, a 28° cone-tipped and a 49° triangular-tipped needle respectively. With the triangular-tipped needle requiring statistically significantly less insertion force then the other two needles for the same diameter. A positive relationship between the needle diameter and insertion force as well as a negative relationship between needle diameter and deflection were also found. No evidence was found for a relationship between the insertion force and angle of the grind on a bevel-tipped needle.

Hirsch, Gibney, Berube, and Manocchio (2012) showed that a 5-faceted bevel pen needle produced significantly lower injection forces into skin substitute then a 3-facited bevel pen needle. An extensive overview on the literature available on needle-tissue interaction can be found in the paper by van Gerwen, Dankelman, and van den Dobbelsteen (2012).

5.3.2. Pre-bend

To increase the steering capability of an asymmetrically steering needle, such as a bevel-tipped needle, the tip of the needle can be pre-bend, increasing asymmetry and steering capability. Majewicz et al. (2012) showed this effect in-vivo in canine. Many studies have shown this effect (Majewicz et al., 2012; Swaney et al., 2013). A pre-bend tip combined with the duty cycling method runs the risk of inflicting addition tissue damage. The rotation of the asymmetric needle results in a helical path being cut into a phantom. Swaney et al. (2013) presented a novel approach using a flexible tip to decrease tissue damage while achieving a similar steering capability to a pre-bent tip.

5.3.3. Coating

Needles are coated in a lubricant by the manufacturer. There is evidence this lubricant reduces insertion forces in synthetic tissue phantoms, whether this effect is present in-vivo is a matter of debate (van Gerwen et al., 2012).

5.4. Performance evaluation of steerable needles found in literature

Quality clinical evidence of steerable needle use in the prostate radiotherapy is absent. A search of the PubMed library for steerable and prostate yields four relevant papers of which none pertain to use in-vivo. Google Scholar as well as Scopus yield no evidence of in-vivo use of steerable needles. The exception being the paper by Majewicz et al. (2012), describing the in-vivo behaviour of bevel-tipped steerable needles in canine.

Scali et al. (2017a) presents a comprehensive overview of steerable needle performance in the second section of the paper. Table 15 presents a summary of these papers and outcomes, papers drawing similar conclusions or without mention of any performance data are excluded. Papers published after the publication by Scali et al. (2017a) have been included provided they meet the same requirements.



	Type of steering	Needle-Tip	Needle Diameter Gauge (mm)	Tissue Phantom	Method of Insertion	Insertion Depth/Deflection [mm/mm]	Smallest Radius of Curvature [mm]
Misra, Reed, Douglas, Ramesh, and Okamura (2008)	Bevel-Tip	Bevel-tip	27g (.4mm)	Plastisol (4:1 ratio plastic to softener)	Robotic	0.78*	179.4
Khadem, Rossa, Usmani, Sloboda, and Tavakoli (2016)	Bevel-tip needle with notches.	Bevel-tip	19 (1.02mm)	80% liquid plastic 20% softener	Manual	0.24*	198
Swaney et al. (2013)	Bevel-Tip with flexure Imitating pre- bend	Bevel-tip	20G (0.91)	Gelatine 10%wt Ex vivo pork Ioin	Robotic	-	121 (gelatine) 176 (pork loin)
Majewicz et al.	Bevel-Tip	Bevel-tip	24g (0.58)	Canine kidney	Robotic	-	164.5
(2012)	Bevel-Tip with Pre-bend	Pre-bent (15°) with bevel-tip	24g (0.58)	Canine kidney	Robotic	-	52.3
Okazawa et al. (2005)	Pre-Curved Stylet in Cannula	-	21g (0.81)	PVC	Handheld robotic	0.35*	-
Ko et al. (2011)	2-Section Programmable Bevel-Tip	Bevel-tip	±8.5 g (4mm)	Gelatine 6% wt.	Robotic	-	±70
Scali et al. (2017c)	4-Section Programmable Bevel-Tip	Bevel-tip	12mm	Gelatine 6% wt.	Robotic	-	178.6
Scali et al. (2017a)	6-Wire Programmable Bevel-Tip	Bundled wires	±16.5g (1.55mm)	Gelatine 5% wt.	Robotic	0.097	
Ryu et al. (2015)	SMA articulated-tip steering	Both bevel and conical tip	16g (1.67mm)	Plastisol (4:1 ratio plastic to softener	Robotic	0.12*	-
Adebar et al. (2016)	Articulated-tip steering	Conical tip	21g (0.82mm)	Ex vivo porcine liver	Robotic	0.42*	82.7
Henken, Seevinck, Dankelman, and van den Dobbelsteen (2017)	Articulated-tip steering	Conical	±15g (1.9mm)	Gelatine 15% wt.	Manual	0.15-0.22*	-

Table 15 Summery of papers on steerable needles *calculated or estimated from provided data

Table 15 serves to give an indication of reported results of needle steering, an overview of existing steerable needle designs and the most used technique. Due to the use of different tissue phantoms, needle diameters, and tip geometries, direct comparison between papers is arduous. The need for a systematic classification and testing of steerable needles was also recognised by the paper from Scali, Pusch, Breedveld, and Dodou (2017b).

Khadem, Rossa, Usmani, Sloboda, and Tavakoli (2018) presented a novel approach using existing beveltipped brachytherapy needles with notches cut out. The notches allowed the needle to flex more during insertion. The goal of the study was to present a steerable needle that can aid in the case of PAI in brachytherapy. Another novel unmentioned approach is presented in the paper by Ryu et al. (2015). Optical heating is used to actuate shape memory alloys, realising steering of a needle. Concerns should be raised about possible tissue damage from excess heat. Burdette et al. (2010) presented the first steerable needle with an integrated interventional tool. A pre-curved canula with an ultrasonic ablator as a stylet was used to ablate porcine livers. van de Berg, Dankelman, and van den Dobbelsteen (2017) used a novel tip-articulated steerable needle to show the increased endpoint accuracy compared to a non-steered linear stage.



Rutigliano et al. (2017) presented a study using the Morrison steerable needle in a bovine phantom. The goal was to reach a target while avoiding obstacles. The paper's conclusion stated: 'The steerable needle performed better than a straight needle with regard to procedure time, needle repositioning events, and CT scans required for placement.' The paper further claimed 'Steerable needles can increase accuracy while decreasing procedure time.' These claims pertain to needle biopsies.

With the exception of some (Rutigliano et al., 2017; van de Berg et al., 2017) most referenced papers report a smallest radius of curvature or largest insertion depth/deflection ratio achieved. While I believe this to be an indication of steerability, deflection controllability and consistency are also of importance. To be useful in practice the needle requires an approximately linear actuation to deflection correlation and constant behaviour.

There are several steering techniques that are presently receiving attention, these techniques are bevel-tip, articulated tip, and programmable-tip steering. These techniques achieve a minimum radius of curvature of 50-200mm and an insertion depth over deflection ratio of 0.1 to 0.8. Due to inconsistencies in testing methods, general comparisons between steering modalities are inconsequential.

5.5. Prospects

Biomimicry in the design of steerable needles is an interesting topic of research being pursued. The paper by Sakes, Dodou, and Breedveld (2016) on buckling prevention in nature gives valuable insights in the design of a steerable needle. Sahlabadi and Hutapea (2018) present a needle tip designed to reduce insertion force based on the barb of a honeybee.

To be able to make active adjustments to a needle, you must be able to see the needle. Studies into visualisation accuracy and tip visibility improve needle visibility and measurement accuracy, which in turn elevates the value of a steerable needle as a precision instrument (Cowan et al., 2011; Sadjadi et al., 2014). Xu et al. (2009) present two algorithms to calculate trajectories for bevel-tipped steerable needles. These trajectories originate in a single or small area and can avoid sensitive tissues such as the penile bulb around the prostate by active steering. The research into steerable needles seems to be moving away from duty cycle bevel-tip steering in favour of articulated-tip and programmable-bevel-tip.

5.6. Conclusion

The topic of steerable needles is an active topic in research. In recent years the focus has slightly shifted away from bevel-tip duty-cycle steering. Biomimicry of insect barbs has received a lot of attention recently. There is a need to systematically classify and test steerable needles to advance the field. While numerous papers present robotic closed-loop systems involving steerable needles, so far, only handheld steerable devices have made it to market.



The place of steerable needles in prostate HDR BT

Abstract

Steerable needles in prostate high dose-rate brachytherapy offer the possibility of steering around anatomical interference, increasing the group of patients eligible for the procedure. Secondly, steerable needles could be used to steer around sensitive tissues, decreasing late toxicities associated with the procedure. Lastly, steerable needles could increase needle positioning accuracy resulting in reduced procedure time and less needle punctures. The drawbacks of steerable needles include increased system complexity and the possible decrease in cost efficiency.



The objective of this literature review is to uncover the possible advantages a steerable needle would have in HDR BT of the prostate. The previous three chapters on HDR BT, prostate anatomy and steerable needles served to provide a brief overview of relevant literature to be able to answer this question. This chapter aims to combine the information of the three previous chapters and explore the possible benefits and drawbacks steerable needles would have in the field of HDR prostate BT.

6.1. Advantages

This section will discuss possible advantages of steerable needles in prostate HDR BT based on found literature.

6.1.1. Anatomical Interference

A steerable needle could aid in patient specific variations. In HDR BT of the prostate, one of these variations that regularly occurs is pubic arch interference (PAI). In PAI the ilia forming the pubic arch occlude parts of the prostate impeding needle implantation (Section 4.6). This phenomenon is especially common in patients with larger prostates. Men with prostates larger than 50-60cc are therefore often advised against undergoing HDR BT (Gibbons et al., 2009).

To overcome this issue the surgeon either has to reposition the patient, reposition himself or attempt freehand needle implantation instead of the usual template-guided implantation (Monroe et al., 2008). A steerable needle would allow for a larger range of patients being eligible for HDR BT. The surgeon could adhere to the routine template guided implantation in the dorsal lithotomy position and circumvent the PAI with the use of a steerable needle (Khadem et al., 2018).

85% of the respondents in the questionnaire by de Jong et al. (2018) agreed steerable needles would be useful to avoid anatomical obstacles. With a majority agreeing with the statement: 'Steerable needles would be advantageous for targeted lesions in the prostate'. A steerable needle could also aid in reaching parts of the prostate occluded by the urethra in a trans-perineal approach while minimising periurethral implantations.

6.1.2. Avoidance of sensitive tissues

Complication rates in trans-perineal biopsies indicate that needle trauma is in part responsible for the complications associated with HDR BT of the prostate (Section 4.5). The specific tissues responsible for these toxicities are largely unknown. It stands to reason that sparing sensitive neural and vascular pathways in the perineum from implantation trauma would decrease the toxicities associated with HDR BT.

The works by Podder, Dicker, Hutapea, Darvish, and Yu (2012); Xu et al. (2009) show that there are approaches that would decrease the size of the insertion area and/or decrease the number of needles necessary to achieve adequate coverage.

Urethral and prostate capsule sparing has historically drastically decreased toxicities in surgical and radiological interventions. This indicates the potential that sparing sensitive tissues has in increasing quality of life for patients after prostate interventions. Steerable needles could play a part in sparing sensitive tissue while still delivering adequate dose coverage of the prostate in BT.

6.1.3. Increased needle positioning accuracy

In a questionnaire by de Jong et al. (2018), 85% of interventional radiologists reported experiencing unwanted needle bending. Unwanted needle bending can lead to unsatisfactory accuracy in implant placement, which is well documented in the literature (Section 4.4). 93% of respondents saw the added value of steerable needles in interventional radiology with 91% being in favour of manual steering and 9% being in favour of robotic control

While implant inaccuracies can be adjusted in HDR BT with inverse treatment planning. A satisfactory implant coverage of the prostate is required to be able to achieve appropriate dose delivery. Being able to correct for needle bending and other inaccuracies could decrease procedure time, decrease needle insertions and manipulations, and increase needle placement accuracy



van de Berg et al. (2017) showed a handheld steerable needle can increase needle placement accuracy over a straight needle. More accurate needle placement means being able to better adhere to the desired implantation locations and thereby decrease the change of needing additional implants to achieve adequate coverage of the prostate. Decreasing needle insertions could result in less toxicity. This is explored further in the next section.

6.1.4. Decreased needle insertions

There is a sizable body of work indicating a relation between the number of needle implants and post-intervention toxicity (Section 4.5). Increased endpoint accuracy would mean treatment plans can be designed to minimise the number of needles necessary, whilst maintaining adequate coverage of the prostate. According to the literature this decrease in the number of implanted needles would result in decreased acute and late toxicity.

Furthermore, a link between periurethral needle manipulation (retracting partially and re-inserting) during implantation and toxicities was found by Eapen et al. (2014). While Rutigliano et al. (2017) found that using a steerable needle in a biopsy simulation could decrease the number of needle manipulations required to reach a particular target in the phantom. This would mean a steerable needle could also have the advantage of decreasing implant related trauma through decreasing the number of required needle manipulations.

6,2. Drawbacks

Every novel technique has its disadvantages. The question is do the advantages outweigh the disadvantages? In this section possible disadvantages of using a steerable needle in HDR BT of the prostate are explored.

6.2.1. System complexity

Many of the proposed steerable needles drastically increase the complexity of implantations. Bevel-tip duty cycle steering requires closed-loop feedback generally realised through MR-guidance and a robotic system to drive the needle. While a system like this could potentially increase needle placement accuracy or be used to avoid certain anatomical structures, the complexity presents a clear drawback. The availability of imaging modalities, reliability of control mechanisms and the CE-certification process of complex equipment all pose challenges to the adoption of the technique.

A second concern in the adoption of steerable needles regarding system complexity is the usability the instruments has to the surgeon. Barring fully automated systems, a surgeon will control the needle. Steerable needles like active-cannula type steerable needles, behave in a manner foreign to most surgeons. This could result in additional complications or increased procedure time.

Introducing a steerable needle for HDR BT implantations will require a system in which the additional complexity of the procedure is outweighed by the advantages for the patient and/or the surgeon.

6.2.2. Intervention costs

To gain large scale adoption a procedure must be cost-effective. Section 3.2.4 showed HDR BT could be cost-effective as a monotherapy and is cost-effective as a boost for EBRT. The use of steerable needles during the implantation will presumably increase the material cost of the procedure. A steerable multi-component needle will be more costly than a regular straight needle. This difference in material cost however, could be offset by a reduction in adverse side-effects of the procedure. These side-effects would require, additional procedures, medication or follow up hospital visits.

Besides direct material cost, increased operation times or training of medical personnel could decrease the cost-effectiveness of an HDR BT implantation using steerable needles.

Offsetting the cost of the procedure itself with a future cost reduction due to improved patient outcome could make the use of steerable needles in HDR BT cost-effective. To gain large-scale adoption the steerable needle system must be designed with cost-effectiveness in mind.



6.3. Conclusion

I believe the potential advantages this paper has shown for steerable needle in high dose rate brachytherapy, warrants the development of such a steerable needle. Steerable needles could be used to deal with anatomical restrictions, decrease tissue damage, increase needle positioning accuracy, and decrease required needle insertions. However, every new technique has its drawbacks. Increased system complexity and intervention cost-effectiveness could stand in the way of adoption of a steerable needle for HDR BT implantations.



Conclusion

The purpose of this paper was to explore the usefulness of a steerable needle in high dose rate brachytherapy of the prostate. First, I investigated the benefits of high dose rate brachytherapy in the treatment of prostate cancer in comparison to other treatment options. This showed there is clear evidence of the efficacy and efficiency of high dose rate brachytherapy in the treatment of prostate cancer. Secondly, I looked at the anatomy of the prostate and the complications that are encountered with current needle implantations. Third, I explored the field of steerable needles and the possible advantages they could present in high dose rate brachytherapy needle implantation. Lastly, these chapters were combined to deliver a verdict about the usefulness of steerable needle in high dose rate brachytherapy of the prostate.

Several possible advantaged and disadvantages of steerable needles in the field of high dose rate brachytherapy of the prostate we presented. Unfortunately, due to the lack of quality literature on for instance the field of steerable needles and the anatomies responsible for toxicities in prostate needle implantations, it is difficult to provide a conclusive ruling on the usefulness of steerable needles in high dose rate prostate brachytherapy.

Phantom experiments and theoretic literature provide, ample proof of the possible advantages of steerable needles in high dose rate prostate brachytherapy. But evidence of its efficacy in practice is scarce. Due to the complexity of needle-tissue interactions and high dose rate prostate brachytherapy toxicities the transferability of the results from phantom experiments and theoretical papers is debatable.

This paper presents several possible advantages and disadvantages of steerable needles in high dose rate brachytherapy of the prostate. Whether these advantages and disadvantages will present themselves in practice is unknown. However, I believe the potential advantages this paper has shown for steerable needle in high dose rate brachytherapy, warrants the development of such a steerable needle. Such a needle should be developed with the cost-effectiveness and usability for the end-user in mind.



Appendix B -Steering example





Appendix C - Theory

$$> eq1 := \frac{\Delta S}{\theta l} = \frac{\Delta S + \Delta S strain}{\theta 2}$$
:

>
$$eq2 := \theta 2 = \frac{-P \cdot L1^2}{2 \cdot Emod \cdot Ixx}$$
: # P is the resultant needle tip force

>
$$eq3 := F = \frac{P \cdot L1}{R}$$
:

>
$$eq4 := \Delta Sstrain = 2 \cdot \frac{F \cdot Lslot}{A \cdot Emod}$$
:

Because Δ Sstrain is calculated for on half of the needle it needls to be doubled

$$ightharpoonup eq5 := \Delta S = \left(\left(r + \frac{R}{2} \right) \cdot \theta I \right) - \left(\left(r - \frac{R}{2} \right) \cdot \theta I \right) :$$

$$\rightarrow eq6 := subs(eq3, eq4);$$

$$eq6 := \Delta Sstrain = \frac{2PL1Lslot}{RAEmod}$$

$$\rightarrow eq7 := subs(eq6, eq1);$$

$$eq7 := \frac{\Delta S}{\theta I} = \frac{\Delta S + \frac{2PL1Lslot}{RAEmod}}{\theta 2}$$

$$> eq8 := subs(simplify(eq5), eq7);$$

$$eq8 := R = \frac{\theta l R + \frac{2PL1Lslot}{RAEmod}}{\theta 2}$$

$$\rightarrow eq9 := subs(isolate(eq2, P), eq8)$$

$$eq9 := R = \frac{\theta I R - \frac{4 \theta 2 Ixx Lslot}{L1 R A}}{\theta 2}$$

$$\Rightarrow eq10 := isolate(eq9, \theta2)$$

$$eq10 := \theta 2 = \frac{\theta I R^2 L1 A}{R^2 L1 A + 4 Ixx Lslot}$$

$$A := \frac{\pi \cdot R^2}{2}$$
:

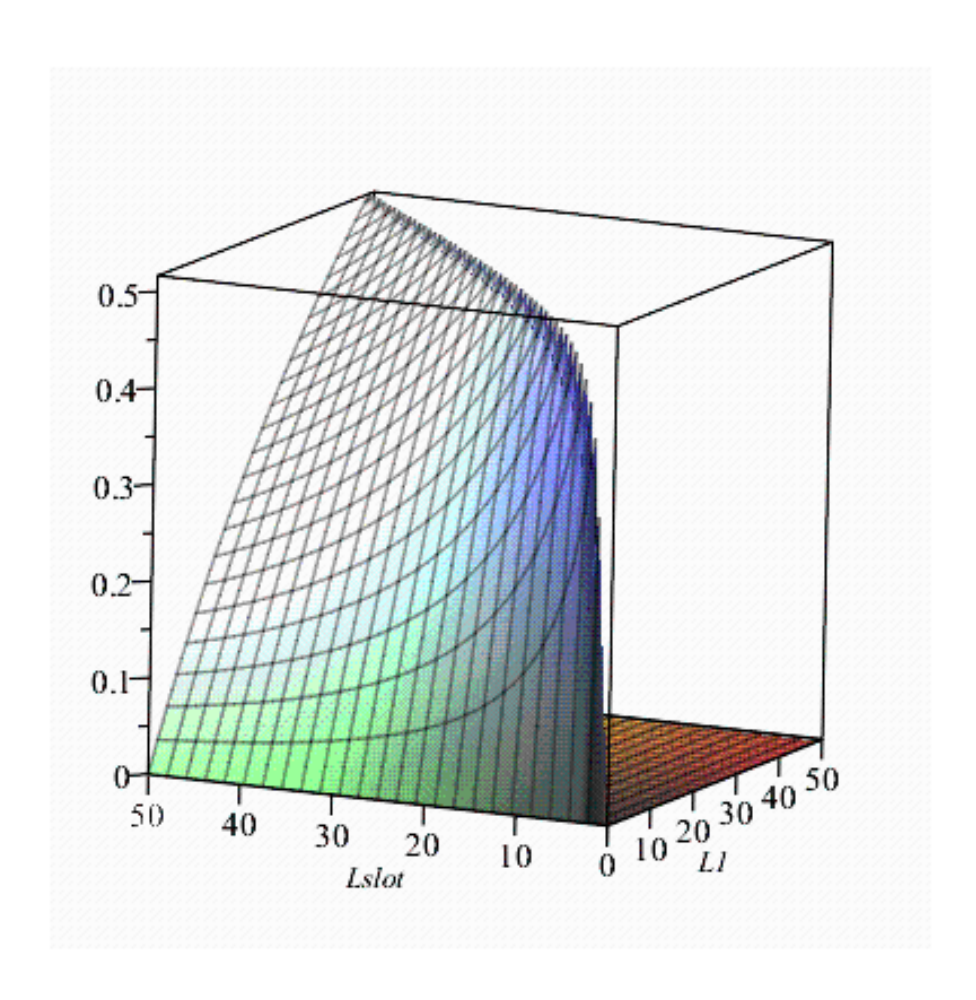
>
$$Ixx := \frac{1}{4} \cdot \pi \cdot R^4$$
:

>

$$\theta 2 = \frac{\theta 1 L1}{L1 + 2 Lslot}$$

 $> \textit{eq11} \coloneqq \textit{piecewise}(0 < \textit{L1} \ \text{and} \ \textit{L1} < \textit{Lslot}, \ \textit{rhs}(\textit{simplify}(\textit{eq10}))) \\$

$$eq11 := \begin{cases} \frac{\theta l L l}{L l + 2 L s lot} & 0 < L l < L s lot \\ 0 & otherwise \end{cases}$$





Appendix D — Expert consultations

D.1. Elekta

On 7/10/19 Martijn de Vries and myself presented the first prototype of the steerable needle to Elekta, a company specialised in developing medical instruments for radiological therapy. We were able to insert the needle into a CIRS 'tissue equivalent ultrasound prostate phantom' under TRUS guidance. (CIRS, 2019) The setup can be seen in Figure 48-1. Figure 48-2 demonstrates the amount of possible steering. A needle was inserted until the deep boundary of the prostate and subsequentially steered medially. Figure 48-3 shows a needle inserted into to medio-superior part of the prostate and subsequentially steered inferiorly. The image

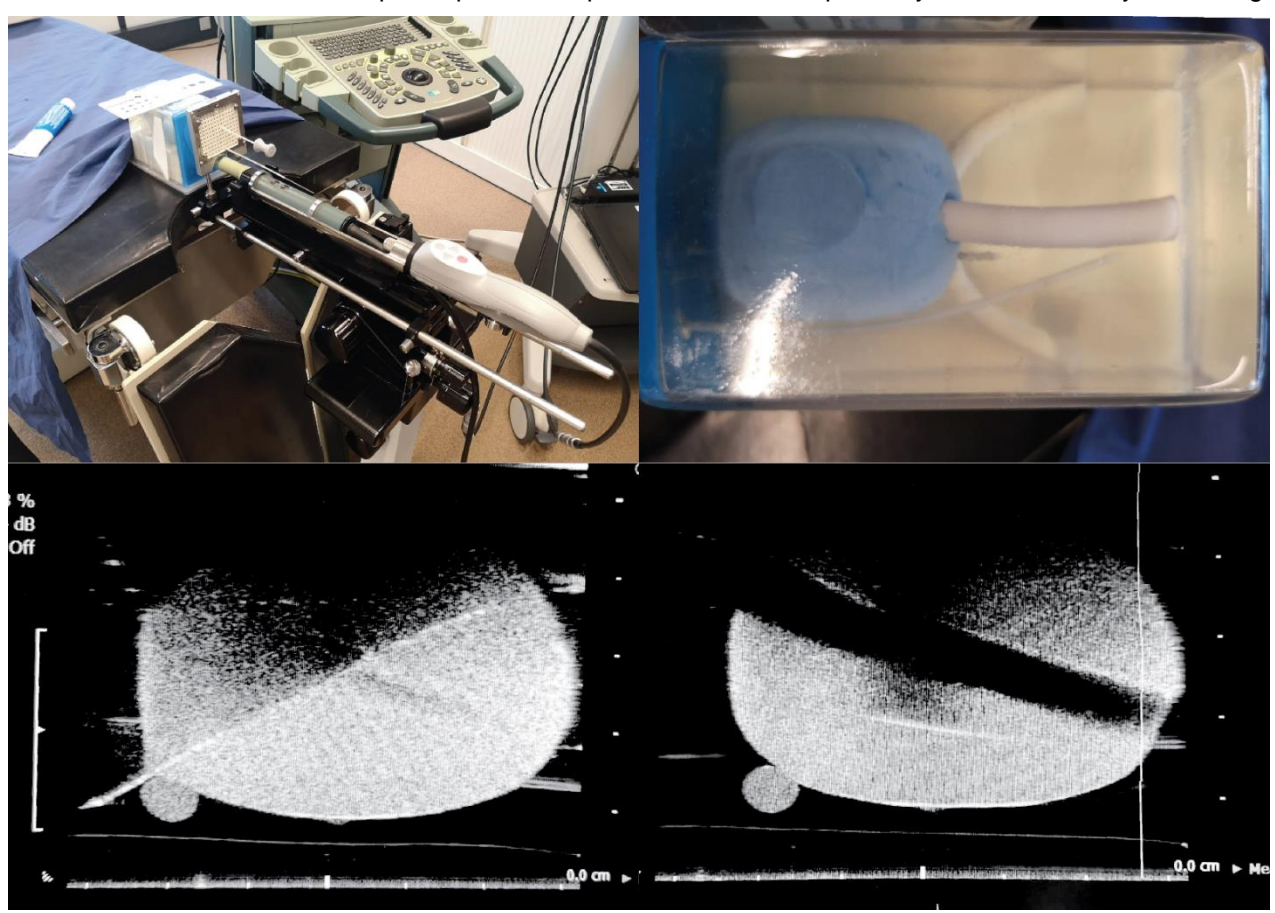


Figure 48 Images taken at Elekta. From top left to bottom right: 1. Prostate phantom and TRUS setup. 2. Prostate phantom with steerable needle. 3. Ultrasound image of steerable needle inserted superiorly into the prostate phantom exiting inferiorly. 4. Ultrasound image of steerable needle inserted inferiorly steering superiorly to follow the curve of the urethra



shows the amount of steering attainable in a relatively short insertion depth. Figure 48-4 shows a needle inserted medio-inferiorly into the prostate and steered superiorly, inferiorly following the curvature of the urethra. The ability to follow the curve of the urethra was an especially welcome sight to the Elekta representatives, as the deep region of the prostate inferiorly to the urethra can be hard to reach in HDR BT.

Some observations made in our visit to Elekta:

- The needle is relatively flexible. Due to this flexibility the insertion requires two hands to stabilise the needle;
- The TRUS setup interferes with the needles ability to steer superiorly;
- Previously placed needles could also interfere with the placement of a steerable needle;
- The needle throws a 'shadow' on the TRUS imaging, representatives from Elekta this deemed shadow larger than the shadow of currently available needles;
- The bare needle is too small to comfortably insert into the prostate, a handle is necessary;
- The needle should be fixated to the sleeve during implantation and easily retractable from the sleeve after implantation;
- The representatives from Elekta were especially enthusiastic about the prospect of reaching the deep region of the prostate inferior to the urethra. Additionally, increasing the number of patients eligible for HDR BT by offering an instrument to deal with PAI also rang true.

D.2. Rien Moerland

On 12/11/2019 Martijn de Vries, John van Dobbelsteen and myself met Rien Moerland, a clinical physicist specialised in brachytherapy, at the University Medical Centre Utrecht (UMCU) to discuss the development of the steerable needle.

Rien Moerland gave valuable insight into the procedure and possible roles the steering needle being developed could fulfil. He noted the benefit a SN could have in focal salvage HDR BT. Recurring malignancies are often located along the periphery of the prostate near the seminal vesicles. In a dorsal lithotomy position, these can be difficult to access due to occlusion by the rectum. Here a SN could aid to make the area more accessible. He also noted the ability to access the region 'behind' the urethra could prove valuable depending on the location of the tumour. Dr. Moerland mentioned a typical HDR BT implantation including prepping takes about 45 minutes with an average of 8 needles placed. He mentioned it takes one or two minutes to place a needle. Surprisingly he noted the average insertion depth of an HDR BT needle to be about 120mm with the prostate being about 50mm of this path. This is a fair amount more than literature seems to indicate.

We met two surgeons about to start an HDR BT procedure and presented our SN. They noted the ability to steer 5-10mm would be a very welcome feature as it would allow them to position the needles more easily in the appropriate location. Surprisingly, they mentioned a welcome increase in needle placement accuracy. From literature and other professionals, we have concluded that there is little clinical advantage of more accurate needle placement.

D.3. UMCU

On 26/11/2019 Martijn de Vries and myself met a number of physicians at the University Medical Centre Utrecht (UMCU) to observe a high dose-rate brachytherapy procedure of the prostate. The procedure in question was a salvage procedure where the needle implantation was guided by TRUS and the inverse treatment planning was done according to MRI imaging.

While salvage HDR BT is not our focus in designing this SN, this procedure bears much resemblance to a regular variant. The section of the procedure we were most interested in was the implantation of the needles. In this procedure a total of 6 needles were implanted through a template. The planned locations for the needles were visible on the TRUS monitor. During implantation feedback was given to the implanting surgeon, by slightly withdrawing the needle, manipulating the needle, template, or patient, and subsequently reinserting the needle, the surgeons attempted to place the needle in the designated pathways as best they could. After every needle, the location was noted in the software and locations remaining to be populated were updated.



Overall, these six needles took about 45 minutes to place. Noteworthy was the fact the surgeon frequently spoke about 'steering' the needle to arrive at the desired location. The emphasis on accurate needle placement could in part be due to the small size of the reoccurring malignancy. When asked, the surgeons stated a steerable needle could be of benefit to the HDR BT procedure. In this application the amount of steering required to be of benefit to the procedure would be minimal. A steering capability of approximately 5mm would be sufficient to nudge most needles to their desired location.

D.4. EMC

On 17/12/2019 Martijn de Vries and myself met two physicians at the Erasmus Medical Centre (EMC) to discuss the concept of a steerable HDR BT needle to be used in prostate cancer treatment. This medical centre performs HDR BT monotherapy in a single implantation with two fractions of 13.5 Gy.

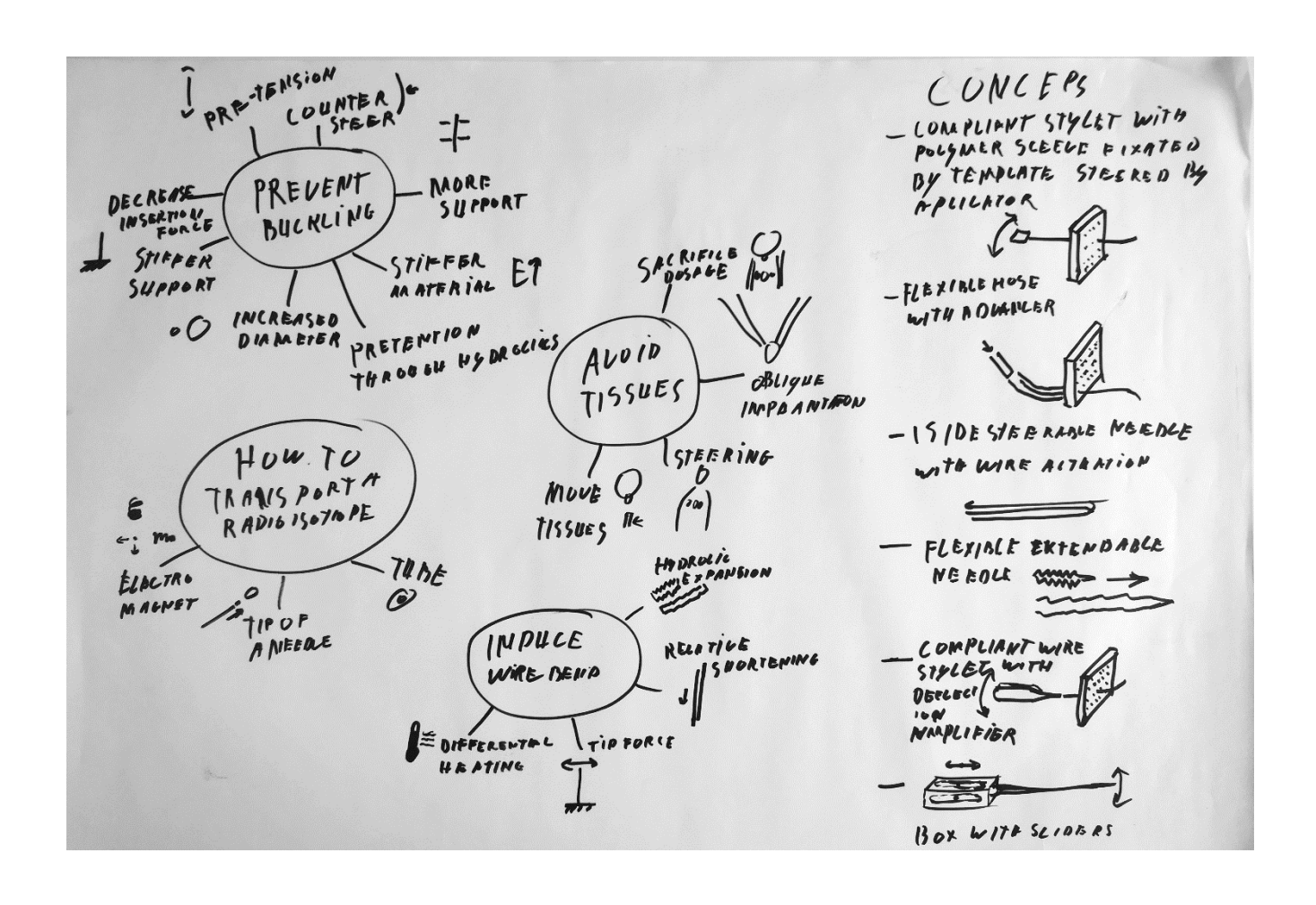
Several possible advantages and concerns of using SN in HDR BT of the prostate came to light. The physicians expressed the desire to have a needle that could be used to increase the ease of needle placement. Especially the possibility of reducing needle trauma by decreasing retractions and insertions and possibly avoiding implantations through the bulbus penis were mentioned. Both could decrease toxicities related with HDR BT. The ability to steer a needle throughout its implantation under TRUS guidance would enable less retractions and reinsertions. The ability to reach tumours ventral to the urethra, reach lateral seminal vesicles and voiding PAI were well received. The physicians estimated that a needle implantation, consisting of between 15 to 20 needles takes on average 30 to 45 minutes.

A number of concerns came up. The physicians questioned the ability to sterilise the needle, due to the geometry of the needle. Another concern was the reproducibility of the steering, as inhomogeneous tissue (such as calcifications) could make the steering difficult to predict. Whether the needle could be steered enough to leave a previously made 'track' was also a concern. A SN could make the quality of outcome more dependent on the performing radiotherapist, which could be an unwanted side effect. Lastly the physicians mentioned the amount of change in procedure should be minimal as to improve adoption among radiotherapist.

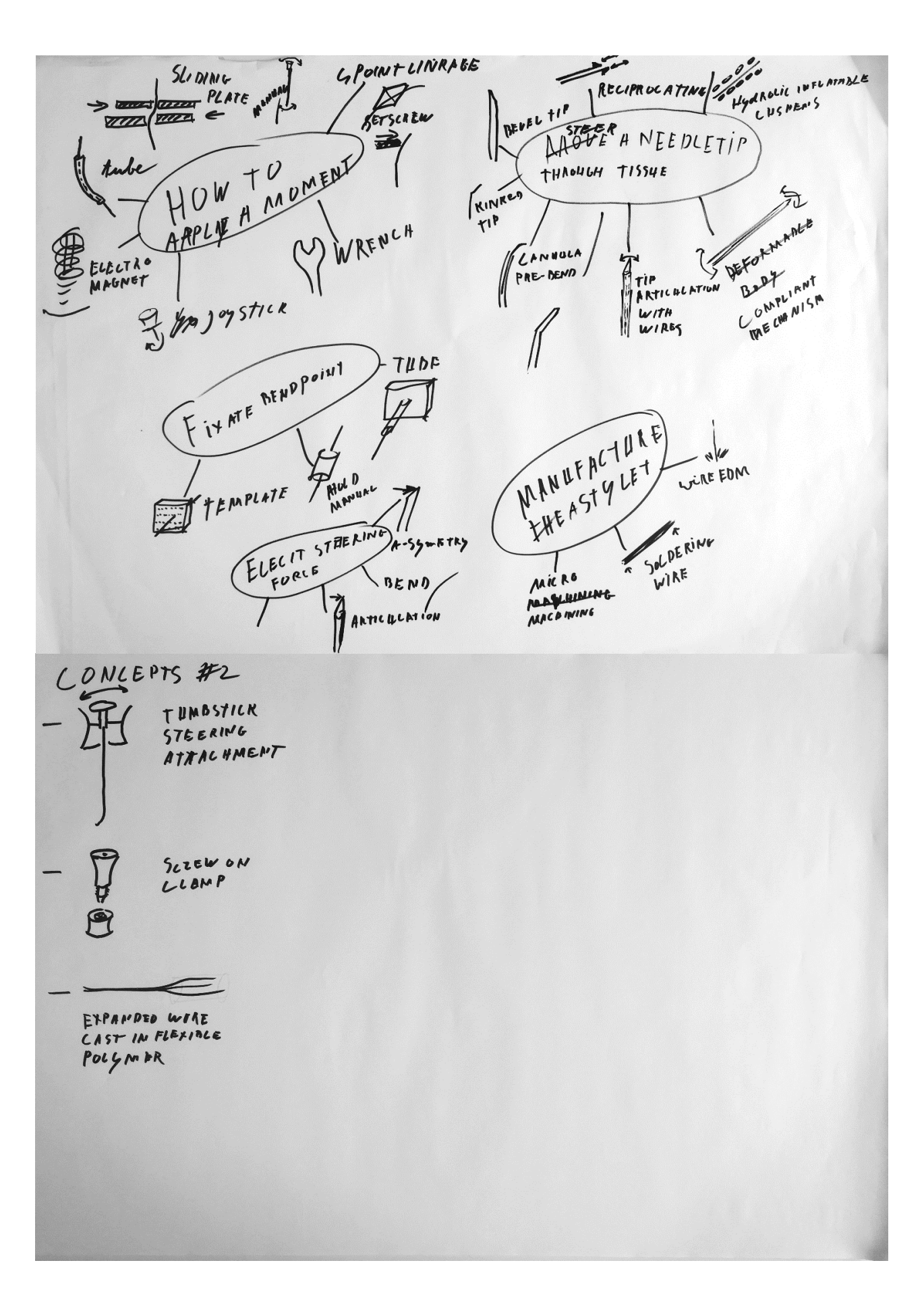
These concerns should be addressed in the development of this SN and provide valuable insight into possible hurdles that need to be overcome.



Appendix E — Idea generation









Appendix F — Experiment run tables and results

F1. Small gelatine experiment

Proximal deflection (angle)	0				20				40			_	60			
Run	1	2	3	4	1	2	3	4	1	2	3	4	1	2	3	4
Deflection (mm)	0.55	3.8	1.1	3.0	9.9	6.0	6.7	4.9	15.3	10.2	19.4	9.4	37.1	15.0	23.0	18.7
Average deflection (mm)		2	.1			6	.9			13	3.6			23	3.5	

F.2. Large gelatine experiment

		0 0						
Concept	Location	Direction	Deflection	This concept does not interfere with existing equipment	This concept requires practice to operate.	This concept is prone to buckling.	This concept increases implantation time.	This concept requires a long assembly.
3	6	1	17.5	3	2	5	2	1
6	5	1	24.4	5	4	3	2	2
5	3	3	4.5	3	2	2	3	4
4	2	4	20.5	4	3	1	3	2
1	7	2	25.5	5	2	4	2	4
7	4	4	13	5	3	4	3	3
2	1	4	22.6	5	3	2	2	4
5	7	1	15	2	2	3	2	4
2	6	3	29.5	5	2	1	2	2
1	1	3	32.5	3	3	5	2	4
7	4	2	8.4	4	3	3	3	3
3	5	2	12.5	3	1	4	2	2
6	3	4	5.5	5	3	4	3	3
4	2	2	4	3	2	1	2	2
2	6	1	24.5	4	2	1	2	3
3	1	3	10.5	3	2	5	2	2
6	3	4	13	5	3	2	2	2
4	4	1	16.5	2	2	1	2	2
5	5	1	7.5	4	2	3	2	3
1	7	1	19	4	2	5	2	3
7	2	1	6	3	3	4	3	1



5	7	4	5	5	3	2	2	4
1	3	1	12.5	5	2	3	2	3
4	4	4	7.5	2	2	1	2	1
6	2	3	10	5	4	4	2	1
7	6	4	16	5	3	4	2	2
2	1	2	16.5	5	2	1	3	3
3	5	1	13.5	2	2	4	2	2
7	1	2	3.5	4	4	4	2	1
6	4	2	3.5	5	3	3	2	1
3	7	3	17	4	1	2	2	3
5	5	3	8.5	4	3	2	2	4
1	3	3	17.14	5	4	5	2	3
4	2	1	26.5	2	1	1	2	3
2	6	1	24.5	2	2	1	2	3
7	2			4	2		2	
-		1	18			5		1
1	6	1	24	4	1	4	1	4
2	7	2	22	5	1	2	2	3
5	3	4	1.5	5	2	3	2	3
4	1	1	23.5	3	1	2	2	3
3	4	3	23	2	1	4	2	2
6	5	3	13.5	1	2	4	2	1
5	6	4	12.5	5	4	2	2	3
1	4	3	35	5	2	4	2	3
3	1	2	14	2	1	3	2	2
-								
2	2	2	29.5	5	2	1 -	2	3
6	7	3	8.5	4	3	5	2	2
4	3	2	9	2	1	1	1	2
7	5	1	26	2	3	4	2	2
1	2	4	34.5	4	2	5	2	4
5	5	3	3	4	4	2	2	3
2	7	3	28	5	2	1	2	3
3	6	1	28.5	2	1	3	2	3
								<u> </u>
7	1	4	17.5	1	3	1	2	1
7	4	4	17.5	4	3	4	2	1
6	3	2	2	4	3	3	2	2
6 4	3 1	2 1	2 21	4 2	3 1	3 1	2	2
6 4 7	3 1 1	2 1 4	2 21 15.5	4 2 5	3 1 4	3 1 4	2 2 2	2 3 1
6 4 7 1	3 1 1 3	2 1 4 3	2 21 15.5 30	4 2 5 4	3 1 4 2	3 1 4 4	2 2 2 2	2 3 1 3
6 4 7	3 1 1	2 1 4	2 21 15.5	4 2 5	3 1 4	3 1 4	2 2 2	2 3 1
6 4 7 1	3 1 1 3	2 1 4 3	2 21 15.5 30	4 2 5 4	3 1 4 2	3 1 4 4	2 2 2 2	2 3 1 3
6 4 7 1 3	3 1 1 3 7	2 1 4 3 4	2 21 15.5 30 21.5	4 2 5 4 2	3 1 4 2 1	3 1 4 4 3	2 2 2 2 2	2 3 1 3 2
6 4 7 1 3 2	3 1 1 3 7 4	2 1 4 3 4	2 21 15.5 30 21.5	4 2 5 4 2 5	3 1 4 2 1	3 1 4 4 3	2 2 2 2 2 2	2 3 1 3 2 3
6 4 7 1 3 2 4 6	3 1 1 3 7 4 5	2 1 4 3 4 4 3 1	2 21 15.5 30 21.5 30 9.5	4 2 5 4 2 5 3 5	3 1 4 2 1 2 1 4	3 1 4 4 3 1 1 3	2 2 2 2 2 2 2 2 2	2 3 1 3 2 3 3 1
6 4 7 1 3 2 4 6 5	3 1 1 3 7 4 5 6	2 1 4 3 4 4 3 1	2 21 15.5 30 21.5 30 9.5 26.5 2.5	4 2 5 4 2 5 3 5 5	3 1 4 2 1 2 1 4 4	3 1 4 4 3 1 1 3 2	2 2 2 2 2 2 2 2 2 2	2 3 1 3 2 3 3 1
6 4 7 1 3 2 4 6 5	3 1 1 3 7 4 5 6 2	2 1 4 3 4 4 3 1 2 2	2 21 15.5 30 21.5 30 9.5 26.5 2.5	4 2 5 4 2 5 3 5 5 5 5	3 1 4 2 1 2 1 4 4 4 3	3 1 4 4 3 1 1 1 3 2	2 2 2 2 2 2 2 2 2 2 2 2 2 2 2 2 2 2 2	2 3 1 3 2 3 3 1 3
6 4 7 1 3 2 4 6 5 7	3 1 1 3 7 4 5 6 2 7	2 1 4 3 4 4 3 1 2 2	2 21 15.5 30 21.5 30 9.5 26.5 2.5 8 25	4 2 5 4 2 5 3 5 5 5 5	3 1 4 2 1 2 1 4 4 3 2	3 1 4 4 3 1 1 1 3 2 4 5	2 2 2 2 2 2 2 2 2 2 2 2 2 2 2 2 2 2 2	2 3 1 3 2 3 3 1 3 1 3
6 4 7 1 3 2 4 6 5 7	3 1 1 3 7 4 5 6 2 7	2 1 4 3 4 4 3 1 2 2 1 4	2 21 15.5 30 21.5 30 9.5 26.5 2.5 8 25	4 2 5 4 2 5 3 5 5 5 5 4 4 2 5	3 1 4 2 1 2 1 4 4 3 2 4	3 1 4 4 3 1 1 1 3 2 4 5	2 2 2 2 2 2 2 2 2 2 2 2 2 2 2 2 2 2 2	2 3 1 3 2 3 3 1 3 1 3 1
6 4 7 1 3 2 4 6 5 7 1 6 3	3 1 1 3 7 4 5 6 2 7 1 4 5	2 1 4 3 4 4 4 3 1 2 2 2 1 4 4	2 21 15.5 30 21.5 30 9.5 26.5 2.5 8 25 15.5	4 2 5 4 2 5 3 5 5 5 5 4 4 5 3	3 1 4 2 1 2 1 4 4 3 2 4 3	3 1 4 4 3 1 1 1 3 2 4 5 4 3	2 2 2 2 2 2 2 2 2 2 2 2 2 2 2 2 2 2 2	2 3 1 3 2 3 3 1 3 1 3 1 3
6 4 7 1 3 2 4 6 5 7 1 6 3 5	3 1 1 3 7 4 5 6 2 7 1 4 5 6	2 1 4 3 4 4 3 1 2 2 1 4 4 4 3	2 21 15.5 30 21.5 30 9.5 26.5 2.5 8 25 15.5 12.5 5.5	4 2 5 4 2 5 3 5 5 5 5 4 5 3 4	3 1 4 2 1 2 1 4 4 3 2 4 3 4 3	3 1 4 4 3 1 1 3 2 4 5 4 3 3 3	2 2 2 2 2 2 2 2 2 2 2 2 2 2 2 2 2 2 2	2 3 1 3 2 3 3 1 3 1 3 1 3 1 3 3 1 3 3 3 3
6 4 7 1 3 2 4 6 5 7 1 6 3 5 4	3 1 1 1 3 7 4 5 6 2 7 1 4 5 6 3	2 1 4 3 4 4 4 3 1 2 2 1 4 4 4 1	2 21 15.5 30 21.5 30 9.5 26.5 2.5 8 25 15.5	4 2 5 4 2 5 3 5 5 5 5 4 5 3 4 2	3 1 4 2 1 2 1 4 4 3 2 4 3 4 1	3 1 4 4 3 1 1 1 3 2 4 5 4 3 3 1	2 2 2 2 2 2 2 2 2 2 2 2 2 2 2 2 2 2 2	2 3 1 3 2 3 3 1 3 1 3 1 3 1 3 2 3 3 3 1 3 3 2 2 3 3 3 2 2 3 3 2 3 2
6 4 7 1 3 2 4 6 5 7 1 6 3 5	3 1 1 3 7 4 5 6 2 7 1 4 5 6	2 1 4 3 4 4 3 1 2 2 1 4 4 4 3	2 21 15.5 30 21.5 30 9.5 26.5 2.5 8 25 15.5 12.5 5.5	4 2 5 4 2 5 3 5 5 5 5 4 5 3 4	3 1 4 2 1 2 1 4 4 3 2 4 3 4 3	3 1 4 4 3 1 1 3 2 4 5 4 3 3 3	2 2 2 2 2 2 2 2 2 2 2 2 2 2 2 2 2 2 2	2 3 1 3 2 3 3 1 3 1 3 1 3 1 3 3 1 3 3 3 3
6 4 7 1 3 2 4 6 5 7 1 6 3 5 4	3 1 1 1 3 7 4 5 6 2 7 1 4 5 6 3	2 1 4 3 4 4 4 3 1 2 2 1 4 4 4 1	2 21 15.5 30 21.5 30 9.5 26.5 2.5 8 25 15.6 12.5 5.5	4 2 5 4 2 5 3 5 5 5 5 4 5 3 4 2	3 1 4 2 1 2 1 4 4 3 2 4 3 4 1	3 1 4 4 3 1 1 1 3 2 4 5 4 3 3 1	2 2 2 2 2 2 2 2 2 2 2 2 2 2 2 2 2 2 2	2 3 1 3 2 3 3 1 3 1 3 1 3 1 3 2 3 3 3 1 3 3 2 2 3 3 3 2 2 3 3 2 3 2
6 4 7 1 3 2 4 6 5 7 1 6 3 5 4 2	3 1 1 1 3 7 4 5 6 2 7 1 4 5 6 3 2	2 1 4 3 4 4 4 3 1 2 2 1 4 4 4 1 1	2 21 15.5 30 21.5 30 9.5 26.5 2.5 8 25 15.5 12.5 5.5 16	4 2 5 4 2 5 3 5 5 5 5 4 5 3 4 2 5 5	3 1 4 2 1 2 1 4 4 3 2 4 3 4 1 2	3 1 4 4 3 1 1 1 3 2 4 5 4 3 3 1 1 2	2 2 2 2 2 2 2 2 2 2 2 2 2 2 2 2 2 2 2	2 3 1 3 2 3 3 1 3 1 3 1 3 1 3 2 3 3 3 1 3 3 2 3 3 3 2 3 3 3 2 3 3 3 3
6 4 7 1 3 2 4 6 5 7 1 6 3 5 4 2 3	3 1 1 1 3 7 4 5 6 2 7 1 4 5 6 3 2 6 7	2 1 4 3 4 4 3 1 2 2 1 4 4 1 1 2 4 4 2	2 21 15.5 30 21.5 30 9.5 26.5 2.5 8 25 15.5 12.5 5.5 16 26.5 15.5	4 2 5 4 2 5 3 5 5 5 5 4 5 3 4 2 5 2 5 2 5 2 5 2 5 2 2 5 2 2 2 5 2	3 1 4 2 1 2 1 4 4 3 2 4 3 4 1 2 2 2	3 1 4 4 3 1 1 1 3 2 4 5 4 3 3 1 1 2 4 1	2 2 2 2 2 2 2 2 2 2 2 2 2 2 2 2 2 2 2	2 3 1 3 2 3 3 1 3 1 3 1 3 1 3 2 3 3 2 3 3 1 3 2 3 3 2 3 3 2 3 3 2 3 3 2 3 3 2 3 3 2 3 3 2 3 3 2 3 3 2 3 3 2 3 3 3 3 2 3 3 3 2 3 3 2 3 3 2 3 3 2 3 3 2 3 3 2 3 2 3 2 3 2 3 2 3 2 3 2 3 2 3 2 3 2 3 2 3 2 3 2 3 3 2 3 2 3 3 2 3 2 3 2 3 2 3 3 2 3 2 3 2 3 3 2 3 3 2 3 3 2 3 2 3 3 2 3 3 2 3 3 3 2 3 3 3 3 2 3 3 3 3 3 3 3 3 2 3
6 4 7 1 3 2 4 6 5 7 1 6 3 5 4 2 3 4 7	3 1 1 1 3 7 4 5 6 2 7 1 4 5 6 3 2 6 7 3	2 1 4 3 4 4 3 1 2 2 1 4 4 1 1 2 4 4 2 3	2 21 15.5 30 21.5 30 9.5 26.5 2.5 8 25 15.5 12.5 5.5 16 26.5 15.5 14.5	4 2 5 4 2 5 3 5 5 5 5 4 5 3 4 2 5 2 5 2 5 2 5 2 5 5 2 5 5 2 5 5 2 5 5 2 5 5 2 5 2 5 5 2 5 5 2 5	3 1 4 2 1 1 2 1 4 4 3 2 4 3 4 1 2 2 2 4	3 1 4 4 3 1 1 1 3 2 4 5 4 3 3 1 1 2 4 1 4	2 2 2 2 2 2 2 2 2 2 2 2 2 2 2 2 2 2 2	2 3 1 3 2 3 3 1 3 1 3 1 3 1 3 2 3 2 2 1
6 4 7 1 3 2 4 6 5 7 1 6 3 5 4 2 3 4 7 2	3 1 1 1 3 7 4 5 6 2 7 1 4 5 6 3 2 6 7 3 5	2 1 4 3 4 4 3 1 2 2 1 4 4 1 1 2 4 2 3 4 4 4 3 4 4 4 2 2 3 4 4 4 4 4 4	2 21 15.5 30 21.5 30 9.5 26.5 2.5 8 25 15.5 12.5 5.5 16 26.5 15.5 14.5 13 42.3	4 2 5 4 2 5 3 5 5 5 5 4 5 3 4 2 5 2 5 2 5 5 2 5 5 5 5 5 5 5 5 5 5 5	3 1 4 2 1 1 2 1 4 4 3 2 4 3 4 1 2 2 2 2 4 3 3	3 1 4 4 3 1 1 1 3 1 1 3 2 4 5 4 3 3 1 1 2 4 1 4 2	2 2 2 2 2 2 2 2 2 2 2 2 2 2 2 2 2 2 2	2 3 1 3 2 3 3 1 3 1 3 1 3 1 3 2 3 2 2 1 3 3
6 4 7 1 3 2 4 6 5 7 1 6 3 5 4 2 3 4 7 2 6	3 1 1 1 3 7 4 5 6 2 7 1 4 5 6 3 2 6 7 3 5 2	2 1 4 3 4 4 3 1 2 2 1 4 4 1 1 2 4 2 3 4 4 4 4 4 4 2 2 3 4 4 4 4 4 4 4	2 21 15.5 30 21.5 30 9.5 26.5 2.5 8 25 15.5 12.5 5.5 16 26.5 15.5 14.5 13 42.3 9.5	4 2 5 4 2 5 3 5 5 5 5 4 5 3 4 2 5 2 2 5 5 5 5 5 5 5 5 5 5 5 5 5 5 5	3 1 4 2 1 1 2 1 4 4 3 2 4 3 4 1 2 2 2 4 3 4 3 4 1 2 2 2 4 3 4 3 4	3 1 4 4 3 1 1 1 3 2 4 5 4 3 3 1 1 2 4 1 4 2 3 3	2 2 2 2 2 2 2 2 2 2 2 2 2 2 2 2 2 2 2	2 3 1 3 2 3 3 1 3 1 3 1 3 2 3 2 2 1 3 2 1 3 1
6 4 7 1 3 2 4 6 5 7 1 6 3 5 4 2 3 4 7 2 6 1 1	3 1 1 1 3 7 4 5 6 2 7 1 4 5 6 3 2 6 7 3 5 2 1	2 1 4 3 4 4 3 1 2 2 1 4 4 1 1 2 4 2 3 4 4 4 4 4 4 4 4 4 4 4 4 4 4 4 4	2 21 15.5 30 21.5 30 9.5 26.5 2.5 8 25 15.5 12.5 5.5 16 26.5 15.5 14.5 13 42.3 9.5 30	4 2 5 4 2 5 3 5 5 5 5 4 5 5 3 4 2 5 2 2 5 5 5 5 5 5 5 5 5 5 5 5 5 5 5	3 1 4 2 1 1 2 1 4 4 3 2 4 3 4 1 2 2 2 4 3 4 3 4 1 2 2 2 4 3 4 3 4 3	3 1 4 4 4 3 1 1 1 3 2 4 5 4 3 3 1 1 2 4 1 4 2 3 5 5	2 2 2 2 2 2 2 2 2 2 2 2 2 2 2 2 2 2 2	2 3 1 3 2 3 3 1 3 1 3 1 3 1 3 2 3 2 1 3 1 3
6 4 7 1 3 2 4 6 5 7 1 6 3 5 4 2 3 4 7 2 6 1 5	3 1 1 1 3 7 4 5 6 2 7 1 4 5 6 3 2 6 7 3 5 2 1 4	2 1 4 3 4 4 3 1 2 2 1 4 4 1 1 2 3 4 4 4 4 4 4 4 4 4 4 4 4 4 4 4 4 4 4	2 21 15.5 30 21.5 30 9.5 26.5 2.5 8 25 15.5 12.5 5.5 16 26.5 14.5 13 42.3 9.5 30 11	4 2 5 4 2 5 3 5 5 5 5 4 5 3 4 2 2 5 2 2 5 5 5 5 5 5 5 5 5 5 5 5 5 5	3 1 4 2 1 1 2 1 4 4 3 2 4 3 4 1 2 2 2 4 3 4 3 4 1 2 2 4 3 4 3 4 4 3 4 3 4 4 3 4	3 1 4 4 4 3 1 1 1 3 2 4 5 4 3 3 1 1 2 4 1 4 2 3 5 3 5 3	2 2 2 2 2 2 2 2 2 2 2 2 2 2 2 2 2 2 2	2 3 1 3 2 3 3 1 3 1 3 1 3 1 3 2 2 3 2 2 1 3 1 3
6 4 7 1 3 2 4 6 5 7 1 6 3 5 4 2 3 4 7 2 6 1 5 2	3 1 1 1 3 7 4 5 6 2 7 1 4 5 6 3 2 6 7 3 5 2 1 4 4 4	2 1 4 3 4 4 3 1 2 2 1 4 4 1 1 2 4 2 3 4 4 4 4 1 1 2 4 4 4 4 4 3 4 4 4 4 4 4 4 4 4 4 4 4 4	2 21 15.5 30 21.5 30 9.5 26.5 2.5 8 25 15.5 12.5 5.5 16 26.5 14.5 13 42.3 9.5 30 11 21	4 2 5 4 2 5 3 5 5 5 5 4 5 5 2 2 2 5 5 5 5 5 5 5 5 5 5	3 1 4 2 1 1 2 1 4 4 3 2 4 3 4 1 2 2 2 4 3 4 3 4 1 2 2 2 4 3 4 3 4 3 4 3 4 3 4 3	3 1 4 4 3 1 1 1 3 1 1 3 2 4 5 4 3 3 1 1 2 4 1 4 2 3 5 3 1 1	2 2 2 2 2 2 2 2 2 2 2 2 2 2 2 2 2 2 2	2 3 1 3 2 3 3 1 3 1 3 1 3 1 3 2 2 3 2 1 3 1 3
6 4 7 1 3 2 4 6 5 7 1 6 3 5 4 2 3 4 7 2 6 1 5	3 1 1 1 3 7 4 5 6 2 7 1 4 5 6 3 2 6 7 3 5 2 1 4	2 1 4 3 4 4 3 1 2 2 1 4 4 1 1 2 3 4 4 4 4 4 4 4 4 4 4 4 4 4 4 4 4 4 4	2 21 15.5 30 21.5 30 9.5 26.5 2.5 8 25 15.5 12.5 5.5 16 26.5 14.5 13 42.3 9.5 30 11	4 2 5 4 2 5 3 5 5 5 5 4 5 3 4 2 2 5 2 2 5 5 5 5 5 5 5 5 5 5 5 5 5 5	3 1 4 2 1 1 2 1 4 4 3 2 4 3 4 1 2 2 2 4 3 4 3 4 1 2 2 4 3 4 3 4 4 3 4 3 4 4 3 4	3 1 4 4 4 3 1 1 1 3 2 4 5 4 3 3 1 1 2 4 1 4 2 3 5 3 5 3	2 2 2 2 2 2 2 2 2 2 2 2 2 2 2 2 2 2 2	2 3 1 3 2 3 3 1 3 1 3 1 3 1 3 2 2 3 2 2 1 3 1 3
6 4 7 1 3 2 4 6 5 7 1 6 3 5 4 2 3 4 7 2 6 1 5 2	3 1 1 1 3 7 4 5 6 2 7 1 4 5 6 3 2 6 7 3 5 2 1 4 4 4	2 1 4 3 4 4 3 1 2 2 1 4 4 1 1 2 4 2 3 4 4 4 4 1 1 2 4 4 4 4 4 3 4 4 4 4 4 4 4 4 4 4 4 4 4	2 21 15.5 30 21.5 30 9.5 26.5 2.5 8 25 15.5 12.5 5.5 16 26.5 14.5 13 42.3 9.5 30 11 21	4 2 5 4 2 5 3 5 5 5 5 4 5 5 2 2 2 5 5 5 5 5 5 5 5 5 5	3 1 4 2 1 1 2 1 4 4 3 2 4 3 4 1 2 2 2 4 3 4 3 4 1 2 2 2 4 3 4 3 4 3 4 3 4 3 4 3	3 1 4 4 3 1 1 1 3 1 1 3 2 4 5 4 3 3 1 1 2 4 1 4 2 3 5 3 1 1	2 2 2 2 2 2 2 2 2 2 2 2 2 2 2 2 2 2 2	2 3 1 3 2 3 3 1 3 1 3 1 3 1 3 2 2 3 2 1 3 1 3
6 4 7 1 3 2 4 6 5 7 1 6 3 5 4 2 3 4 7 2 6 1 5 2 6	3 1 1 1 3 7 4 5 6 2 7 1 4 5 6 3 2 6 7 3 5 2 1 4 4 1	2 1 4 3 4 4 3 1 2 2 1 4 4 1 1 2 4 2 3 4 4 4 2 3 4 4 4 1 1 1 1 2 3 4 4 4 4 4 1 1 1 1 1 1 1 1 1 1 1 1 1 1	2 21 15.5 30 21.5 30 9.5 26.5 2.5 8 25 15.5 12.5 5.5 16 26.5 15.5 14.5 13 42.3 9.5 30 11 21 8.5	4 2 5 4 2 5 3 5 5 5 5 4 5 5 2 2 2 5 5 5 5 5 5 5 5 5 5	3 1 4 2 1 1 2 1 4 4 3 2 4 3 4 1 2 2 2 4 3 4 3 4 1 2 2 2 4 3 4 3 4 1 2 2 4 3 4 3 4 4 3 4 3 4 4 3 4 4 3 4 4 3 4 4 3 4 4 3 4 4 3 4 4 3 4 4 4 3 4	3 1 4 4 4 3 1 1 1 3 2 4 5 4 3 3 1 1 2 4 1 4 2 3 5 3 1 1 3	2 2 2 2 2 2 2 2 2 2 2 2 2 2 2 2 2 2 2	2 3 1 3 2 3 3 1 3 1 3 1 3 1 3 2 2 3 2 1 3 1 3
6 4 7 1 3 2 4 6 5 7 1 6 3 5 4 2 3 4 7 2 6 1 5 2 6 3 3	3 1 1 1 3 7 4 5 6 2 7 1 4 5 6 3 2 6 7 3 5 2 1 4 4 4 1 6	2 1 4 3 4 4 3 1 2 2 1 4 4 1 1 2 3 4 4 4 2 3 4 4 4 1 1 1 2 3 4 4 4 4 1 1 1 1 1 1 1 1 1 1 1 1 1 1 1	2 21 15.5 30 21.5 30 9.5 26.5 2.5 8 25 15.5 12.5 5.5 16 26.5 14.5 13 42.3 9.5 30 11 21 8.5 13.5	4 2 5 4 2 5 3 5 5 5 4 5 5 2 2 2 5 5 5 5 5 5 5 5 5 5 5	3 1 4 2 1 1 2 1 4 4 3 2 4 3 4 1 2 2 2 4 3 4 3 4 1 2 2 2 4 3 4 3 4 3 4 3 4 3 4 2	3 1 4 4 4 3 1 1 1 3 2 4 5 4 3 3 1 1 2 4 1 4 2 3 5 3 1 1 3 4	2 2 2 2 2 2 2 2 2 2 2 2 2 2 2 2 2 2 2	2 3 1 3 1 3 2 3 3 1 1 3 1 3 1 3 2 2 3 2 1 3 1 3
6 4 7 1 3 2 4 6 5 7 1 6 3 5 4 2 3 4 7 2 6 1 5 2 6 1 5 2 6 3 1 4	3 1 1 1 3 7 4 5 6 2 7 1 4 5 6 3 2 6 7 3 5 2 1 4 4 1 6 2 3	2 1 4 3 4 4 3 1 1 2 2 1 1 4 4 1 1 2 4 4 1 3 3 4 4 4 1 3 3 3 2 4 3	2 21 15.5 30 21.5 30 9.5 26.5 2.5 8 25 15.5 12.5 5.5 16 26.5 12.5 13 42.3 9.5 30 11 21 8.5 13.5 29.5	4 2 5 4 2 5 3 5 5 5 5 4 5 5 2 2 2 5 5 5 5 5 5 5 5 5 5	3 1 4 2 1 1 2 1 4 4 3 2 4 3 4 1 2 2 2 4 3 4 3 4 1 2 2 2 3 4 3 4 3 4 3 4 3 4 3 4 3 4 3 4 3	3 1 4 4 4 3 1 1 1 3 2 4 5 4 3 3 1 1 2 4 1 4 2 3 5 3 1 1 2 4 1 4 2 3 5 1 1 3 4 5 1 1	2 2 2 2 2 2 2 2 2 2 2 2 2 2 2 2 2 2 2	2 3 1 1 3 2 3 3 1 1 3 1 3 1 3 1 3 2 2 3 2 1 3 1 3
6 4 7 1 3 2 4 6 5 7 1 6 3 5 4 2 3 4 7 2 6 1 5 2 6 1 5 2 6 3 1 4 5	3 1 1 1 3 7 4 5 6 2 7 1 4 5 6 3 2 6 7 3 5 2 1 4 4 1 6 2 3 7	2 1 4 3 4 4 3 1 1 2 2 1 1 4 4 1 1 2 4 4 1 1 3 3 4 4 4 1 3 3 1 1	2 21 15.5 30 21.5 30 21.5 30 9.5 26.5 2.5 8 25 15.5 12.5 5.5 16 26.5 15.5 14.5 13 42.3 9.5 30 11 21 8.5 13.5 29.5 11 12.5	4 2 5 4 2 5 3 5 5 5 5 4 5 5 2 2 2 5 5 5 5 5 5 5 5 5 5	3 1 4 2 1 1 2 1 4 4 3 2 4 3 4 1 2 2 4 3 4 3 4 1 2 2 2 4 3 4 3 4 2 2 4 3 4 4 3 4 4 3 4 4 4 4	3 1 4 4 4 3 1 1 1 3 2 4 5 4 3 3 1 1 2 4 1 4 2 3 5 3 1 1 2 4 1 4 2 3 5 1 3 5 1 3 4 5 1 3 3	2 2 2 2 2 2 2 2 2 2 2 2 2 2 2 2 2 2 2	2 3 1 1 3 2 3 3 1 1 3 1 3 1 3 2 3 2 2 1 3 3 1 3 3 1 3 3 3 3
6 4 7 1 3 2 4 6 5 7 1 6 3 5 4 2 3 4 7 2 6 1 5 2 6 1 5 2 6 3 1 4 5 7	3 1 1 1 3 7 4 5 6 2 7 1 4 5 6 3 2 6 7 3 5 2 1 4 4 1 6 2 3 7 5	2 1 4 3 4 4 3 1 2 2 1 4 4 1 1 2 4 2 3 4 4 1 3 3 3 2 4 4 1 2 2 3 1 2	2 21 15.5 30 21.5 30 21.5 30 9.5 26.5 2.5 8 25 15.5 12.5 5.5 16 26.5 15.5 14.5 13 42.3 9.5 30 11 21 8.5 13.5 29.5 11 12.5 2.5	4 2 5 4 2 5 3 5 5 5 5 4 5 5 2 2 2 5 5 5 5 5 5 5 5 5 5	3 1 4 2 1 1 2 1 4 4 3 2 4 3 4 1 2 2 2 4 3 4 3 4 1 2 2 2 4 3 4 3 4 4 3 4 4 3 4 4 4 4 4 4 4	3 1 4 4 4 3 1 1 1 3 2 4 5 4 3 3 1 1 2 4 1 4 2 3 5 3 1 1 3 4 5 1 3 4 4 5	2 2 2 2 2 2 2 2 2 2 2 2 2 2 2 2 2 2 2	2 3 1 3 1 3 2 3 3 1 3 1 3 1 3 2 2 1 3 1 3
6 4 7 1 3 2 4 6 5 7 1 6 3 5 4 2 3 4 7 2 6 1 5 2 6 1 5 2 6 3 1 4 5	3 1 1 1 3 7 4 5 6 2 7 1 4 5 6 3 2 6 7 3 5 2 1 4 4 1 6 2 3 7	2 1 4 3 4 4 3 1 1 2 2 1 1 4 4 1 1 2 4 4 1 1 3 3 4 4 4 1 3 3 1 1	2 21 15.5 30 21.5 30 21.5 30 9.5 26.5 2.5 8 25 15.5 12.5 5.5 16 26.5 15.5 14.5 13 42.3 9.5 30 11 21 8.5 13.5 29.5 11 12.5	4 2 5 4 2 5 3 5 5 5 5 4 5 5 2 2 2 5 5 5 5 5 5 5 5 5 5	3 1 4 2 1 1 2 1 4 4 3 2 4 3 4 1 2 2 4 3 4 3 4 1 2 2 2 4 3 4 3 4 2 2 4 3 4 4 3 4 4 3 4 4 4 4	3 1 4 4 4 3 1 1 1 3 2 4 5 4 3 3 1 1 2 4 1 4 2 3 5 3 1 1 2 4 1 4 2 3 5 1 3 5 1 3 4 5 1 3 3	2 2 2 2 2 2 2 2 2 2 2 2 2 2 2 2 2 2 2	2 3 1 1 3 2 3 3 1 1 3 1 3 1 3 2 3 2 2 1 3 3 1 3 3 1 3 3 3 3



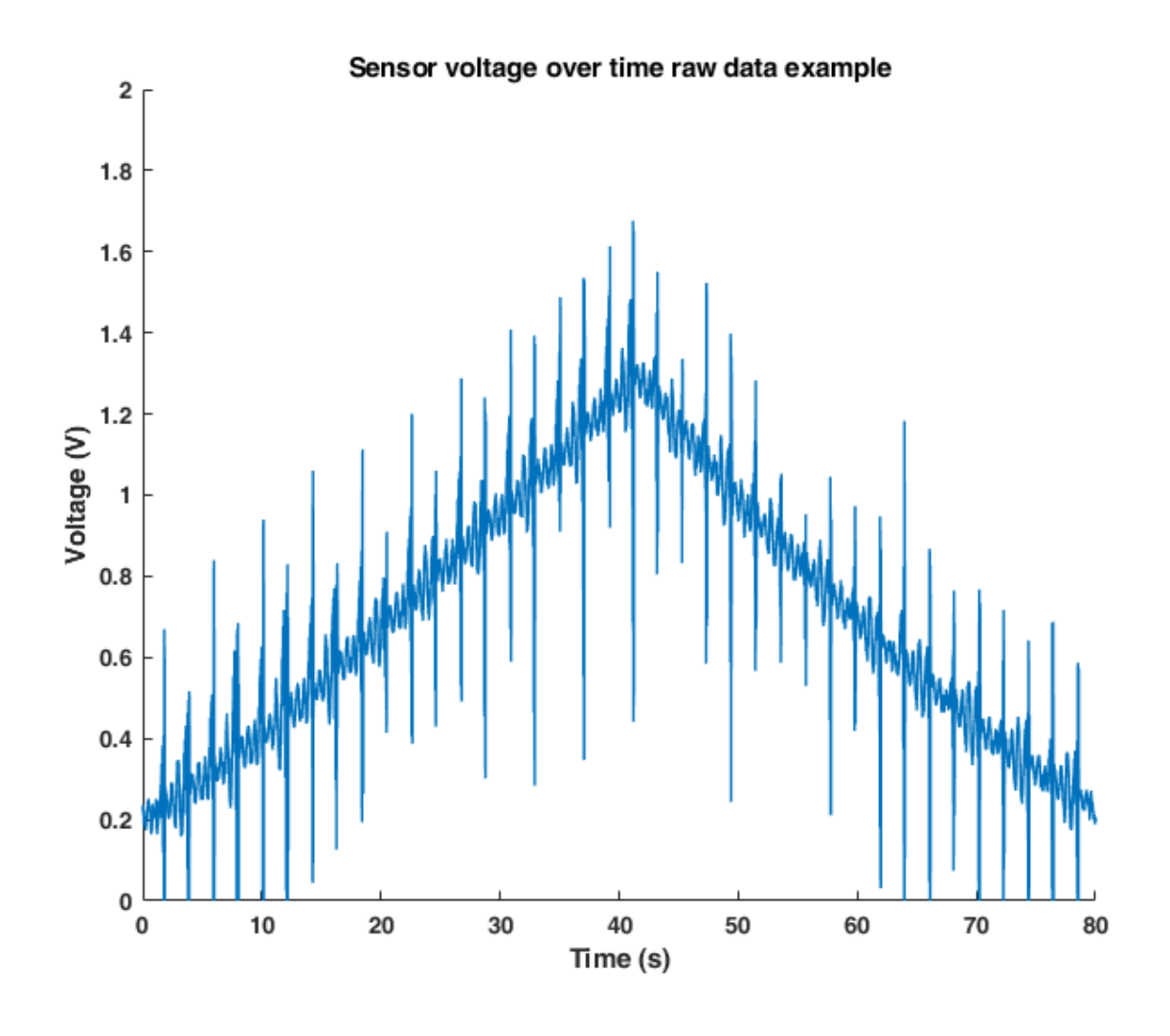
7	5	4	10.5	5	3	4	2	1
2	4	3	30	5	2	1	2	3
5	6	2	1	5	4	4	2	3
6	2	1	14.5	5	3	3	2	1
1	3	2	22	5	3	5	2	3
6	1	2	6.5	5	3	4	2	2
7	3	2	9	4	3	4	2	1
2	2	1	34.5	5	3	1	2	3
3	4	2	14.5	2	1	3	2	4
4	7	2	9	2	2	1	2	4
1	5	2	18	5	3	4	2	3
5	6	2	0	5	3	2	2	3
7	7	3	10.3	5	2	4	2	1
2	5	1	31.5	5	3	1	2	3
4	2	3	10	3	1	1	2	4
3	1	3	19	3	1	3	2	4
5	3	2	4	5	3	2	2	3
1	4	3	24.5	5	3	5	2	3
6	6	3	2	5	3	4	2	2
3	7	2	14	3	1	3	2	4
5	1	3	2.5	5	4	2	2	3
4	2	4	15.5	2	1	1	2	4
1	5	4	32	5	3	4	3	3
6	4	2	5	5	4	4	2	1
7								
-	6	3	6	4	3	4	2	1
2	3	1	49	4	3	1	2	3
6	6	2	3	5	3	3	2	2
7	1	1	36	4	2	4	2	1
5	4	4	10.5	5	3	3	2	3
1	2	1	46	5	4	5	2	3
4	7	3	15.5	2	1	1	2	4
2	3	2	18.5	5	3	1	2	3
3	5	3	18	2	1	3	2	3
6	2	1	10	5	3	3	2	1
4	1	4	10.5	2	2	1	2	3
5	4	3	10.5	5	4	2	1	4
7	6	3	10	4	2	4	2	1
1	5	2	32	5	3	5	2	4
3	7	1	20	4	2	4	2	4
2	3	4	30.5	5	3	1	3	3
4	4	3	13	3	2	1	2	3
7	3	1	24	5	3	4	2	1
1	6	2	21.5	5 5	4	5	2	3
3	5	4	15	2	2	4	2	4
2	1 -	4	30.5	5	4	1	2	3
5	2	2	1	5	2	2	2	3
6	7	4	10.5	5	4	3	2	3
7	1	3	11	5	2	4	2	2
6	3	1	15	5	4	4	2	1
4	2	4	13.5	3	2	1	2	4
5	5	4	7	5	4	2	2	3
2	7	3	25.5	5	3	1	2	3
1	4	4	28.5	5	2	5	3	3
3	6	4	11	3	2	4	2	4
_								

Experimental Condition	Experimental Condition				Significance
1	2	-41.5814	-3.775	34.03141	0.999947
1	3	-2.88141	34.925	72.73141	0.092391
1	4	13.86859	51.675	89.48141	0.001095
1	5	49.19359	87	124.8064	3.73E-08
1	6	30.69359	68.5	106.3064	1.94E-06
1	7	17.86859	55.675	93.48141	0.000284
2	3	0.89359	38.7	76.50641	0.040783
2	4	17.64359	55.45	93.25641	0.000308
2	5	52.96859	90.775	128.5814	3.71E-08
2	6	34.46859	72.275	110.0814	3.96E-07

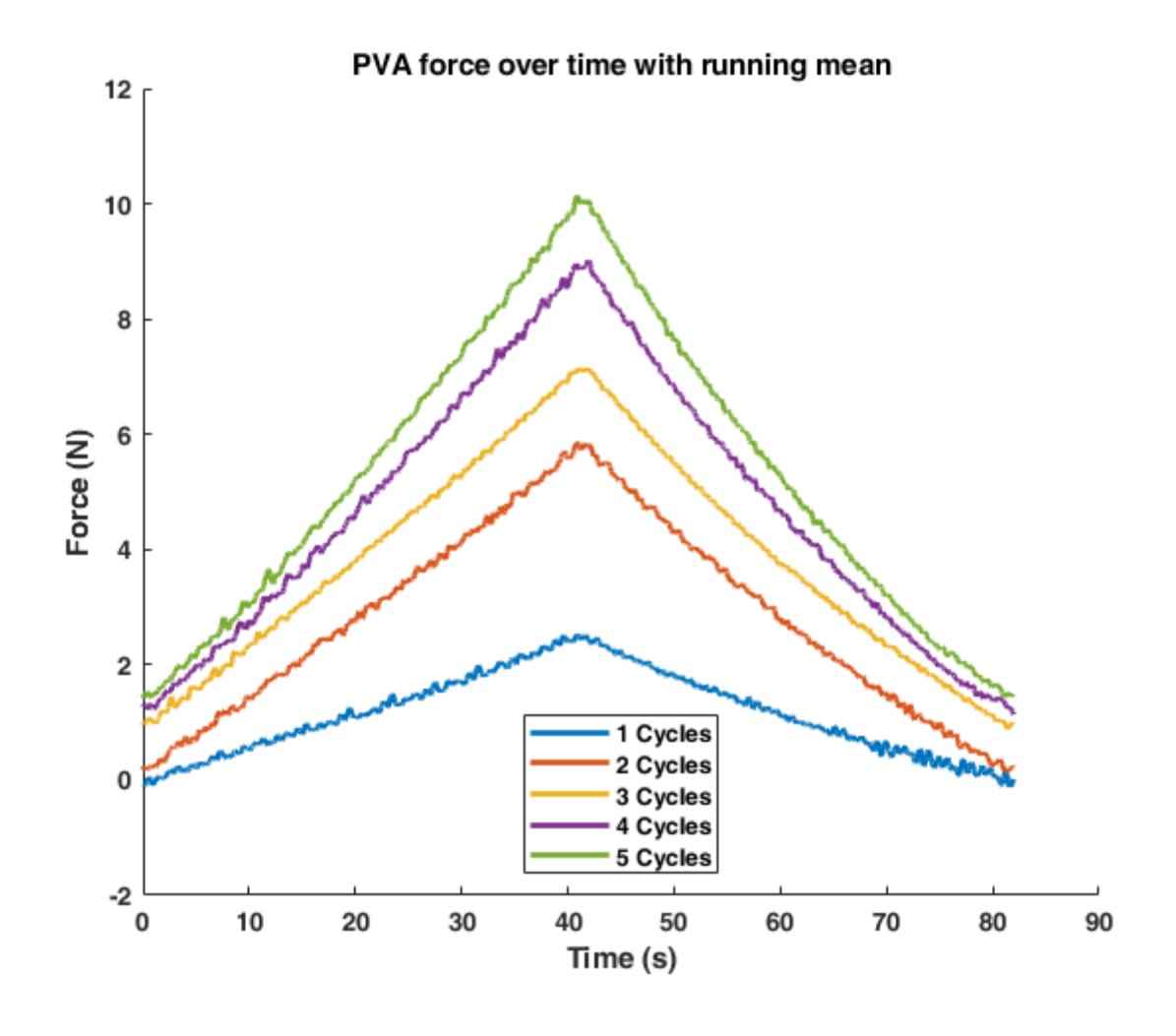


2	7	21.64359	59.45	97.25641	7.26E-05
3	4	-21.0564	16.75	54.55641	0.849339
3	5	14.26859	52.075	89.88141	0.000961
3	6	-4.23141	33.575	71.38141	0.120362
3	7	-17.0564	20.75	58.55641	0.67055
4	5	-2.48141	35.325	73.13141	0.085182
4	6	-20.9814	16.825	54.63141	0.84659
4	7	-33.8064	4	41.80641	0.999926
5	6	-56.3064	-18.5	19.30641	0.778503
5	7	-69.1314	-31.325	6.48141	0.180789
6	7	-50.6314	-12.825	24.98141	0.954125

F.3. Phantom validation







F4. Performance evaluation experiment

		Low stiffness phan	tom		High stiffness phantom						
Condition	Location	Deflection (Y- coordinate = PL0)	Deflection (X- coordinate = PL1)	Note	Condition	Location	Deflection (Y- coordinate = X)	Deflection (X- coordinate = Y)	Not		
4	1	0.543			5	5	0.182	•			
2	3	2.778	1.676	skip	1	3	0.915	1.372	sk		
3	3	1.176			4	2	2.734				
5	1	0.41			3	3	2.005				
1	3	1.481	1.64	skip	2	3	3.008	6.525	ski		
2	3	3.398	0.39	skip	4	4	2.709				
4	4	2.193			1	3	2.221	0.44	ski		
5	1	3.414			2	3	3.61	9.163	ski		
3	3	0.57		phantom damage	5	4	1.602				
1	3	1.469	1.814	skip	3	3	0.888				
4	4	0.558		phantom damage	2	3	6.151	4.83	ski		
2	3	0.067	0.92	skip	3	3	2.548				
5	4	2.939		phantom damage	4	1	2.73				
3	3	1.094		phantom damage	5	5	3.962				
1	3	1.561	0.184	skip	1	3	1.296	3.077	ski		
1	3	0.436	0.781	skip	4	2	2.711				
2	3	2.089	1.561	skip	3	3	2.525				
5	2	0.729			1	3	2.244	0.486	sk		



4	1	3.918		phantom damage No photo	5	1	0.114		
3	3	2.301		phantom damage	2	3	6.314	1.791	skip
5	1	2.643		No photo phantom damage	2	3	0.909	8.349	skip
2	3	0.353	0.823	skip	4	2	1.446	0.010	- Citip
4	4	1.791	0.020	o.up	3	3	0.602		
3	3	1.753			1	3	0.592	1.048	skip
1	3	1.355	0.184	skip	5	2	1.883		
3	3	1.572			5	5	0.758		
5	2	0.296			1	3	2.02	0.666	skip
4	1	4.534		wrong defined	3	3	0.207		
2	3		4 000	target	2	3		F 007	alsia
1	3	0.023	1.823 2.457	skip	4	5	1.043	5.097	skip
2	3	0.23	2.688		5	1	0.319		
3	3	2.438	2.000		2	3	2.314	6.594	akin
1	3	0.23	0.115	akin	3	3	3.008	0.394	skip
4	5	1.618	0.115	skip	1	3	0.231	0.162	skip
5	2	2.141			4	4	0.231	0.102	SKIP
2	3	1.883	2.135	akin	1	3	1.944	1.157	akin
-			2.133	skip				1.137	skip
5	3	1.823	1 252	akin	4	5 3	1.079	7.404	akin
3	3	1.185	1.253	skip	3	3	3.633	7.404	skip
		1.355					0.159		
4	4	3.165			5	2	0.597		
4	1	3.577	0.755	alria		4	0.321		
2	3	0.551	2.755	skip	4	1	1.92	4.004	-1-:
5	4	1.071			2	3	2.985	4.201	skip
3	3	3.121	0.755	-14-	1	3	1.722	1.676	skip
1	3	0.253	2.755	skip	3	3	0.482	4.074	alria
1	3	2.939	0.666	skip	1		1.936	1.071	skip
3	3	1.185	0.000	-14-	3	3	1.079	0.045	-1-:
2	5	2.453 0.251	0.393	skip	5	2	1.607	6.245	skip
4						4	1.423 0		
3	5 3	0.456 1.002			5	2	0.23		
2	3	1.666	0.81	akin	3	3	0.995		
4	4	0.661	0.61	skip	2	3	8.173	2.663	akin
5	5	0.433			1	3	2.192	1.236	skip skip
1	3	1.817	2.648	skin	4	4	0.413	1.230	SKIP
1	3	1.139	2.734	skip skip	1	3	1.607	1.263	skip
5	2	0.505	2.734	экір	5	5	1.194	1.203	SKIP
3	3	1.731			3	3	1.388		
4	2	0.217			4	5	0.849		
2	3	3.283	0.344	skip	2	3	1.469	8.127	skip
1	3	2.25	1.148	skip	5	1	1.249	U. 121	опр
2	3	0.528	1.929	skip	2	3	1.561	6.245	skip
3	3	1.148	1.020	onip	1	3	1.782	0.255	skip
4	5	2.802			3	3	1.041	0.200	опр
5	1	2.073			4	5	0.092		
3	3	2.64			5	5	0.671		
2	3	3.771	1.296	skip	2	3	3.448	3.633	skip
1	3	0.528	0.39	skip	1	3	1.157	1.944	skip
5	5	0.253	0.00	onip	3	3	1.686	1.0-17	опр
4	2	0.253			4	1	2.457		
3	3	1.116			4	1	0.482		
1	3	1.504	0.648	skip	1	3	1.584	1.538	skip
2	3	0.888	2.802	skip	2	3	1.481	1.273	skip
4	5	1.276	2.002	July	5	4	2.227	1.273	σκιμ
5	4	1.217			3	3	0.551		
-	4	1.21/			3	ა	0.001		



5	4	0.735			5	2	0.413		
4	5	1.171			1	3	1.897	0.602	skip
3	3	0.365			4	5	0.879		
2	3	0.574	1.561	skip	2	3	7.867	3.008	skip
1	3	0.872	0.941	skip	3	3	0.393		
3	3	2.204			5	1	0.161		
2	3	2.802	0.957	skip	3	3	0.833		
4	2	2.457			1	3	1.319	0.347	skip
1	3	0.463	1.203	skip	2	3	2.847	5.212	skip
5	5	2.25			4	2	0.255		
2	3	0.138	1.997	skip	1	3	0.888	1.253	skip
5	4	1.319			3	3	0.866		
1	3	0.98	2.096	skip	4	4	1.597		
4	2	2.106			5	1	0.482		
3	3	2.112			2	3	0.207	5.097	skip
4	1	4.859		phantom damage	1	3	0.393	2.615	skip
5	5	2.135			4	2	0.069		
1	3	0.758	2.457	skip	2	3	0.023	6.773	skip
3	3	0.228			5	4	1.378		
2	3	1.814	0.184	skip	3	3	0.253		
3	3	0.023			1	3	2.02	0.735	skip
5	2	0.987		Photo without needle, but with measurement	5	4	2.244		
4	2	0.62			4	1	4.836		
1	3	2.709	1.722	skip	3	3	1.435		
2	3	0.452	1.876	skip	2	3	1.342	7.45	skip

